# DESIGN AND OPTIMIZATION OF A FORMULA SAE RACECAR

A Major Qualifying Project Report:

Submitted to the Faculty of

WORCESTER POLYTECHNIC INSTITUTE

In partial fulfillment of the requirements for the

Degree of Bachelor of Science

By:

_____          _____

William Davis. billygolfer@wpi.edu          Krysten Carney. kcarney@wpi.edu


_____          _____

Jonathan Leith. jleith@wpi.edu          Anton Kirschner. antonk20@wpi.edu


_____

David Piccioli. dpiccioli@wpi.edu


Date:

Approved by:


_____

Professor David C. Planchard

## Abstract

The purpose of Formula SAE is to provide students an opportunity to design, fabricate, and then demonstrate the performance of a prototype race car. This project focused primarily on a major redesign of the previous WPI Formula SAE car by determining its strengths and weaknesses. The areas addressed for improvement include the chassis, front suspension components and geometries, tuning the continuously variable transmission (CVT), the air intake, exhaust system, engine mounting, fuel tank, braking components, and the uprights for the front suspension. With weight reduction in numerous systems of at least ten percent, analytical design of the intake, exhaust, and front suspension, and increased height of the chassis roll hoops and length between the front roll hoop and bulkhead, the final product is lighter, more efficient, and provides more room and comfort for the driver than its predecessor.

## Acknowledgements

The group would like to thank the following people:

Barbara Furhman, for her help with ordering parts and guidance

James Loiselle, for his guidance with machining

Torbjorn Bergstrom, for facilitating our use of the Washburn Labs

Adam Sears, for his assistance with machining

Corey Stevens, for his technical advice with high speed machining

Al Smyth, for creating many opportunities for the team we would have never otherwise had

Brian Barnhill, for his guidance throughout the project

Professor Planchard, for advising us throughout the project

This project could not have been completed without the help and support from these people.

# Table of Contents

# List of Figures

## List of Tables

# List of Equations

## Introduction

The Society of Automotive Engineers hosts a number of student design competitions, one of which being Formula SAE. Collegiate teams are given the opportunity to design and fabricate a Formula-style race car prototype and compete against one another. Teams are evaluated on the potential for their prototype to be a production item.

The project team consisted primarily of students that were contributing factors to WPI's FSAE team's success this past year in FSAE Michigan 2011. With the team familiar in practical, real-world testing on the previous WPI FSAE car, refinements on the original design were possible. Using the performance in braking, skid pad, acceleration, and autocross from the previous year's car as a benchmark, the project was oriented around redesigning specific aspects of the car. The objective for this project was developed with using information gathered from competition and analyzing every system of the 2011 car to determining which aspects of the car needed to be redesigned and which aspects could be carried over. These aspects included the chassis, front suspension components and geometries, tuning the continuously variable transmission (CVT), the air intake, exhaust system, engine mounting, fuel tank, braking components, and the uprights for the front suspension. Aspects that were carried over from the 2011 car include the front suspension geometry and kinematics, much of the chassis geometry, and the solid rear axle.

# Chapter 1: Analysis of the 2011 Car

The Formula SAE race car completed in 2011 was successful in the 2011 Formula SAE competition for the first time since 2008, however the car posed several areas for improvement. It was decided that the 2012 Formula SAE MQP would be based partly on its predecessor. To determine the scope of the project the 2011 car was analyzed.

The areas of the 2011 car that proved to be effective, thus were carried over were the engine, front suspension geometry and kinematics, general chassis geometry, and solid rear axle. Since the car would be designed and fabricated in one academic year, the engine was reused since the team already had an immense amount of knowledge on the engine. Using a new engine would have resulted in many major changes in most of the aspects of the car and the likelihood of completing a car for competition would have been unlikely. There was also no apparent need to change the suspension kinematics and geometry which resulted in little need to change the chassis geometry. Finally, since the car would only reach speeds of about 60 mph a solid rear axle was suitable for the application and received positive feedback from the judges at competition.

The main objective for this project other than addressing areas of extreme concern was to reduce weight and cost and increase manufacturability and adjustability. Areas that needed improvement included the chassis, front suspension, engine mounting, intake, exhaust, fuel system, CVT tuning, hubs and uprights, and belt tensioning. The 2011 chassis was overbuilt and too small for taller drivers. The bell crank was in bending and placed bolts in single sheer. There was no obvious concern with the hubs and uprights, however since the system is unsprung and rotating mass the goal was to reduce its weight by 30 percent. The 2011 method for mounting the engine caused the driver to sit and a more reclined and uncomfortable thus this became an area that was to be modified. The previous intake was not tuned for the engine, it was not properly sealed thus it leaked, and it was extremely bulky. The exhaust system was not properly designed for an odd-fire engine. Finally the continuously variable transmission was never tuned to hold the engine at the RPM that produced the peak power due to a lack in understand of how a CVT operated and was tuned.

## Chapter 2: Chassis Design and Fabrication

For a typical racecar, torsional rigidity is critical in chassis design. Torsional flex in the frame essentially adds another spring to the system, making suspension tuning unpredictable. It is nearly unavoidable to have some chassis flex during hard cornering. However, when it is minimized it will allow for calculated suspension adjustment with immediate and predictable results. Therefore, the goal is to make the chassis as stiff as possible.

Torsional rigidity is less important in the new car because of the swing-axle rear suspension. Unlike typical Formula SAE cars that use independently acting suspension left to right, both sides of the 2012 car are rigidly linked and can only move together. This style suspension has infinitely stiff roll stiffness in the rear. Since it's desirable to have some torsional roll to prevent the car from under steering, having a chassis with an above-average torsional compliance is acceptable.

An important constraint taken to each component being designed this year is minimizing weight. The chassis is no exception. All tube sizes that were not explicitly dictated by the Formula SAE rulebook have been analyzed under loading conditions and reduced in size until they were considered at a point where they would be strong enough to support the loads and still lighter than the previous design. While the chassis was stretched slightly to accommodate taller drivers, several chassis members forward of the front roll hoop have been reduced in size. This helps maintain the mass moment of inertia as focused on the center of the car as much as possible. These actions were taken to simultaneously keep the weight of the vehicle low and to reduce the mass moment of inertia. Physically reducing the mass moment of inertia allows for more responsive handling characteristics.

The design templates dictated by the Formula SAE rulebook provided several of the constraints for designing the chassis. The design of the 9-10-11 Formula SAE car also provided a number of constraints to base the new design on. It was found in the previous design that the chassis was not suitable for taller drivers. To fix this, alterations were made to the seating position as well as the bulkhead supports.

### 2.1 2011 Chassis Design and Fabrication

The previous chassis was fabricated from tubular 4130 Chrome Moly steel. Chrome Moly is widely available, relatively inexpensive, and can be easily welded. A substantial portion of the design was based on the constraints given by the Formula SAE rules. The rules require specific tubing sizes for teams that choose a tubular space frame. Tubular members not specifically dictated by the rules were included to increase rigidity and overall safety, although many were not optimized. The design was focused on simplicity, using only a small handful of tube sizes, which lead to an unnecessarily heavy chassis.

It was found that while the initial chassis model fit all of the associated templates, once electronics and braking components were added, they no longer fit. This caused poorly executed alterations that detracted from the overall design in order to pass technical inspection. To prevent this from happening again for the 2012 Formula car, refer to Section 2: Design Approach.

## 2.2 Goal Statement and Task Specifications for the Chassis

To design a new chassis that would address the known issues in the 9-10-11 Formula SAE car while still meeting the Formula SAE rules.

- Any alterations to the chassis must meet Formula SAE rules

- Changes to the driver's seating position must be accounted for to increase overall legroom, elbowroom, and headroom, allowing for a greater range of physical driver sizes

- Decrease overall chassis weight while still maintaining favorable structural rigidity

- Maintain initial suspension geometry for the front and rear

- Maintain an active effort to maximize serviceability and keep future packaging constraints in mind.

## 2.3 Design Approach

The triangulations used in the previous design presented no known issues in the analysis, so the existing chassis was used as a baseline for the new design. Chassis members not explicitly sized according to meet Formula SAE rules were then analyzed independently. These resulted in finding what standard tube sizes could be used in place of the heavier initial ones.

After adjusting all of the appropriate tube sizes, individual issues were addressed. The most prevalent issue in the previous design was fitting the 95th percentile male and 5th percentile female (read: PERCY). Although the PERCY template did pass technical inspection, the chassis disallowed for the majority of average sized drivers to operate the vehicle comfortably. This was due to a forced alteration to the seating position that placed drivers in an uncomfortably reclined position that left unreasonably reduced legroom. This issue was addressed by moving the fuel tank, previously mounted deep underneath the driver seat. Moving the fuel tank allows for the driver to sit upright, extending legroom. Secondly, the bulkhead was stretched forward from the front suspension mounts. By changing the seating position and stretching the bulkhead, legroom increased by at least six inches.

Due to Formula SAE rules on the upright seating position the main and front roll hoops were then adjusted. As per Formula SAE rules, the driver's helmet should have at least two inches of clearance between the plane created by the tops of the main and front roll hoops, indicated by the red dotted line in Figure 1.
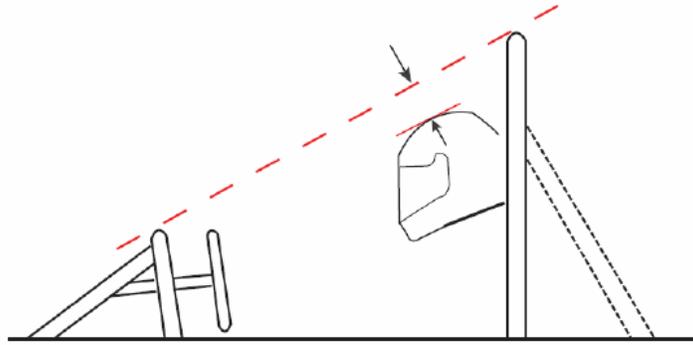
**Figure 1: Helmet Clearance**

The main and front roll hoops were extended to accommodate the higher position due to the driver now sitting upright. Corresponding head restraint supports and the harness bar were also adjusted accordingly. In extending the height of the front roll hoop, the driver will also be able to have more knee room. This also allows for better steering control, since the steering wheel will now be raised off of the driver's lap.

The last major alteration was due to the foot well template. It was found on the previous car that in practical application, the template was barely legal, and would need to be adjusted for the new design. The joints around the front suspension pick up points were widened to prevent the issue arising this year. To maintain the previously calculated suspension geometries, the pick-up tabs to the front control arms needed to be shortened. While this reduces overall camber adjustability, it was determined through the experience with the previous car that such a wide range of camber adjustment was unnecessary. Final Design figures comparing the 2012 chassis to the 2011 Chassis can be found in Appendix A.

## 2.4 Design Analysis

The most notable stress production onto the chassis would be found under braking. Considering the tube sizes that are affected by braking loads were changed, this was the primary focus for analysis. The maximum braking load is estimated at 2g. Each of the suspension pickup points can see upwards of 300lbs of resultant force. These forces were calculated using standard suspension calculation methods. With the forces known at each of the pickup points, the analysis showed a maximum deflection of 0.94mm, which is an acceptable value. With a deflection of 0.94mm, there will not be an excessive deformation in the suspension geometry. While this value is higher than the amount reported in the previous chassis design, it is expected given the goal to reduce chassis weight. It is more beneficial for the small loss in weight compared to the small increase of deflection and reduced rigidity. The deflection is still found to be within an acceptable range.
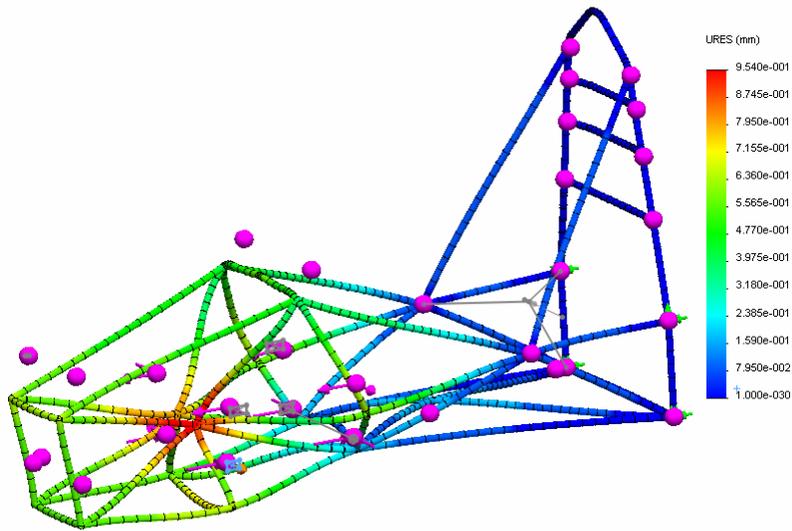
**Figure 2: Chassis Displacement under 2g Braking**
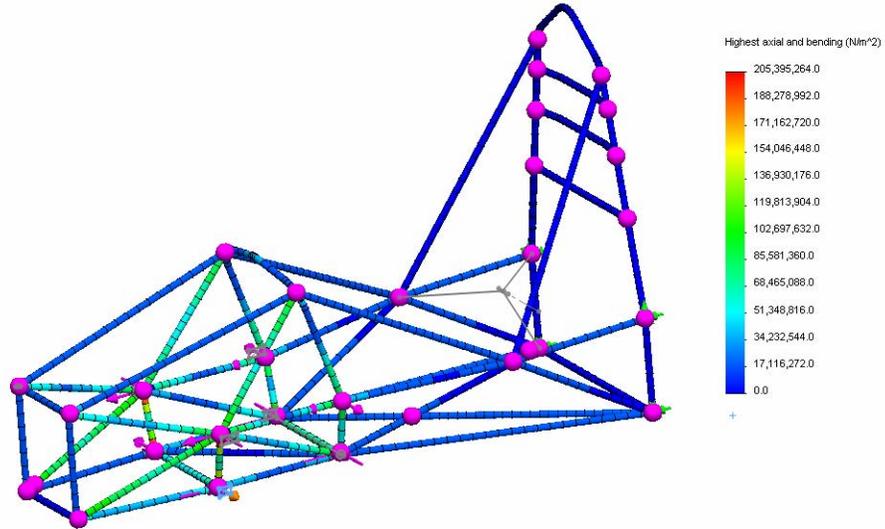


**Figure 3: Chassis stress under 2g braking**

Per the SAE rules the headrest must be able to take a 200 lb load directed into the headrest. It must be proven that the headrest and its supports will not fail under such a loading. An analysis was performed in which a non-uniform load of 100lb was applied to each headrest support beam with the main roll hoop fixed. This study showed small deflections with a safety factor of 2.44. This indicated that the headrest will be able to take the required force without failure. Although when the headrest is designed the mounting hardware must be able to transfer this 200lb of load into the supports. The deflection study can be seen in figure 4.
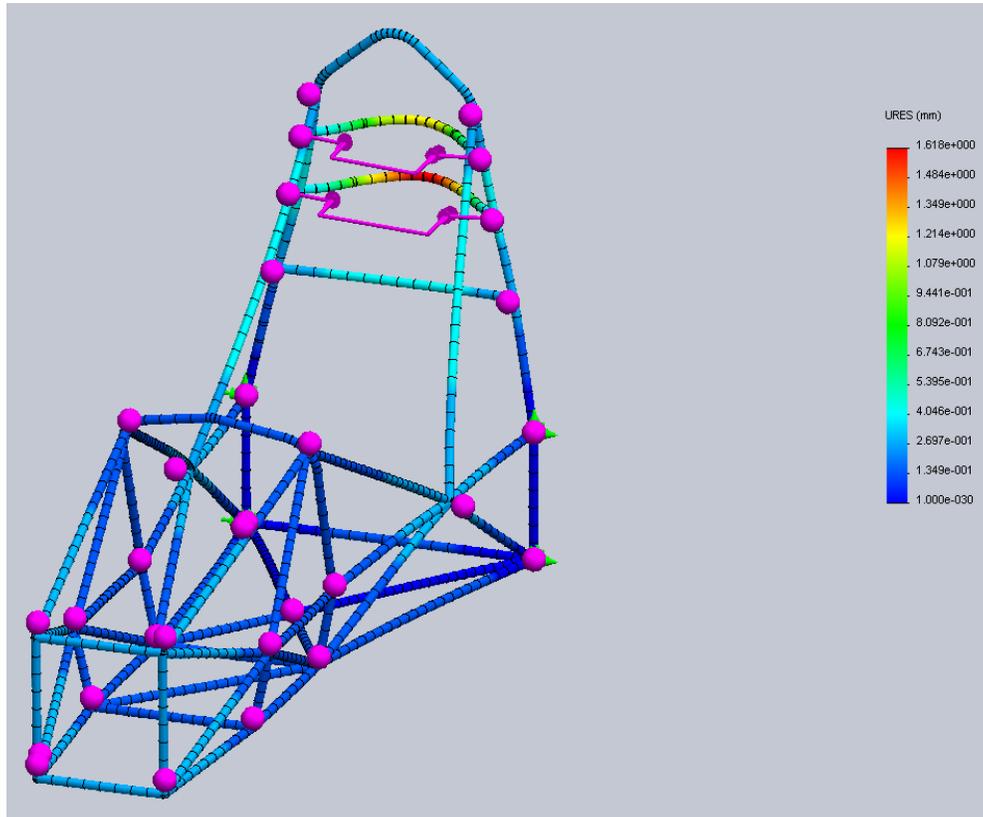


**Figure 4 Headrest Analysis**

Worst case analyses were performed, such as loading the car as it would if it was dropped onto one wheel with the driver in it. The deflection in such a case was higher than one would like, however the car would not be expected to turn in such a situation and only failure would be considered in such a case. The chassis will not fail and it has a reasonable safety factor such that it could see this loading multiple times without failure.

Lastly the torsional strength was tested. Yet again a worse case force was chosen. It was loaded and located from both the front and back in torsion located off of the shock mounts. The rear loading is shown in Figure 5, it is less than realistic as the shock forces would not be in that direction. It is still a useful test for torsional rigidity as it shows different deformation than frontal loading. Loading from the front is a more realistic loading and those results can be seen in Figure 6.
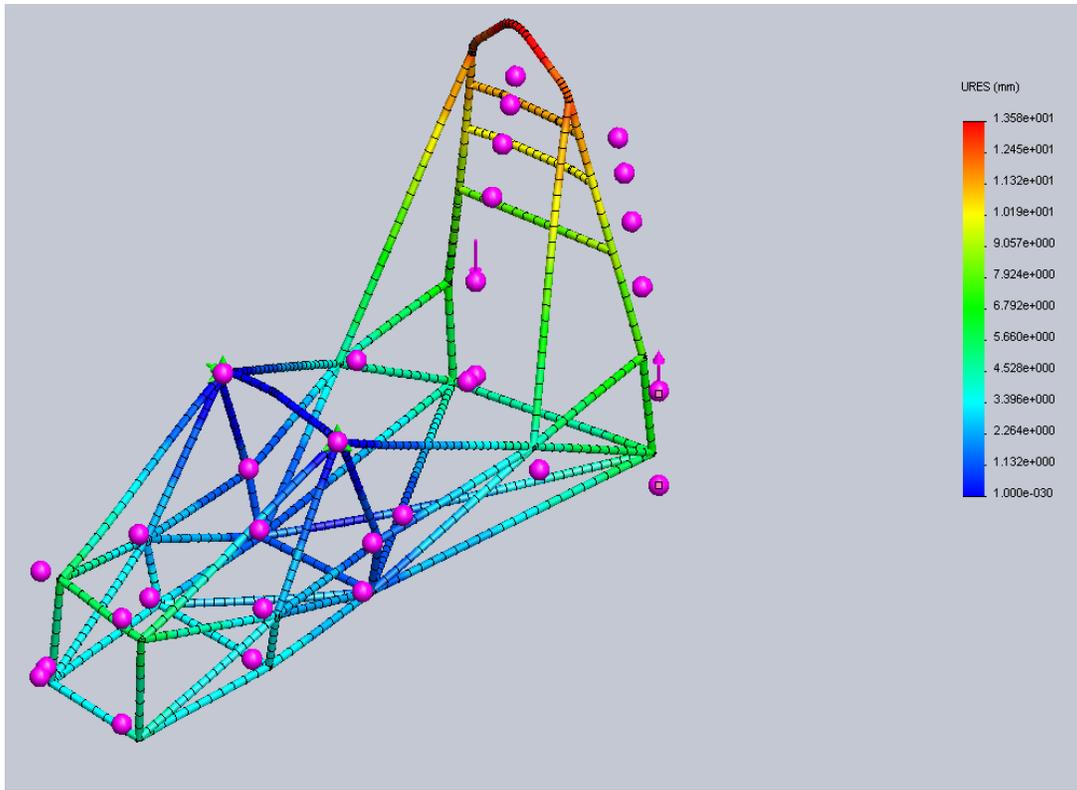
**Figure 5: Rear Torsional Loading Displacement**
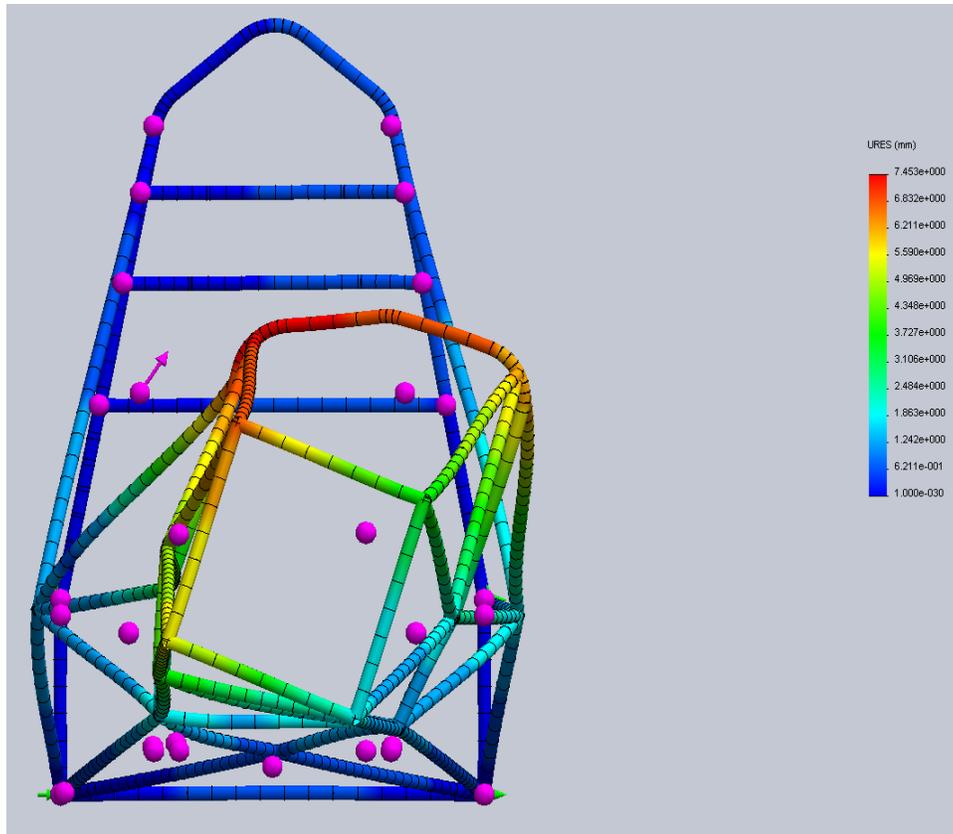
**Figure 6: Front Torsional Loading Displacement**

## 2.5 Fabrication

The chassis tubes were laser notched by Carroll Racing Development (CRD) and bent by the MQP group using a manual rotary tube bender. Although the design was satisfactory, the fabrication proved to be less than ideal. The quality and method of notching used by CRD was poor and left gaps at the joints. In addition there were noticeable tolerances and errors in bending the tubes due to the use of an old bender that was in poor condition. This also led to many gaps at the joints, some of which were too large to fill with the weld.

### 2.5.1 Preparation Procedure

Tubing was provided by Aircraft Spruce, and was later laser notched by Carroll Racing Development (CRD). This was thought to be an appropriate means of expediting the chassis fabrication process. While this prevented the team from having to hand notch each tube in its entirety, fitment was imperfect for any joint that included a bent member. This was a combination of generally poor notching on behalf of CRD as well as poor bending performed by the team at WPI using an old manual rotary tube bender.

Tubes were first placed for the three primary hoops: the front bulkhead, front roll hoop, and main roll hoop. Bent members joining the front roll hoop and bulkhead proved to be exceptionally difficult to fit, and required trimming the notches by hand for each connection.

When connections were prepared for welding, they would first be cleaned using Scotch-brite or similar wire mesh cleaning material. Joints would then be cleaned using fresh cloths and acetone to minimize contamination.

Several tubes were then tacked into place joining the front roll hoop and bulkhead. Some joints were welded near to completion to be able to heat the front roll hoop and correct the previous bending error in it. This proved successful, although some gaps did occur.

### 2.5.2 Resulting Weld Quality

The resulting quality of the chassis construction ranges from average to above average when considered for Formula SAE. Because of design intent, several joints mate different wall thickness tubes together. The increased difficulty of welding different wall thickness tubes necessitated an above average skill welder to complete. While these welds did not turn out pristine, the work was completed voluntarily by a WPI alumnus at no cost to the team. Additionally, any welds that join similar wall thickness materials turned out above average in quality. Below are figures of areas that had been deemed trouble areas, as well as photographs of areas that have been completed as expected.



**Figure 7: Chassis Welding**

**Figure 8: Chassis Welding Gap**



**Figure 9: Chassis Welding 2**

### 2.5.3 Resulting Solutions

To ensure safety in the rigidity of the chassis, several measures were taken. To begin, any problem areas where a gap is too large to be filled with weld instead had 4130 sheet of equal or greater wall thickness cut to shape and welded in to fill in the gap. Figure 10 is an example of a gap previously photographed with the filler plate.



**Figure 10: Display of Filler Plate**

**Figure 11: Display of Gusset Plate**

Where areas have minimal contact, such as the upper front suspension tabs, filler plates were used. Additionally, gusset plates were placed to increase overall strength of each of these points. While the FEA passed during design, and the joints would be strong enough with the filler plates alone, gusset plates were also placed to ensure the safest measures are taken in the chassis' strength. Figure 11 displays a sample gusset plate on a suspension mount. Similar plates were placed at each corner of these mounts to ensure the largest possible contact patch. Gusset plates are widely used and a commonly accepted method for strengthening welded joints when needed.

## 2.6 Conclusion

The chassis has grown considerably more spacious; allowing a larger range of driver's to handle the vehicle properly. While still following the Formula SAE rules, there have been over a 10% decreases in overall weight, saved mostly by changes in the engine mounting support and adjusting tube diameters. While there has been a marginal decrease in overall rigidity, it has still been found to be more than acceptable and can be used for the 2012 Formula SAE car.

To accelerate the fabrication process for the chassis, each tube member was created as individual parts in SolidWorks 2012. This allowed individual profiling tube-by-tube that was outsourced to be laser notched. In previous years, notching the chassis was done by hand at WPI. This has proven to be extremely time consuming for very minimal gains. It has been accounted for in the budget this year to allow for chassis fabrication to be outsourced. This allows for higher precision notching, quicker turnaround, and allows for continued engineering by the team to keep moving forward towards the final product.

The combination of less than ideal notching and inaccurate tube bending lead to difficulties in assembling of the chassis. Although the team was able to fix the issues that came about time and frustration could have been saved if a different company was chosen to outsource the chassis to.

CRD was marginally cheaper than Cartesian, another company the team looked into, which heavily influenced the decision to go with CRD. In the future the team recommends outsourcing the chassis to Cartesian or another similar company. Cartesian, while being costly, CNC notches and bends tubes.

## Chapter 3: Engine Mounting

The previous method of supporting the engine creates an unusual seating position for most of the drivers who drove at competition last year. The previous front engine mount creates a structural member to protect the fuel tank from being loaded by the seat, but leaves drivers sitting in an uncomfortably reclined position. This later caused the design of the seat to need to be altered to fit the Formula SAE driver's template, PERCY, while meeting SAE standards for chassis requirements. The seat alteration, while fitting PERCY, became very uncomfortable for drivers to operate the vehicle.
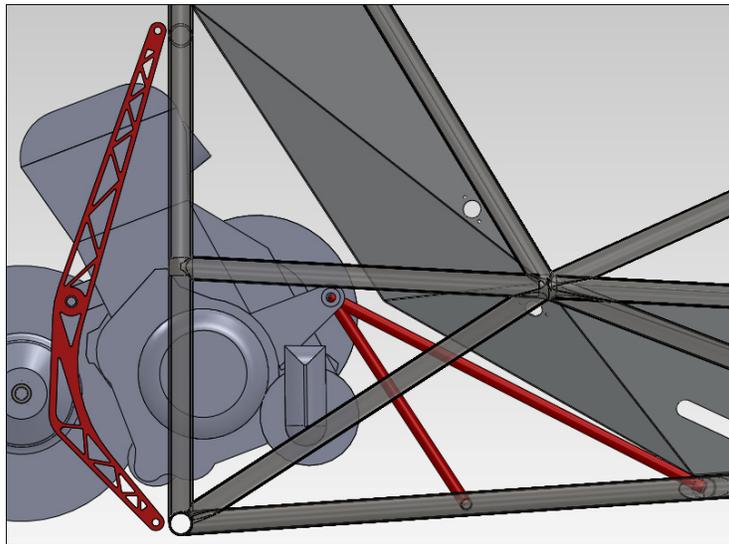


**Figure 12: 2011 Engine Mounting Method**

### 3.1 2011 Engine Mounting

The existing rear engine mounts were created from 7075-T651 Aluminum, having a yield strength of 54,000psi. They were precision water-jetted at Vangy Tool Company (Worcester, MA), who offered free water-jetting services to the previous MQP team. The tabs welded to the chassis for the rear mounts were also water-jetted to ensure accuracy in assembly. The front engine mounts were created from 4130 Chrome Moly, and was welded to the chassis.

The existing design was oriented around keeping the center of gravity of the engine low. This required the engine to be rotated to leave room for the intake manifold while still being able to move as much of the engine underneath the seat as possible. It was rotated to 20* off-vertical, the maximum allowable tilt according to Yamaha Engineers. The front mount was intentionally designed to support the seat and place the driver in a reclined position. Secondly, since the previous MQP team intended on putting the fuel tank below the driver's seat, the engine mount

would act to protect the fuel tank from seeing any loads, as dictated by Formula SAE rule B9.4.2.

## 3.2 Goal Statement and Task Specifications for the Engine mounting

To create and analyze a detailed design of the engine mounting for the 2011-2012 Formula SAE racecar that will be structurally sound and provide a simple approach to installing the engine.

- Must be able to take a 1400lb load from the belt tension force or under acceleration/braking

- Must be able to support the weight of the engine

- Must be within 1lb of the previous engine mounting strategy, ideally lighter

- Must not interfere with the positioning of the seat and driver

- Must provide a simple approach to installing or uninstalling the engine in case of engine failure

## 3.3 Design Approach

Conceptualizing all of the forces involved in the engine mounts proved to be a difficult task. The force towards the rear of the car due to the primary sheave was calculated as approximately 1200lbs in the worst case scenario. This was if the car was unrestricted, so these loads should never be seen. There are also a multitude of torques due to the output shaft of the engine and the inertial torques from the crank itself.
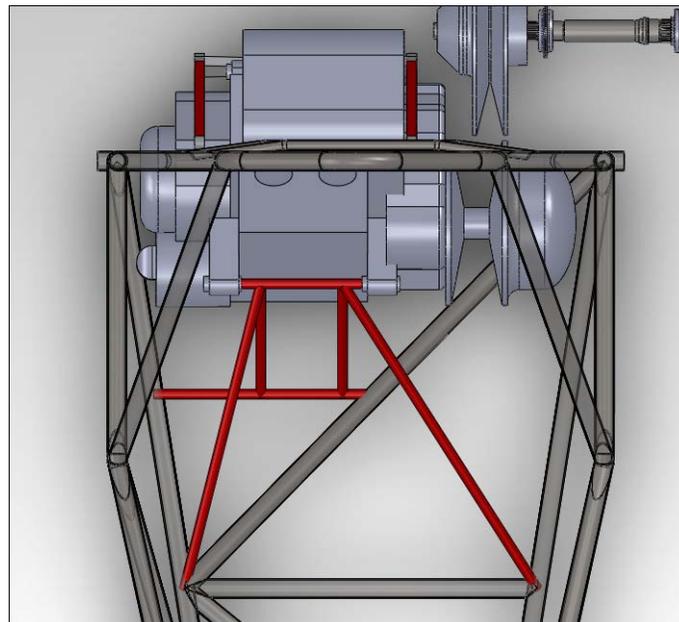


**Figure 13: Top View of 2011 Engine Mounting**

In a general internal combustion piston engine, those forces share a common axis. However, with the Genesis 80 FI, the output shaft is offset from the crank because of the internal, pre-CVT gear reduction in the engine. The engine mounts must also be able to support the static weight of the engine as well as additional forces from accelerating or decelerating the engine. An example of this would be keeping the engine coupled with the car as the car accelerates or decelerates.

It would be simply impossible to reuse the front engine mounting solution from the previous year car. The front engine mount doubled as a structural chassis member and the supporting tubes to allow this structure have been removed to save on weight. Also, the team felt that it was very important to adjust the seating position from the previous year's car. Most of the discomfort in the seating position was caused by the front engine mount being directly under the buttocks of the driver. The design of the rear engine mounts, referred to as the "bananas", can be reused. They cannot be pulled directly off of the old car, however. Because of the changes in the driver seating position, the top of the banana mount to the chassis will need to be raised, causing the dimensions of the banana to need to be changed to accommodate the raised harness bar.

The CVT poses several clear issues with mounting the engine simply. Without the CVT, the engine could have 3 simply triangulated chassis members to each front engine mount with bananas supporting the rear. However, the CVT's placement is directly where all 3 simply triangulated chassis members would need to pass to properly support the left side of the engine while not being obtrusive to the seating position. The theory on having rigid supports absorbing the force towards the rear of the car only on one side of the car began to be designed.

Design iterations began with creating a 3-bar solid mount on the right side of the engine to the chassis. The rear bananas were adjusted to fit the new chassis to support the rear. To support the left side of the engine, a mount was created by connecting the mounts on the engine and the mounting points on the harness bar and main roll hoop base. The simple shape ended up resembling the number six or a claw, thus the component was named the claw. The final weight of the banana is 0.85 pounds and the final weight of the claw is 2.52 pounds. They can be seen in the figures below, see the appendix for more figures and mass properties.
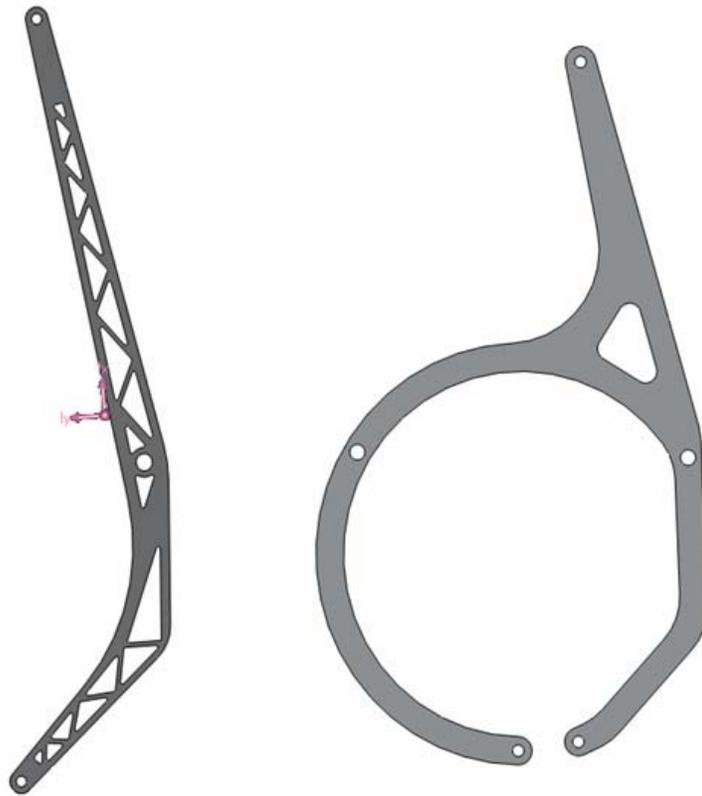
**Figure 14: Engine Mounts- the "Banana and Claw"**

## 3.4 Design Analysis

The Claw and Banana were analyzed using SolidWorks Simulation. To simplify the process, individual components were analyzed independently and forces were inferred based on intuition and conceptualized maximum loading. The first component that was analyzed was the claw. It was loaded with the entire force due to the torque load of the engine, the weight of the engine, and a 1400 pound force under acceleration or braking.

### 3.4.1 Finite Element Analysis on the Banana

For the analysis of the banana the top and bottom holes were defined as fixed geometry since they will be fixed to the chassis by tabs. To simulate the weight of the engine a force of 65 pounds was applied in the negative y direction on the hole that would connect directly to the engine. This resulted in a maximum stress of 4,883,529.5 $N/m^2$, a minimum safety factor of 56.312, and a maximum displacement of $3.219 \times 10^{-3}$ mm. To simulate the torque on the engine an 80 ft-lb torque was applied to the hole that would be directly connected to the engine, resulting in a maximum stress of 826,525.8 $N/m^2$, a minimum safety factor of 332.7, and a maximum displacement of $3.219 \times 10^{-3}$ mm. To simulate the force on the mount from accelerating or breaking the worst case scenario of 700 pounds was applied to the engine mount resulting in a maximum stress of 64,562,852 $N/m^2$, a minimum safety factor of 1.92, and a maximum

displacement of 1.532 mm. However this is about two time the expected load since all of the engine mounts together should be able take a 1400 lb load the banana that only supports a quarter of the engine should only see a 350 lb load.
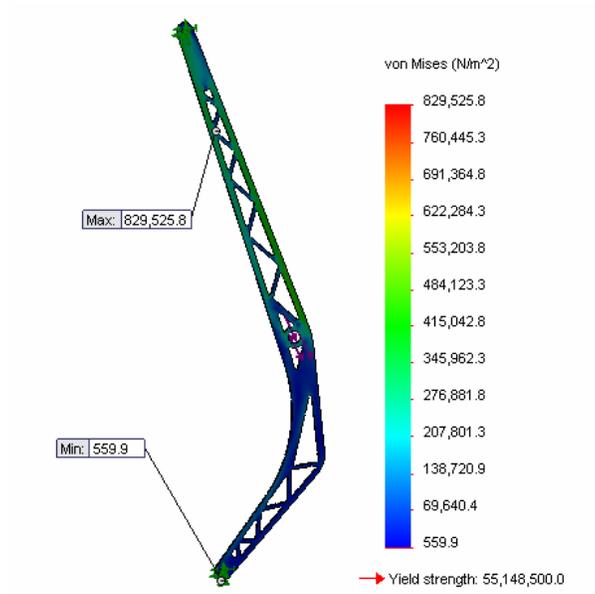


**Figure 15: "Banana" Stress from Acceleration/Braking**
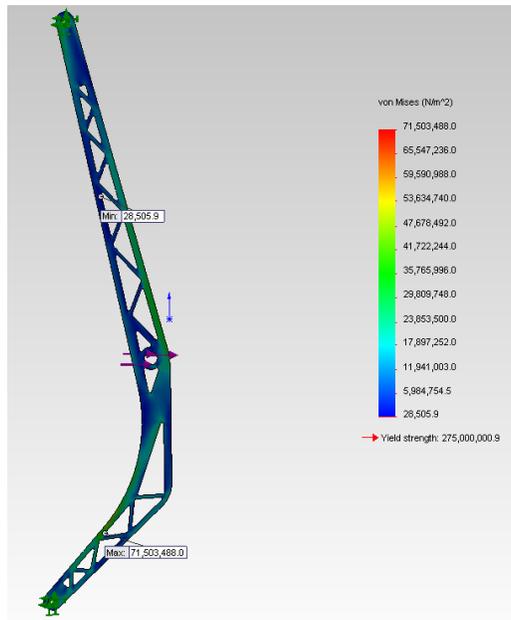


**Figure 16: "Banana" Stress from Engine Torque**
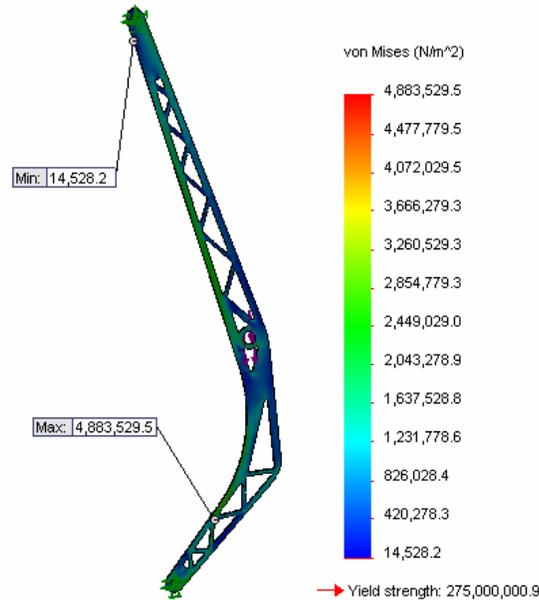
**Figure 17: "Banana" Stress from Engine Weight**

### 3.4.2 FEA on the Claw

The top and bottom holes on the claw were also defined as fixed geometry since they would be fixed to the chassis by tabs. Loading the claw under the weight of the engine resulted in    a maximum stress of 6,754,867.5 N/m$^2$, a minimum safety factor of 40.7, and a maximum displacement of 3.303x10$^{-2}$ mm. The loading from the torque of the engine resulted in a maximum stress of 1,540,494.9 N/m$^2$, a minimum safety factor of 178.514, and a maximum displacement of 6.475x10$^{-3}$ mm. The loading from accelerating or braking resulted in a maximum stress of 222,036,128.0 N/m$^2$, a minimum safety factor of 1.2, and a maximum displacement of 1.086 mm. The combination of the three forces is predominantly driven by the force from acceleration or braking, as such the impact of the weight and torque of the engine have a minimal impact on the mounts as compared to the force from acceleration or braking.
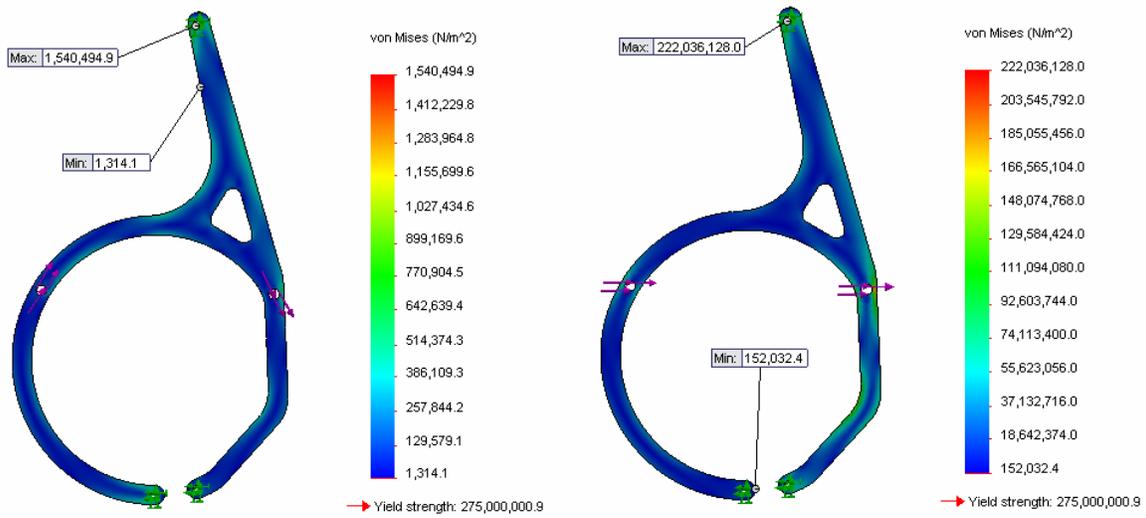
**Figure 18: Stress on the Claw from Acceleration/ Braking**
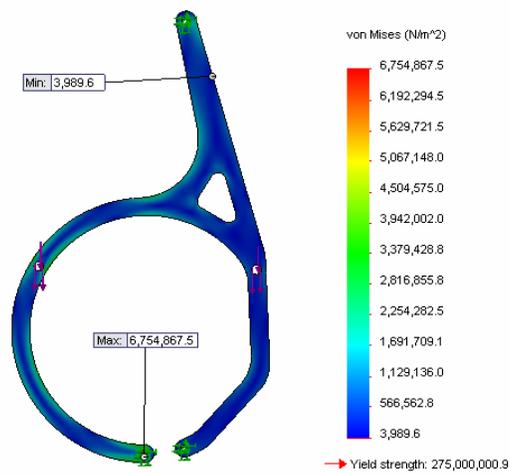


**Figure 19: Stress on the Claw from Engine Torque**
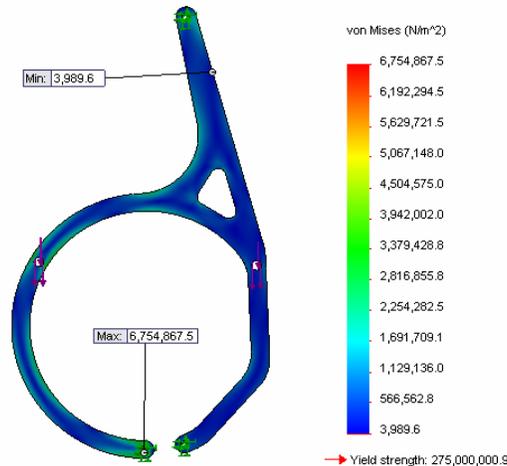
**Figure 20: Stress on the Claw from Engine Weight**

## 3.6 Conclusion

The new engine mounting design eliminates the unreasonably reclined driving position previously implemented, allowing for a more comfortable seating position and allowing the drive to sit more upright. The SolidWorks simulation produced satisfactory results. Since the proposed banana is strongly based off the existing banana the team can be confident in the simulation results. Although the worst case scenario for acceleration or braking of 1400 pounds on the claw produced a minimum safety factor of only 1.2, that force will be split between all of the engine mounts, and it is likely that the claw would only see a 700 pound force which would result in a safety factor of nearly 2.5.

As expected in the design of the mounts, when installed in the actual car the mounts facilitate easy installation and removal of the engine. The new mount design also allows for the oil to be changed in the car, even with the gas tank installed. Removal of the seat is all that is required to replace the oil filter. It also appears that the mounting solution is strong enough to withstand all of the forces, which further reinforces the analysis.


# Chapter 4: Front Suspension

The previous front suspension on the 9-10-11 car is a conventional pushrod suspension set up with Cane Creek 2010 TTX25 dampers. However, the previous set up is in single shear, and acting in two different planes which creates hazardous bending loads on the suspension. The following sections discuss new design concepts that address the issues found in the previous set up, and the calculations that lead to the decision to utilize the new Cane Creek shock model, 2011 TTX25 MKII.

## 4.1 2011 Front Suspension

At the Michigan FSAE competition in May 2011, the Design Judge's criticized the actuation of the front shock assemblies, as they placed bolts in single shear, and required an immensely stiff

bell crank to withstand the forces and large moments that it was subjected to.  One of the main objections for the design of the front suspension on the new car was to address this issue by redesigning the way the shocks were actuated; minimizing the changes, if any, to the front suspension geometry.  It was decided that there would be no changes to the suspension geometry as the car behaved well during competition, and wore tires well through endurance, while allowing for enough adjustment to set up the car sufficiently for all events.

## 4.2 Goal Statement and Task Specifications for the Front Suspension

To design a new front suspension set up that would address the known issues found in the 9-10-11 car.

- Must be simply adjustable using standard automotive tools

- Critical mounts must be in double shear to minimize shear stresses

- Must not be in significant bending

- Must have a rising rate

## 4.3 Design Approach

By manipulating 3-Dimensional sketches in SolidWorks, two methods of shock actuation were explored, pushrod actuation and direct acting. It was determined that pullrod actuation, another common design, was not feasible, as it requires packaging the shocks below the driver's legs. The previous chassis design does not permit this option since there would not be enough space when passing the Formula SAE templates through the chassis.  The pushrod design results in a very long pushrod actuating a rocker mounted on the top forward facing chassis members.
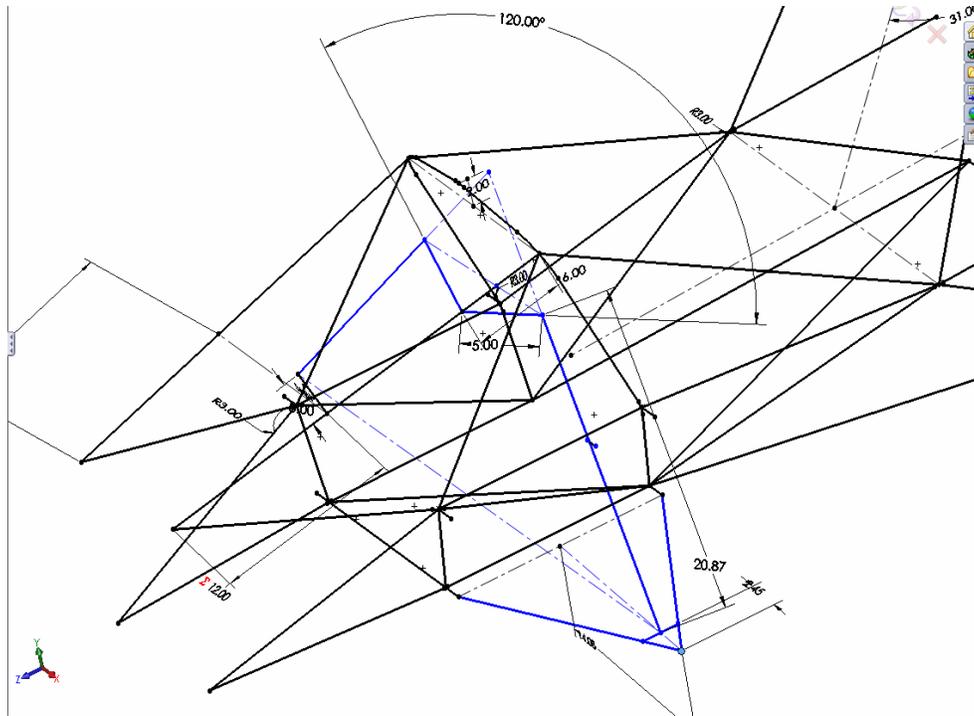
**Figure 21: Pushrod Actuated Shock Design**

This design requires adding a cross member for the shocks to attach to, which would not be triangulated well without additional supports. It also requires designing rockers and mounts for the rockers on the chassis members. The addition of mounts, members, and rockers above the bulkhead and forward in the chassis results in a slightly higher center of gravity. Using this design would also require the pushrod to be very robust to meet acceptable compliance and buckling being such a long length. This also would require the design to be considerably heavier than the existing suspension design.
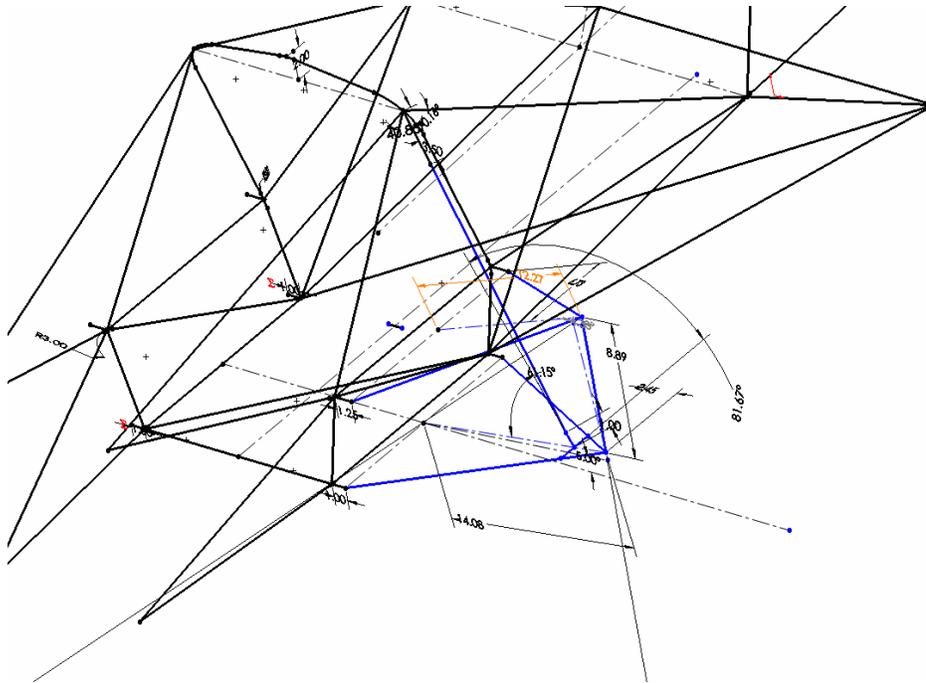
**Figure 22: Direct Acting Shock Design**

The second concept involves a shock that is directly actuated by the control arm itself. This design has the least moving parts, would be easiest to manufacture, and would require minimal changes to the existing design of the car. Drawbacks include inability to make major changes to the motion ratio throughout suspension travel, as well as there not being close triangulated chassis areas to mount the shock to. The issue resulting from this problem is that most short travel shocks that could be used in such applications would require heavy, long, and robust shock extensions to meet the lower control arm. The nearest place to mount the shock is also not in the same plane as the tab where it attaches to the lower control arm, which applies small, longitudinally vectored forces during suspension travel.

Directly locating the shock on the control arm also partially contributes to the addition of unsprung weight, which negatively affects ride and overall mechanical grip when the wheel attempts to keep contact with the road over bumps. However, the existing control arm is already designed to be subjected to these forces during braking, and could be easily adapted for such conditions. Manufacturing this design is also less expensive than a pushrod or pullrod design, which requires adding an additional cross-member, and fabricating rockers. The simplicity and minimal increase in weight at the expense of slightly increased unsprung weight led to further investigation of the feasibility of this design.

### 4.3.1 Design Feasibility
The first step to understanding the feasibility of a direct acting shock was to do a motion study to determine if the motion ratio between wheel travel and shock travel was suitable.

**Equation 1:**

$$\text{Motion Ratio (MR)} = \frac{\text{Wheel Travel}}{\text{Shock Travel}}$$

A desirable motion ratio is generally anywhere between 0.5 and 2.0, as most shocks available do not have spring rates and damping velocities outside of this range.  However, having a lower motion ratio will result in lower shock velocities. This directly promotes excessive friction in the seals of the shock, affecting the damping effectiveness.  Most shocks that would be used in the FSAE application usually have a shock travel in the range of 2 to 3 inches, and having too low of a motion ratio would not give enough suspension travel to meet the 1 inch of compression and 1 inch of droop dictated by the FSAE rules. It is also generally desired for the motion ratio to not increase as the suspension compresses.  A decreasing motion ratio through suspension compression creates a digressive rate suspension, which decreases effective spring rate during suspension bump and promotes unstable cornering characteristics as roll rate increases and the car rolls through the middle of the corner.  A progressive rate suspension is typically desired in FSAE applications, as it allows for choosing spring rates that provide the correct load transfer dynamics while decreasing the chance of bottoming out of the suspension during situations of extreme suspension loads.

The motion ratio study was conducted measuring the effective distance between the proposed shock mount location and the shock tab on the lower control arm as the suspension traveled from full droop to full compression, using a 3DSketch and Design Table in SolidWorks.  Negative suspension travel indicates droop, zero travel is at resting ride height, and positive travel indicates compression.
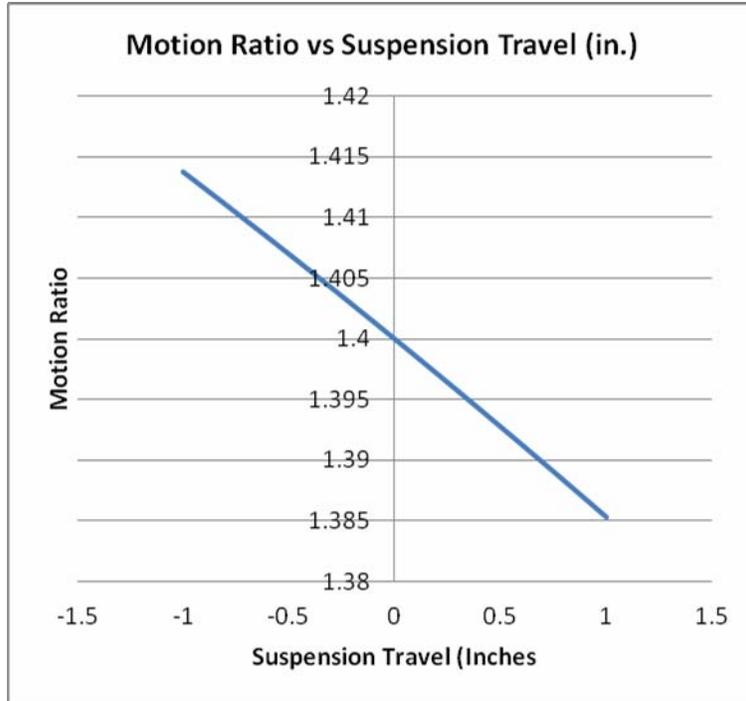
**Figure 23: Motion Ratio of Front Suspension through Suspension Travel**

**Table 1: Motion Ratio**

| Suspension Travel | Suspension Travel@abs0 (in.) | Shock Travel (in.) | Shock Travel (mm) | Motion Ratio |
|---|---|---|---|---|
| -1.5 | 0 | 0 | 0 | 1.41921 |
| -1.4 | 0.1 | 0.07047516 | 1.790069 | 1.41894 |
| -1.3 | 0.2 | 0.141079211 | 3.583412 | 1.417643 |
| -1.2 | 0.3 | 0.211813885 | 5.380073 | 1.416338 |
| -1.1 | 0.4 | 0.282680922 | 7.180095 | 1.415023 |
| -1 | 0.5 | 0.353682069 | 8.983525 | 1.413699 |
| -0.9 | 0.6 | 0.424819083 | 10.7904 | 1.412366 |
| -0.8 | 0.7 | 0.496093729 | 12.60078 | 1.411024 |
| -0.7 | 0.8 | 0.567507782 | 14.4147 | 1.409672 |
| -0.6 | 0.9 | 0.639063025 | 16.2322 | 1.408312 |

| | | | | |
|---|---|---|---|---|
| -0.5 | 1 | 0.710761254 | 18.05334 | 1.406942 |
| -0.4 | 1.1 | 0.782604274 | 19.87815 | 1.405563 |
| -0.3 | 1.2 | 0.854593901 | 21.70669 | 1.404176 |
| -0.2 | 1.3 | 0.926731963 | 23.53899 | 1.402779 |
| -0.1 | 1.4 | 0.9990203 | 25.37512 | 1.401373 |
| 0 | 1.5 | 1.071460765 | 27.2151 | 1.399958 |
| 0.1 | 1.6 | 1.144055224 | 29.059 | 1.398534 |
| 0.2 | 1.7 | 1.216805554 | 30.90686 | 1.397101 |
| 0.3 | 1.8 | 1.289713648 | 32.75873 | 1.395659 |
| 0.4 | 1.9 | 1.362781413 | 34.61465 | 1.394207 |
| 0.5 | 2 | 1.436010771 | 36.47467 | 1.392747 |
| 0.6 | 2.1 | 1.509403656 | 38.33885 | 1.391278 |
| 0.7 | 2.2 | 1.582962022 | 40.20724 | 1.3898 |
| 0.8 | 2.3 | 1.656687836 | 42.07987 | 1.388312 |
| 0.9 | 2.4 | 1.730583081 | 43.95681 | 1.386816 |
| 1 | 2.5 | 1.804649758 | 45.8381 | 1.38531 |
| 1.1 | 2.6 | 1.878889886 | 47.7238 | 1.383796 |
| 1.2 | 2.7 | 1.953305498 | 49.61396 | 1.382272 |
| 1.3 | 2.8 | 2.027898649 | 51.50863 | 1.38074 |
| 1.4 | 2.9 | 2.10267141 | 53.40785 | 1.379198 |
| 1.5 | 3 | 2.177625872 | 55.3117 | 1.377647 |

Through this motion study, it was determined that there is a decreasing motion ratio though suspension travel, resulting in a progressive rate suspension. However, the rate of rise of effective spring rate is not very high, and could be considered almost linear. This is not necessarily undesired, as it keeps roll rate during cornering consistent, allowing predictable

cornering characteristics. Knowing the motion ratio throughout the full suspension travel confirmed the ability to use a direct acting shock design, as it is was the simplest, lightest, most cost effective way to replace the bellcrank design used previously.

## 4.4 Design Analysis

To redesign the existing car for direct acting shocks, the angle of the shock mounts on the chassis, and the shock tabs on the lower control arms needed to be changed. This was done in the 3D Sketch that was used to study the motion ratio at ride height. The distance between the eye of the upper shock mount and the lower shock tab are known from ride height as well, which allows for the sizing of the shock extension and rod end assembly. This is simply done by subtracting the length of the Cane Creek TTX25 shock from the mount to tab distance at ride height.

To complete FEA on each suspension component, theoretical forces through them needed to be calculated first. This is first accomplished by determining wheel loading during extreme situations, such as a 2g bump or corner. Using these wheel loads and static analysis based on the suspension geometry, the forces through each of the components can be calculated. These forces can then be used to perform FEA in SolidWorks Simulation to determine failures in the design, find stress concentrations, as well as find the magnitude of the deflections of the components to determine compliance.
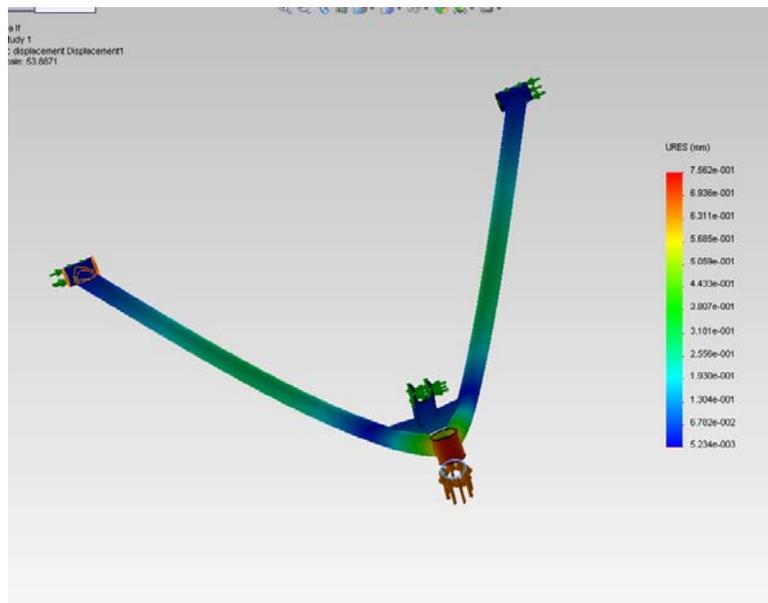


**Figure 24: Stress Concentration FEA Lower Control Arm**

For the lower control arm, FEA was done to check the redesign of the shock tab, as well as ensure that the control arm was strong enough to resist forward loading during suspension compression.
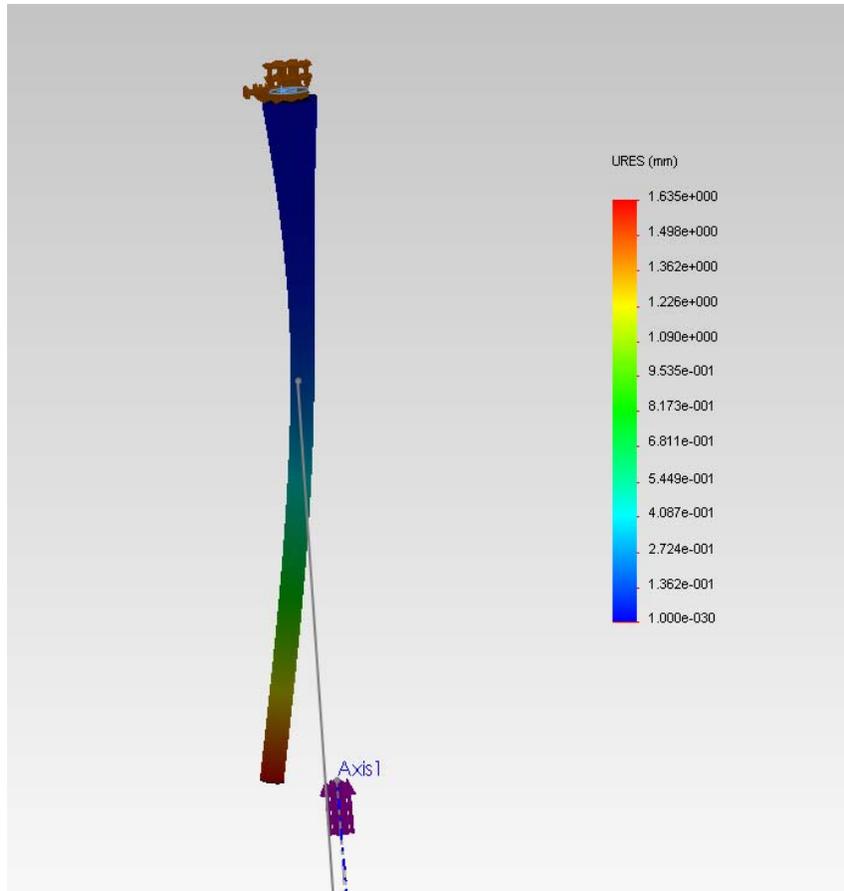
**Figure 25: Off-Axial Loading for Shock Extensions**

The most important aspect of the shock extensions is that deflection is minimized, or they will exert a bending load on the shocks themselves. Such case would cause binding during compression. FEA was completed assuming a worst case scenario of the shock spacing hardware binding and the suspension applying an off axial load. Through iterations, if the deflection was too high, the overall extension shaft diameter was increased. Similarly, if there were high stress concentrations at its base, the fillet distance at the base was increased. This process was repeated until an optimization point was found. Mass properties were also checked through each iteration to keep the shaft weight reasonable. The end result came out to .62 lbs, compared to a 20 inch long, .375 diameter, .075 wall steel tube necessary for a pushrod actuated suspension (.60 lbs). However, this is the only component needed for actuating the suspension, in comparison to the parts required for rockers, bearings and mounts to the chassis needed for push rod actuation.

### 4.4.2 Suspension Calculations

The two components that respond to the dynamic forces seen by the wheel on a car are the spring and the damper. In order to calculate the desired spring rate and damping curves needed to select

the spring and damper, the system will be treated as spring-mass-damper system. Essentially, there is a mass on a spring, the spring controls the forces on the mass, and the damper controls the oscillation of the spring. The following section summarizes the calculations that were done in order to determine the appropriate springs and dampers to be used in the front and rear suspension, the complete calculations can be found in Appendix A.

As previously discussed, the front and rear motion ratios are 1.40 and 2.00, respectively. Having full knowledge of the theoretical motion ratios are important because they control the relationship between the forces at the wheel and those seen by the shock.

In order to begin the calculations, the mass that the shock supports (spring mass) needs to be determined. Based on the 9-10-11 car the weight of the 2012 car with a driver was assumed to be 550 lb (The weight of the car is represented by the letter M in the calculations). Assuming a 45/55 Front/Rear weight distribution, and an even distribution left and right, the front left and right weights of 123.75 lb, and rear left and right weights to be 151.25 lb. it was also assumed based on the 9-10-11 car that the front spring mass was 98.75 lb at each wheel, and the rear sprung mass was 123.27 lb at each wheel.

To determine the spring rate a ride frequency must be chosen. As stated by Matt Giaraffa, "a ride frequency is the undamped natural frequency of the body in ride". Lower frequencies result in softer suspension, higher frequencies result in stiffer suspension. Formula cars and cars that have substantial downforce do not need softer suspension to provide comfort when passing over a bump. Racecars typically don't see large bumps on well-prepared tracks and require stiffer suspension in order to keep from bottoming out. A front ride frequency was chosen to be 3.2 Hz. Lower frequencies would result in the car bottoming out under normal driving conditions. Higher frequencies could result in less mechanical grip. Essentially, the ride frequency is a compromise between mechanical grip provided by softer frequencies and quicker vehicle response in corner entry from stiffer frequencies. This results in desired spring rate ($K_{sf}$) of 220.402 pounds per inch.

A rear ride frequency was chosen to be 2.8Hz. Typically the rear ride frequency is about 10-20% less than the front ride frequency. Maintaining a higher ride frequency in the front over the rear for rear wheel drive cars allows fast transient response by the front wheels. This results in a desired spring rate of ($Kr_f$) 396.82 pounds per inch for the rear.

The center of gravity of the 9-10-11 car was measured to be 16.3 inches above the ground. The calculations can be found in Appendix B. It can be assumed that the center of gravity of the 2012 car will be roughly 13 inches above the ground. This will be achieved by making the overall car lighter and mounting as many components as possible low to the ground.

Roll rates determine how much the body rolls relative to how hard the vehicle is cornering. The roll gradient is expressed in degrees of body roll "per g" of lateral acceleration. A good roll gradient for higher downforce cars is between 0.7-1.0 deg/g. A center of gravity of 13 inches

above the ground results in a roll gradient from the ride springs of 0.757 deg/g. Since this roll gradient is acceptable, an anti-roll bar is not necessary to modify the roll gradient.

## 4.5 Determining the Dampers

The existing WPI Formula SAE car utilizes Cane Creek 2010 TTX25 shock absorbers. Initially, the direct-acting suspension would utilize these shocks again, saving on cost. The following section discusses the theoretical calculations that show that the 2010 TTX25 shocks are not suitable for the front suspension in the new design and the approach taken to finding suitable shock absorbers.

Dampers control oscillations caused by the springs. Over damped systems are slow to respond, allow minimal oscillation of the spring. Under damped systems allow an unreasonable amount of spring oscillation. Critically damped systems allows for minimal oscillation and return to the neutral position at a rate that is equally unsettling to the vehicle. Referencing the design, a damping ratio must first be selected. The damping ratio provides a trade-off between the responsiveness of the suspension and how much the shock "overshoots" the neutral position before returning to its neutral position. Ideally, the ratio should minimize both of these conditions. A damping ratio of 0.7 was chosen because it provides adequate body control as well as quicker response than a critically damped shock would provide.

There are two ranges in which the shock will operate, high and low speed. The point at which the damper switches from low to high speed is a frequency defined as:

**Equation 2:**

$$\sqrt{2} * ride\ frequency$$

Transmissibility is the relationship between the body of the car and the wheel depending on how fast the car is traveling when it comes in contact with a bump. Essentially at lower speeds the wheel and the body move roughly the same amount over a bump, and at higher speeds the wheel moves more than the body over a bump. The crossover point in the front was estimated to be 4.525 Hz. Assuming that the shock moves one inch before the body starts to move, the velocity at the crossover point was determined to be 4.525 inches per second.

Using Optimum G as a guide, the following theoretical damper curves were developed with a crossover from low speed to high speed point of 4.525 inches per second (assuming the shock movement before the body moves to be 1 inch). The high and low speed slopes were then calculated for compression (blue) and rebound (red). Assuming the low speed portion of the graph has a y-intercept of 0; linear equations were determined and plotted in the graph shown in Figure 4. The force on the shock at the crossover point in compression was calculated to be 21.72 pound force, and the force on the shock at the crossover point in rebound was calculated to be 48.87 pound force.
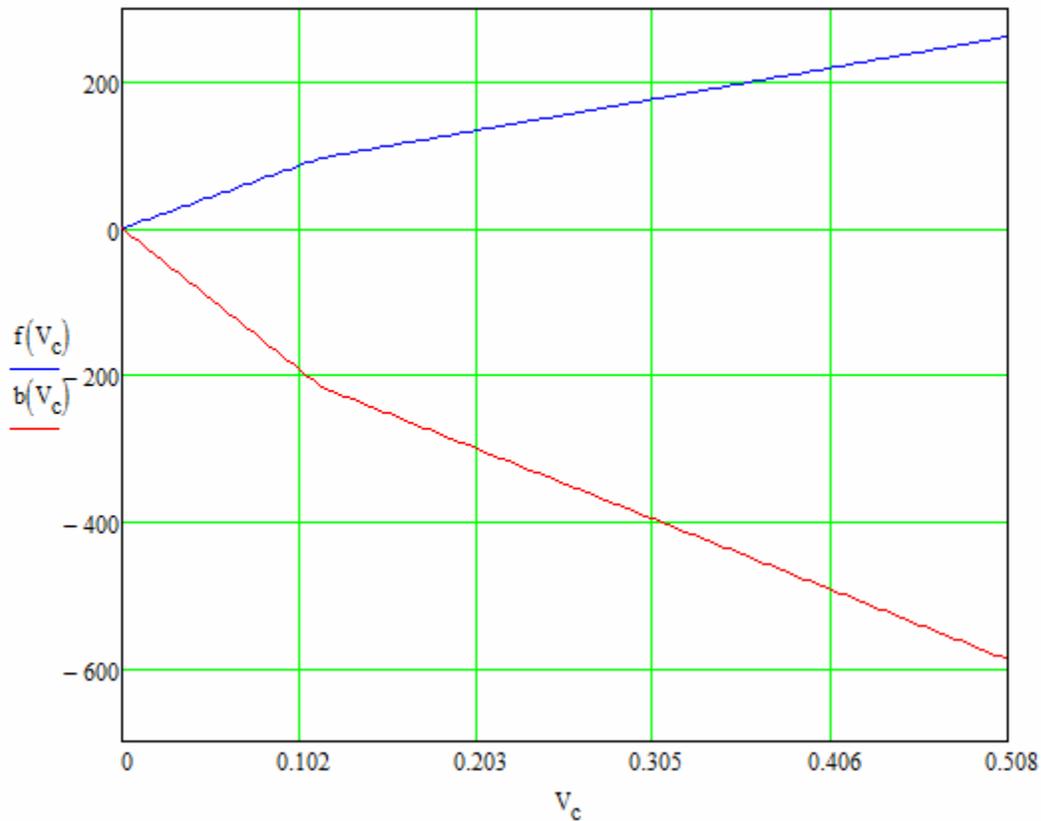
**Figure 26: Front Damper Velocity Curves**[1]

**Table 2: Definition of Variables**

| $V_c$ | Velocity of the shock |
|---|---|
| $f(V_c)$ | Force as a function of velocity in compression |
| $b(V_c)$ | Force as a function of velocity in compression |

The plot above was then compared to the plots given by Cane Creek through the Motorsports Spares website on the 2010 TTX25 dampers. It was determined that the compression curve fell on the very minimum settings for this model, and the rebound curve fell just below the lowest settings. (Meaning that it did not require being at the lowest setting).

The plot was then compared to the 2011 TTX25 MKII damper plots. Both the compression and rebound curves fell roughly in the middle of the adjustable ranges. This meant the TTX25 MKII

---

[1] Note: the units of the x-axis is in meters per second and the units of the y-axis are in newtons

dampers could be adjusted as needed in either direction. The damper curves from Cane Creek can be found in Appendix C.

Although the TTX25 MKII's looked ideal, it needed to be proven that the TTX25 dampers were enough out of the ideal range of use on the physical car to be used on the new design. Essentially, it needed to be proven that the new design would never need to be put on lower settings than the minimum compressive settings offered on the TTX25 dampers. Through testing, it was found that the 9-10-11 car was slightly over damped even at the lowest settings. Theoretical damper curves were created to compare the 9-10-11 car to the new design to help better understand the comparisons between the two damper options. The results from this test confirmed the decision to run the TTX25 MKII dampers for the front suspension. The theoretical damper curves can be found in Appendix B.

Similarly to the front suspension, damper curves were calculated for the rear suspension to determine the ideal dampers to run. These curves, which can be seen below, fit well into both Cane Creek model shock damper curves. From a manufacturing standpoint running the same shocks on both the front and rear was ideal. However, because of budget constraints, it was decided to use the new model shocks in the front, where more adjustability is needed, and the existing model shocks in the rear, where stiffer suspension is needed.

The crossover point in the rear was calculated to be 2.28 inches per second. The force on the shocks at the crossover points are 26.05 pound force in compression and 58.61 pound force in rebound. The calculated rear damper curves can be seen in Figure 27.
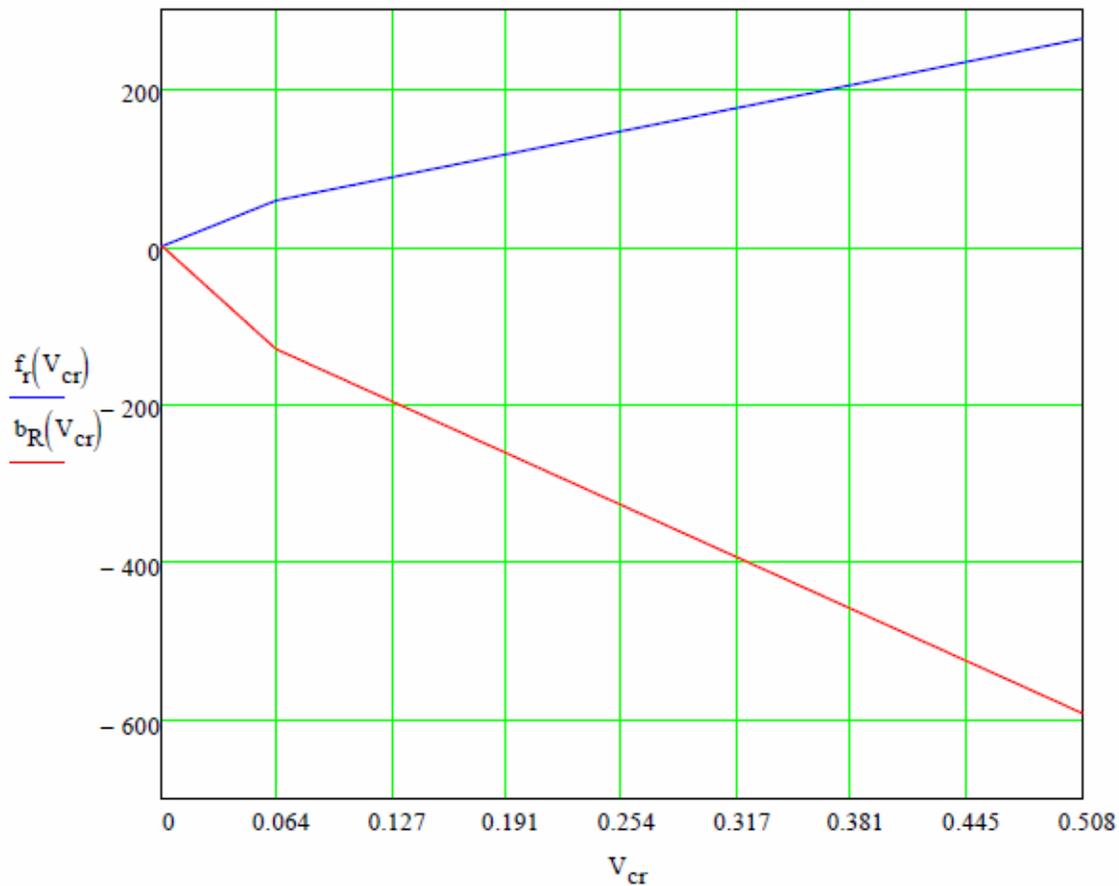
**Figure 27: Rear Damper Velocity Curves**

In conclusion it was determined to utilize the new Cane Creek model shocks in the front suspension, and the previous Cane Creek model shocks in the rear suspension. Ideally, the 2011 TTX25 MKII model shocks would be used in both the front suspension to reduce the number of different types of components. However, due to budgeting constraints, the 2010 TTX25 dampers will be used in the rear.

## 4.6 Other Design Aspects

### 4.6.1 Suspension Bearings

There was discussion with the group as to whether delrin would be an acceptable material for suspension bushings between the control arms and their mounting points. Delrin is the material used on the previous car for bushings, and there was concern that they deflected too much under loading. It was suggest that the bushings could be made fully of oil-impregnated bronze, which is also self-lubricating but is stiffer and heavier. This was investigated by first determining the forces through the bushings. It was concluded that the most force that goes through the bushings occurs during braking. SolidWorks Simulation was used to determine how this loading affects

the deflection of the bushings in lateral loading, as well as longitudinal loading for a bushing made of each material.

| Bushing Deflection Under Braking | | |
|---|---|---|
| Control arm bushing and loading | Bronze (mm) | Delrin (mm) |
| Upper lateral | $1.471 \times 10^{-4}$ | $6.702 \times 10^{-3}$ |
| Upper front longitudinal | $1.399 \times 10^{-3}$ | $5.771 \times 10^{-2}$ |
| Upper rear longitudinal | $8.620 \times 10^{-4}$ | $3.555 \times 10^{-2}$ |
| Lower lateral | $2.459 \times 10^{-4}$ | $1.113 \times 10^{-2}$ |
| Lower front longitudinal | $2.612 \times 10^{-4}$ | $1.097 \times 10^{-2}$ |
| Lower rear longitudinal | $2.459 \times 10^{-4}$ | $1.113 \times 10^{-2}$ |

The deflections of each bushing was reflected in a 2D suspension geometry sketch to see how camber and toe would be affected by such compliance, as these parameters can affect the behavior of the vehicle under hard braking.
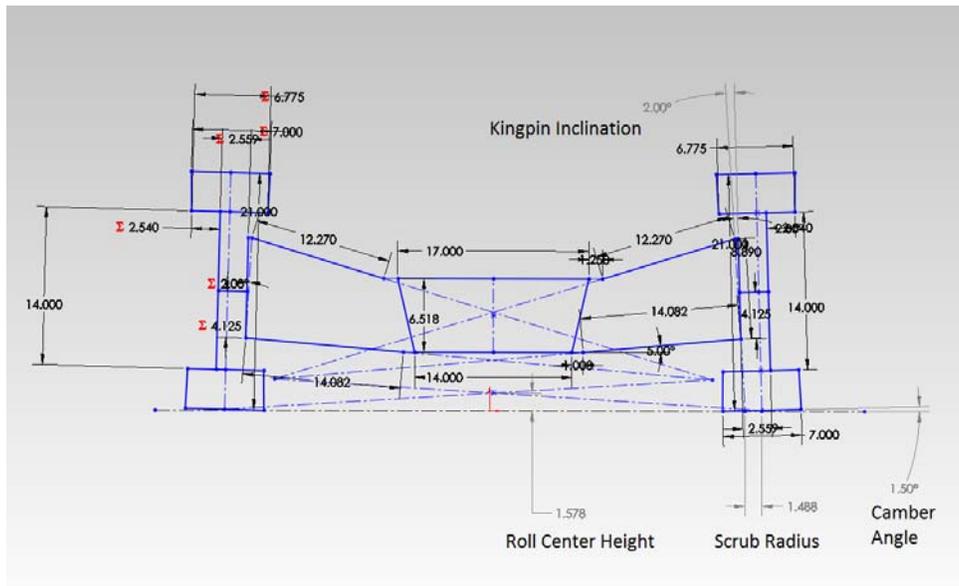


**Figure 28: Front View 2D Sketch of Front Suspension Geometry**
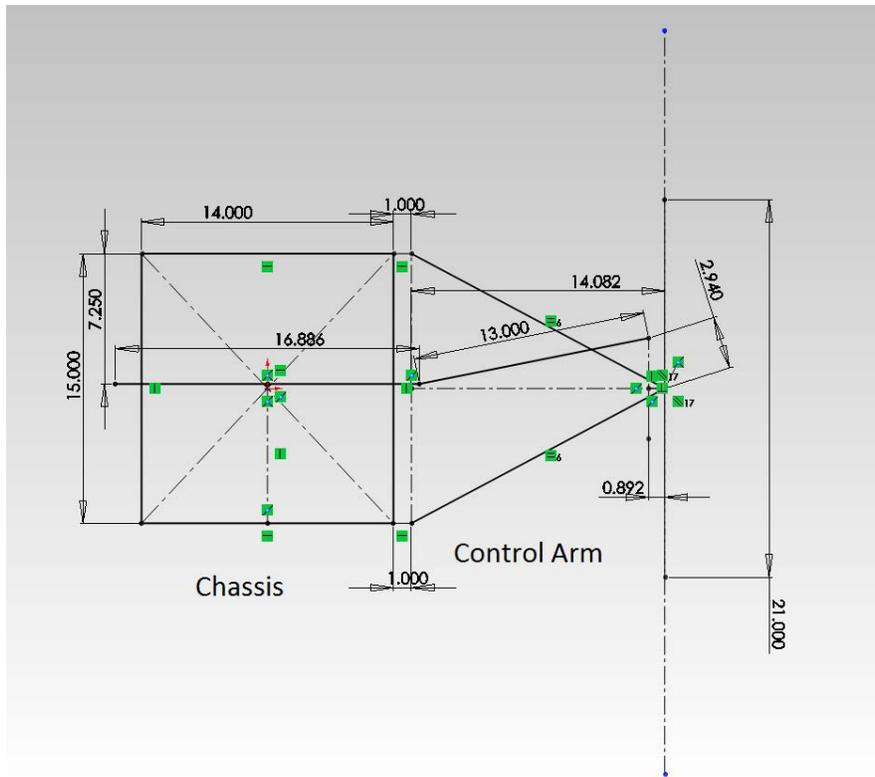
**Figure 29: Top View Steering and Toe Geometry Sketch**

It was determined after applying these changes that there was negligible camber and toe change for either oil-impregnated bronze bushings or delrin suspension bushings under extreme loading. Since the delrin bushings are lighter, it was decided that it would be best to use it as the material for the bushings on the car again.

### 4.6.2 Increasing Serviceability by Aiding in Ease of Reassembly

During repeated disassembly and reassembly of suspension components on the previous car, it was clear that certain assemblies around rod ends and spherical ball were difficult to put back together. This was due to the fact that spacers would not stay aligned during reassembly, making it difficult to push a bolt through. To prevent this issue, there were two ideas suggested. One was using high misalignment ball joints, which have a wide ball width, and have the equivalent of a spacer built into them, reducing number of parts and increasing ease of assembly. Unfortunately, these types of ball joints were not available in the correct size for our application, Modifying certain areas to accept these ball joints would not be possible due to spatial constraints. Another option was to oversize the ball joint bore, and design spacers that sat concentrically aligned at the face of either side, allowing for self-alignment during assembly. This allowed for custom thicknesses, but was not able to be applied at all ball joint and rod end locations. This was because oversizing was not possible in certain location and there is simply not enough space. This concept was applied to where the ball joints in the upper and lower control arms. These areas had enough space for this addition, yet are particularly difficult areas

to service as the upright and control arms make it difficult to reach to align spacers during assembly.
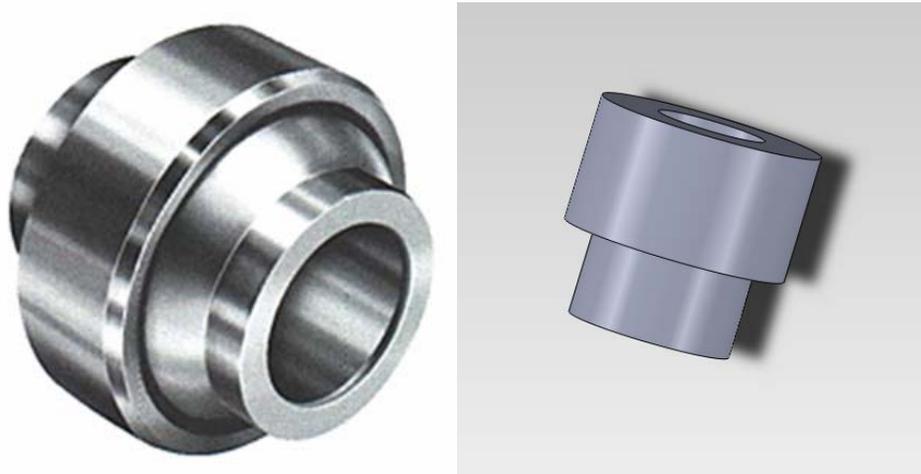


**Figure 30: High Misalignment spherical with Wide Ball (left). Spacer Designed to Fit Into Oversized Spherical (right)**

### 4.6.3 Redesigning Camber Adjustment

Another issue that the team wanted to address was the system for camber adjustment on the previous car. This system utilizes a series of premade inserts that are located in the upper control arm mounts for different camber angles. Unfortunately, this system has finite increments of adjustment, and does not allow fine adjustment. Without fine adjustment, there is no way to compensate for tolerances in manufacture of the chassis as well as the suspension components when setting static camber.
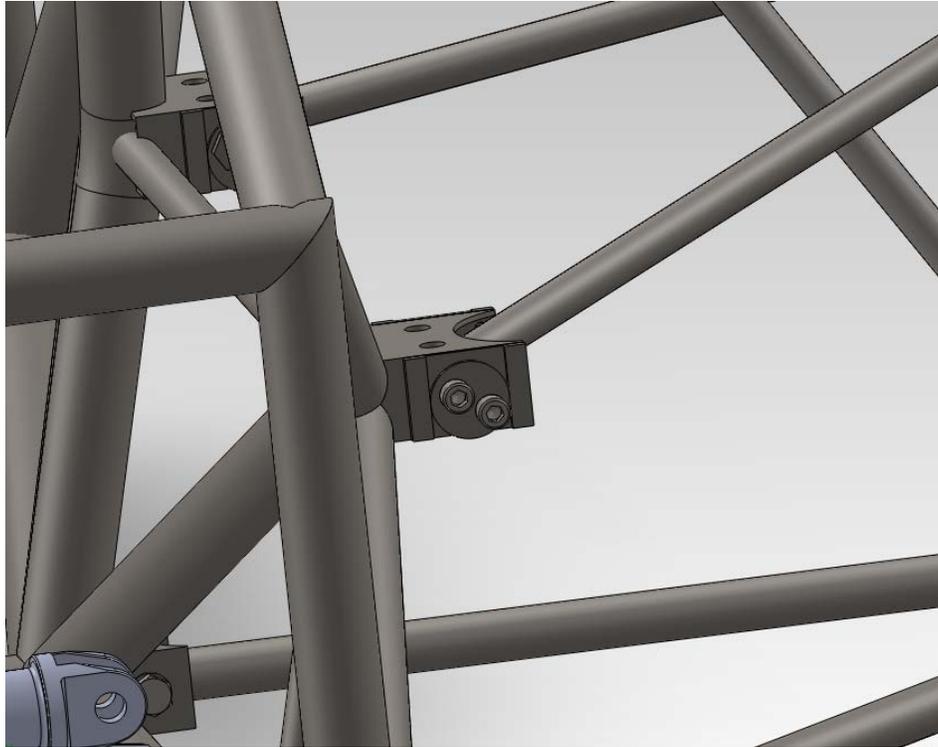
**Figure 31: Camber Adjustment in the Upper Control Arm Mounts**

The new design utilizes eccentric washers with a notched ¼-28 socket head cap screw held in place by notched plates to guide the bolt along a slot cut in the upper control arm mounts.  This allows for fine adjustment, and is tightened when set.  The previous range of adjustment had to be shortened because the chassis was widened at the front suspension pick up points, keeping the front suspension geometry the same. This causes interference between a bolt and one of the side impact members at full negative camber adjustment. However, this range of camber adjustment should never be needed. This can be verified by the even tire wear on the previous car performing at FSAE Michigan 2011, as well as its handling characteristics in steady state cornering, as well as straight line braking. The new design for camber adjustment allows for an infinitely incremental adjustment from -.3$^o$ to -2.7$^o$ of static front camber.

## 4.8 Conclusion

Through testing of the final design, the actual desired spring rates and damping settings will be chosen through driver feedback as well as a data acquisition system designed to measure suspension travel displacements and velocities.  It will also determine whether a linear spring rate is sufficient enough for the application to prevent bottoming out while providing the correct ride compliance and stiffness for mechanical grip and cornering.  This analysis will also reveal the accuracy of the assumptions and estimates used when calculating total load transfer of the vehicle in all directions, particularly laterally due to the difficulties in calculating such with a zero roll rear suspension design.

Recommendations for changes of the front suspension design include finding a new location for mounting the upper connection for the shock. Ideally, it would be best to reduce the length of the shock extension to prevent bending loads on the shock itself, which can be detrimental to the shaft and seals. In addition to a design change for the actuation geometry, it was discovered during fabrication and manufacture of the control arms that the tolerances for the ball joint pockets are very difficult to hold for correct press fit of the sphericals, and the tooling to make them is very difficult to use and expensive. Pegasus Racing offers a ready-made solution (part number 1825-150-0812) that uses the same ball joints specified for the previous suspension design (13/16 OD, .375 ID Spherical) that has a slightly different outer diameter, and different vertical location of the ball joint within the pocket, and overall height. It would be advised to just purchase these premade pockets, and change the design of the control arm to locate the spherical correctly to utilize the previous geometry.



**Figure 32- Pegasus Racing ball joint pocket with respective snap ring**

## Chapter 5: Front Upright and Hub Design and Fabrication

The upright connects the control arms to the hub which connects the upright to the wheels, allowing the vehicle to move. The uprights also connect to the steering arm, allowing the driver to steer the vehicle, and the caliper, allowing the driver to stop the vehicle. The hub is directly connected to the wheel, and is connected to the upright. The upright is to remain stationary relative to the chassis while the hub is to rotate with the wheel. This is done by placing a bearing between the hub and upright. Typically a spindle is pressed into the upright and does not rotate and a bearing is pressed into the hub, and the spindle is pressed into the bearings allowing the hub to rotate about the spindle.

Unsprung mass is the mass of the wheel, hub, rotor, caliper, uprights, spindle, and brake pads. Essentially unsprung mass is the mass that is not supported by the shocks (for example the chassis and everything supported by the chassis is sprung mass). It is important to reduce

unsprung mass in order to increase acceleration. The greater the unsprung mass, the slower the accelerations.

## 5.1 2011 Front Upright and Hub Design

The previous car utilized a hub design that had a rotating aluminum section to locate the brake rotor and wheel, with a steel spindle for its axis of rotation. This steel spindle provided strength of the hub assembly against bending during cornering and bump situations, while the aluminum section worked in resisting torsion during braking. The aluminum hub section has to be a large diameter to accommodate the wheel's lug pattern as well as meet a brake rotor of approximately 7 inches, and also provides a race for the wheel bearing. This makes for a rather large hub that can be designed to withstand bending forces in addition to those in torsion without adding a considerable amount of mass in aluminum. This would allow for the removal of a heavy steel spindle. The steel spindle weighs 0.78 lbs, and when combined with the aluminum (.82 lbs) weighs 1.6 lbs.

Although the previous design has worked well for the car to this point there are many issues with it. While the previous uprights meet all of the essential requirements for an upright they are far from ideal. The uprights use a very standard design and using the ability to roll back the design in Solidworks it was possible to see the modeling process which gives hints about the design process. The upright is a rectangular piece of aluminum with slots cut for the upper and lower ball joints. The center of the upright has a hole in the middle for the spindle to be pressed into. The design however had three issues which became important design points for the future uprights. The first issue which was to be addressed was the lack of a steering pickup. The old upright used a toe tab which is a second part which bolts to the upright. While this reduces the complexity of the upright it adds weight to the design. To attach the toe tab to the upright two bolts are used. This requires two additional holes in the upright to be tapped which increases the time it takes to manufacture the upright and increases the price in the cost report. This also made the toe tab susceptible to separation and excessive movement of the tab in relation to the upright. Because of this it became a design goal to incorporate the steering pickup into the upright.

Another design problem with the original design is the rectangular design which added unnecessary weight. Although the rectangular design makes the upright easier to design and less expensive to manufacture, it adds weight to the part without adding any strength. The old uprights have very wide areas at both the top and bottom where the ball joints connect which is not used for any connections and is unnecessary for strength reasons. One of the design goals for the new upright is to minimize this unnecessary material and simply connect the points using the least material in the most efficient manner possible.

The final major issue with the old upright is the adjustments on it. The upright contains the adjustments for the caster and Ackermann angles. These use the same replaceable tab method of adjustment as the camber for the car. This involves using tabs with varying hole locations to change the pickup locations slightly to make the adjustments. However this has problems when

manufacturing tolerances are looked at. If there are any tolerances in the manufacturing of any of the components it could become impossible to get the same caster or Ackermann on both sides of the car. After much discussion about the old car and research into other FSAE cars it was decided that quick adjustable Ackermann was not required. This simplifies the upright at the steering pickup and does not detract from the usable function of the upright for normal operation. A new method of caster design is one design goal which came from the analysis of the old system.

## 5.2 Goal Statement and Task Specifications for the Uprights and Hubs
To design and fabricate a new design that reduces unsprung mass.

- Reduce unsprung mass

- Must be the sole component in resisting forces in torsion and bending

- Must withstand 310lb-ft of braking force

- Must allow minimal compliance during cornering and bump loading

- Must fixture a full floating rotor with an effective diameter of 7.25 inches

- Must locate the wheel at the proper track width of 42 inches

## 5.3 Design Approach

### 5.3.1 Brake Calculations
Calculations of the parameters involved in braking are fairly straightforward. The excel spreadsheet was designed to solve directly and to allow for a guess and check method. The calculations begin by taking in the mass and static mass distribution front to back of the car. It also requires the center of gravity (CG) height, and wheel base. Then a deceleration rate is chosen (1.5g of deceleration is used in this case as this is the normal limit of grip that the Hoosier R25A tire can provide). The amount of weight transfer is determined from this data, also determining the loading on the front and rear under deceleration. This information also shows the weight distribution under braking, however this is not used in any of the calculations and is just for reference. The calculations then require the tire diameter in order to calculate the torque required from the front and rear brakes. Torque for the front and rear brakes is determined with equation 1.

**Equation 3:**

$$Brake\ Torque = Deceleration\ Loading \times Tire\ Radius \times Deceleration\ Rate$$

Once the torque is determined, more data is required in order to calculate brake line pressure. The necessary data is: caliper piston surface area, effective rotor diameter, and brake pad coefficient of friction. The caliper piston surface area is determined by using the supplied caliper

piston bore from the manufacturer, and the number of calipers per axle. Normally there are two calipers per axle, however our rear brake setup only utilizes one caliper. When calculating surface area for opposed pistons, the surface area is not double, contrary to what one might assume.

The effective rotor diameter is essentially the diameter of the rotor at the point where it is in the middle of the brake pad, this is where the point force from the braking friction force would be applied. Typically, it is the actual rotor diameter minus the height of the brake pad, unless all of the brake pad is not utilized. Finally, the brake pad coefficient of friction is the most difficult to quantify. No brake pad manufacturer publicizes their coefficients of friction, however a range of standard values are common. The coefficients of friction of brake pads usually fall in the 0.30 to 0.50 range, and will be lower when the pads are colder. In this calculation we assume the pads are cold, but are a quality racing pad, so a value of 0.35 is utilized. The cold coefficient is used in order to make the calculations a worst case analysis. Now that all of the variables for brake line pressure have been defined, brake line pressure is determined with equation 2.

**Equation 4:**

$$Brake\ Line\ Pressure = \frac{Brake\ Torque}{2\ x\ Caliper\ Surface\ Area\ x\ Rotor\ Radius\ x\ Brake\ Pad\ \mu}$$

The final part of the calculations involves determining the required master cylinder size to achieve the requested braking performance from the rest of the braking components. The first parameter for calculating this is the force being exerted by the driver onto the master cylinder rod. To determine this value, the pedal ratio and driver's foot force is required. The pedal ratio of our brake pedal assembly is 6:1, and it is assumed that the driver will be able to apply 80 pounds of force to the brake pedal. This makes the pedal force at the balance bar of the linkage 480 pounds. The pedal force is then multiplied by the setting of the brake bias bar, initially this is set at an even 50/50 split front to rear. Now that the necessary values are determined, master cylinder size can be calculated using equation 3.

**Equation 5:**

$$Master\ Cylinder\ Size = 2\ x\ \sqrt{\frac{Master\ Cylinder\ Force\ x\ \pi}{Brake\ Line\ Pressure}}$$

Brake master cylinders are only commercially available in a limited set of sizes; typically in 1/8" increments starting at 5/8" up to over 2". The initial calculations referenced a 14 inch (from the ground) center of gravity. This resulted in the master cylinder volumes of approximately ½" and 1 1/8". However, ½" master cylinders are not commercially available. The brake bias bar was then adjusted until common sizes for master cylinders were found. This ended up being biased 78/22 towards the front. The sizes for the 78/22 bias resulted in 5/8" and ¾" master cylinders.

The highest acceptable brake bias is around theoretical 80/20 distribution; anything beyond that begins to compromise the ability to adjust the brakes once they are on the physical vehicle. To provide a sanity check, the chosen master cylinder sizes the brake forces calculations (Eq. 2 and Eq. 3) were run backwards with the chosen master cylinders and leaving the Brake line pressure unknown.

Multiple center of gravity heights were also considered throughout the calculations. Any center of gravity that falls between 4 inches and 15 inches high will be acceptable in the terms of utilizing the chosen brake components. Such a large range should not be needed, but ensures the difference between theoretical CG and the physical CG to not affect the braking components. It is likely the physical CG height will fall between 12 and 15 inches for the new car. The previous car's CG height was determined empirically to be 15.6 inches. This goes to explain the poor braking performance the car had; the calculations to size its braking components assumed 12 inches CG. The assumed CG being so far from the physical CG can also explain why the car had issues with the tilt test at the FSAE Michigan 2011 competition.

### 5.3.2 Results
The final braking setup consists of several improvements over the existing car. First, the front rotors have been increased in size to 7.75" (effective) diameter in order to make more braking torque. This should make the front wheels able to lock up easier, helping brake control and being able to pass the Formula SAE braking test. The front calipers have been changed to Brembo P32 calipers instead of Wilwood Dynalite single piston floating calipers.  The P32's are significantly lighter and are less expensive. The P32's are also smaller, which is also allowing the front rotor size to increase as much as it has. This should also help with packaging the upright and hub assembly in the front wheels. The rear braking setup will remain the same. The design utilizes a 5/8" and a ¾" bore master cylinder, both of which had been purchased previously for the 9-10-11 car. The setup will also include 2psi bleed back valves on each master cylinder to prevent pad kickback from brake fluid draining out of the calipers. There will be 10 inch long braided stainless flexible brake lines to connect the hard lines to the brake calipers at all three calipers. The brake lines between the master cylinders and the flex lines will consist of 3/16" hand bent steel hardline with double flare ends; approximately 10 feet will be required.

### 5.3.3 Hub and Upright Design
In order to reduce the unsprung mass it was decided that instead of using an aluminum hub and steel spindle, the hub would have an extension that would be the effective spindle. The 2012 car will also use a floating rotor which is held on to the hub by buttons which allow the rotor to "float" on the hub.

To accommodate the new hub design with no spindle a brand new upright was required. This design would use a large double angular contact bearing as the center of the upright in which the hub would be put into. Although the bearing will be a large mass in the upright it also replaces the large spindle that would normally be in the upright. This works towards the overall goal of decreasing the unsprung mass.

*Initial Design*

The hub's main duty is to prevent excessive deflections, particularly in bending. In torsion, which is mainly experienced during braking, excessive deflections can cause excessive fatigue in the hub as well as other components. Deflection during bending can affect overall camber angle during bump and cornering, and can affect toe during braking and cornering. Small toe changes can negatively affect the car's handling, as this will effectively steer the car if the displacement is high enough. Small changes in camber do not necessarily cause immediate change in car behavior, but will change the tire's contact with the road, which can affect overall cornering ability and also cause poor fatigue situations for the hub itself.

The hub must connect the inner face of the wheel, the rotor and the upright. As mentioned before the hub and upright are typically connected by a steel spindle. This design includes the hub and an effective spindle in once piece.

The design of the hub was bounded by various conditions such as track width, wheel bearing size, caliper dimensions, and the bolt pattern on the wheel. The track width of the 2012 car is to be 44 inches in the front, the suspension and the chassis make up for most of that distance, however, the uprights and hubs make up for the remaining distance. Since it was decided that the hub and spindle would be one component the effective spindle dimensions was driven by the selected bearing. The distance between where the caliper bolts onto the upright and the center of the brake pads drove the placement of the rotor support. Finally the bolt pattern on the wheels was 4 bolts on a 4 inch circle.

Since the upright design was also bounded by many of the stated conditions the two components were designed simultaneously. Some of the hub dimensions could not be finalized until the upright's dimensions were finalized.

The initial design determined the rough geometry of the hub to address the task specifications. The front face of the hub matches the bolt pattern of the wheel. Roughly halfway between the front face and the beginning of the effective spindle is the rotor support which allows the rotor to float on the hub with titanium buttons. The geometry of the design with the rotor and buttons can be seen in the figure below.
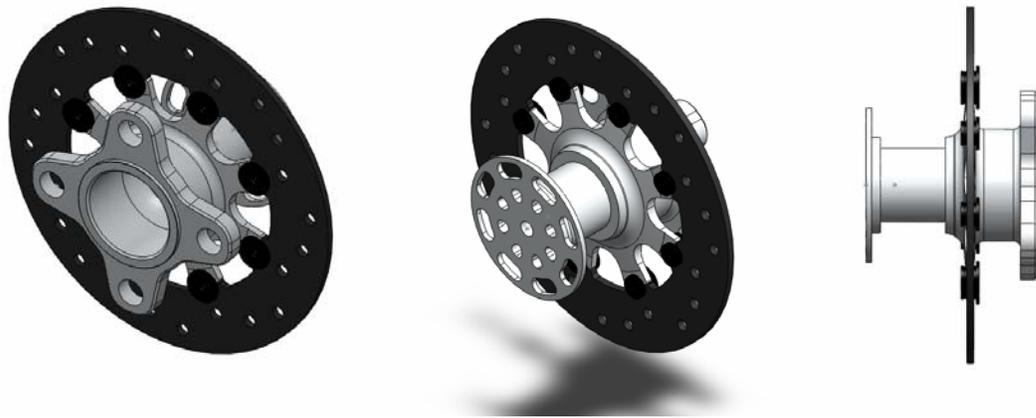
**Figure 33: Hub Design Geometry**

As seen in the side view of the assembly the portion of the hub on the right is the effective spindle. The portion directly to the left of the effective spindle will rest against the bearing. The grove to the left of the portion that is to rest against the bearing was inserted to reduce stress concentrations. A cap on the end is designed to hold the hub to the upright assembly.

The combination of a hub and effective spindle causes large stress concentrations which can lead to premature failure of the component. In cases like these there is no way to avoid stress concentrations; however there are many options to reduce stress. The hub is essentially a stepped shaft that decreases in size at the point in which it is pressed into the bearing. The most obvious method to reduce the stress concentrations at the step is to design a corner with a radius, however the hub needs to have a flat face to locate the bearing axially and radially on the spindle of the hub.

To reduce the stress concentration material was removed directly behind the step to improve the force streamlines. This method also eliminates the need for a washer which reduces the number of extra hardware needed.

The upright is responsible for locating the suspension and steering in relation to the wheel and tire. In addition to this the upright also carries the brake calipers and must be able to withstand all of the braking forces. These functional requirements provided the initial constraints for the upright design. To maintain the suspension geometry the location of the upper and lower ball joints must remain in their set locations. The steering pickup point must also remain in the same location for the steering geometry to remain as designed. With these restraints in place, an initial design was created by simply placing all of the required points and experimenting with packaging inside of Solidworks. The first design was very different from the design which ended up becoming final. Initially to reduce stresses and optimize load paths an innovative inboard brake design was created. This design used an upright with heavily curved upper and lower

mounts to minimize the hub length and eliminate the common right angle loading which uprights normally see. This design would have been an optimal design however it was determined that the team had neither the time nor resources to design or manufacture such an upright. The manufacture cost alone would be more than double that of a normal upright due to either the immense amount of machining or casting involved. While this design would have been optimal it was required to move on and design a more conventional upright.

The design of the upright was a simple task once all of the data involved was collected. By using a sketch with all of the important points a bearing cup for the bearing to be press fit into was designed and used as the center for the upright. As all of the forces are centered on the bearing this was the most important part of the upright to keep strong. Next the pickup locations for the upper and lower ball joints were placed and the bearing cup connected. Each of the connections was designed to contact tangentially for ideal load paths. From these points a basic structure was formed which makes up the backbone of the upright. Once the basic support was established, additional features were added. These include the second side of each ball joint pickup and the steering pickup. Next the brake tabs were modeled using the same tangential design method as previous features. A sketch was used to find an ideal placement for the brake caliper. With all of the important points located and structures put in place the model was cleaned up by adding fillets to reduce stress concentrations and allow the part to be machined.

In order to ensure that design for manufacturability of both the hub and upright is maximized the manufacturing lead was involved during the entire design process. This is slowly becoming the norm in industry, and was thus incorporated into the project. In this project both the hub and upright will be machined, as it is the limitation of the available resources. Machining may not be the best process to utilize, especially for the upright design where casting can often lead to not only a more manufacture-able product, but also a better one.

The design of a typical FSAE upright typically involves a lot of chip removal as well as small intricate features with very small radii. While the large amount of chips produced is nearly impossible to negate without utilizing a casting process, one is able to make it significantly easier to quickly remove material in the design. This can be accomplished by maximizing the open area of the upright and reducing the small pockets from which a small tool would be needed to remove the material.

Small pockets are but one of the types of small features which should be minimized. The second most prevalent in FSAE upright design is the small webbing. This typically shows up as minimally supported slender beams inside of larger pockets. Not only does this effectively create many small pockets the webbing is also typically weak in bending. During machining, high machining forces can cause damage to this webbing which will cause excess part scrapping during a production run.

Small radii will also increase machining time. In this case if the product is designed with large pockets and without intricate webbing one will be able to utilize a very large tool and high removal rate to remove the majority of the material. However, one would still have to switch to a much smaller tool to finish machine all of the radii, in order to actually create such a small radii. If the radii are even smaller, it would require a tool which lacks sufficient cutting length and would require machining the feature from both sides. In the worst case it would require expensive special tooling in order to achieve the depth of cut. Not only would these tools be weaker than the standard length tooling but they would deflect more, resulting in a loss of surface finish and tolerance.

The hub faces similar design for manufacturability constraints. In this case, the majority of the hub features were to be turned, which requires extra thought be put into the tool clearances. Typically tooling clearances form milling becomes second nature to designers; however turning provides different limitations with the vastly different tooling geometries. In this case the hub only needed one undercut lessened in order to be significantly more manufacturable. This undercut was created by the stress relieving integrated washer. All which was required was its height reduced as such a deep undercut would require the use of the cut off tool in a pecking operation. This is a time consuming operation and would result in a poor surface finish. The poor surface finish would result in more stress concentration than the feature prevents.

From a manufacturing stand point the material choice was clear, 6061-T6 aluminum. While some believe that all FSAE uprights and hubs should be made from 7075 aluminum, without exception, 6061-T6 has is merits. First and foremost, it is significantly cheaper per unit, for just the material alone. Secondly, as a softer material it yields long tool life and increased material removal speed. On these merits alone 6061-T6 saves over $100 per part.

### *Final Design*
The final design depended on the dimension of the bearing and calipers that would be used. The bearing that was chosen was the INV-WB643437 Upright wheel bearing from Taylor Race Engineering. This bearing has an outer diameter of 75 mm, and inner diameter of 42 mm, and a width of 37mm. The calipers that were chosen were the Brembo 20695011_21-P32G calipers. The distance between the center of the brake pads and mounting face of the caliper is 16mm.

The figure below shows which dimensions are dependent on the upright, caliper and bearing. The distance from the front face of the hub to the center of the rotor support (A) is driven the caliper. Distance A must exceed the distance from the center of the brake pads (or rotor) and the front face of the caliper (35 mm). The distance between the center of the rotor support and the face of the hub that rests against the bearing is controlled by the distance from the caliper bolts relative to the face of the bearing, and center of the brake pads (dimension B). Dimension C is purely driven by the width of the bearing used. The total distance from the front face to the face that rests against the bearing (A+B) must also take into consideration the desired track width of the car.
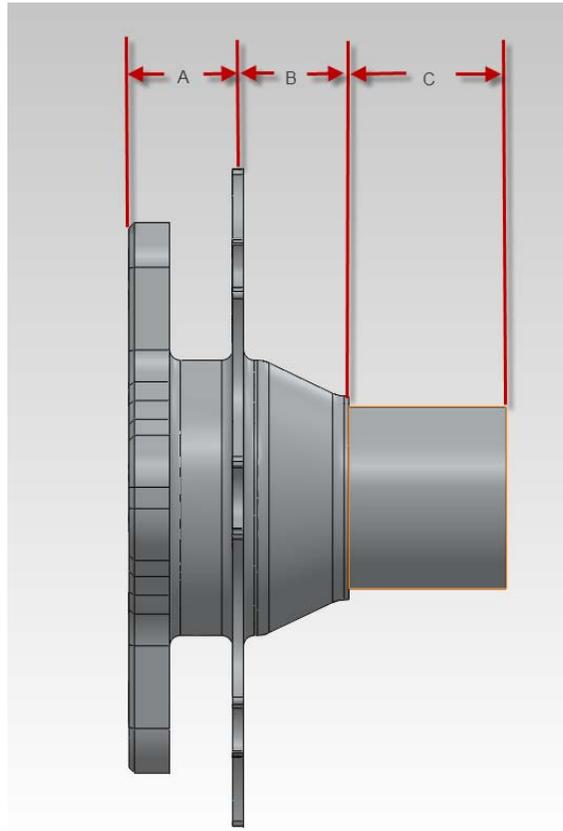
**Figure 34: Hub Driven Dimensions**

In addition the effective washer was removed to increase manufacturability. Additionally, the face of the hub that rests against the bearing must not exceed the thickness of the bearing thrust face, which does not leave enough material for an effective washer. Since the bearing is pressed onto the hub, stress concentrations are reduced by eliminating the ability of bending at the step.

The final upright design also uses the same method of adjustment as the camber adjustments on the rest of the front suspension. By using the eccentric bolts the caster can be changed in an analogue fashion without the stepped design of the previous upright. The steering pickup however has been designed without any adjustment available. This greatly reduces the complexity of the upright and allows the Ackermann angle to be adjusted by other means. This is how many other teams adjust their Ackermann and is an accepted practice in FSAE.
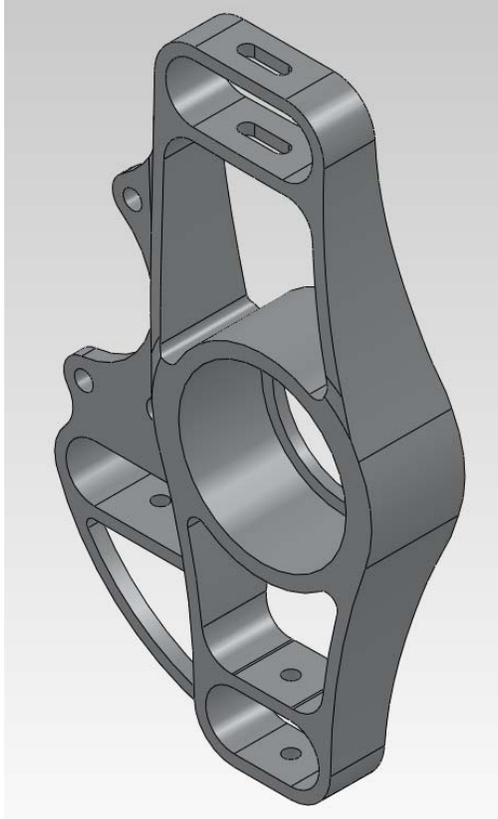
**Figure 35: Final Upright Design**

## 5.4 Design Analysis

Although many of the design modifications came from finalized dimensions, finite element analysis created a few concerns on the design. The major concern was with the rotor support. With the existing geometry it was likely to see stresses that would break the spokes attaching the rotor to the hub. Several modifications including using circular holes instead of triangles or trapezoids and tapering the support so that the base was thicker were made to achieve a minimum safety factor of 7.51 in braking.
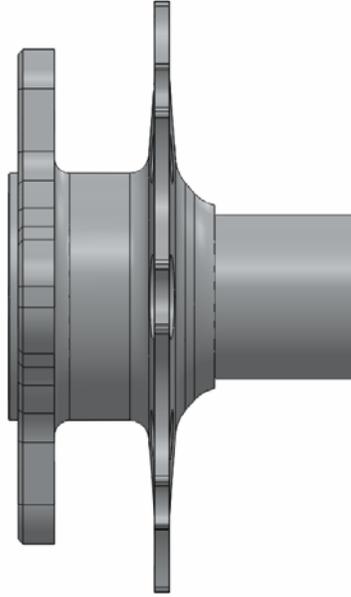
**Figure 36: Hub Final Design, Side View**

For the FEA studies, two scenarios were done to calculate the highest loading the hub would see, which were under hard braking. The input forces were 2g loading at the front wheels (maximum grip the tires can provide) which include a 310 ft-lbf torque applied along the axis of the hub, as well as a 350 lbf bending load applied upward on the outside wheel due to dive. Higher forces are expected from high jounce from bumps, however calculation of such forces are very difficult to approximate, and are considered outside of the expected use. They are accounted for using a high safety factor. These forces could be approximated better if during testing, an accelerometer output was logged from the suspension using data acquisition methods. The results from the FEA are shown in the figures below.

**Figure 37: Von Mises Stress under Braking**
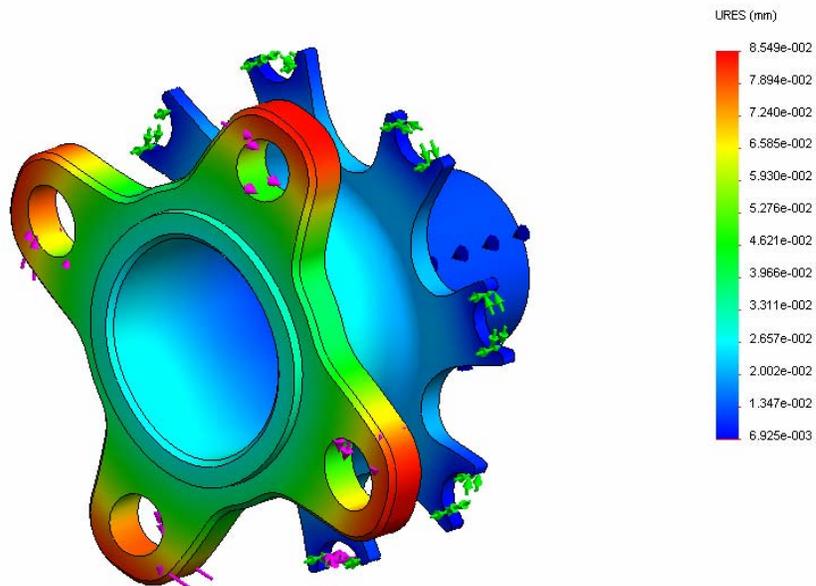


**Figure 38: Hub Displacement under Braking (Deformation Scale 217.631)**
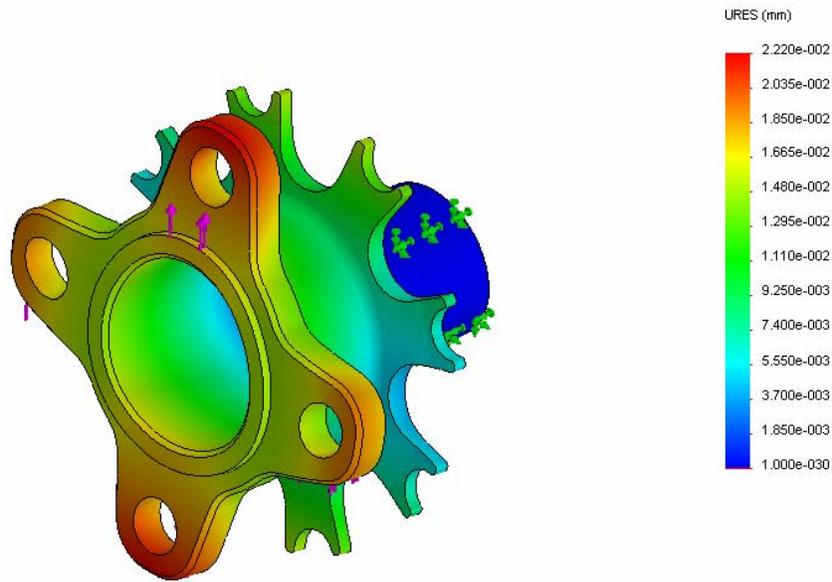
**Figure 39: HubVon Mises Stress**

The bump FEA simulates a 2g bump situation of the ground acting upon the wheel in and upwards direction. The deflections were the most important aspect to consider during this loading situation, and they result in a change of .021 degrees, which is a minimal change in cambe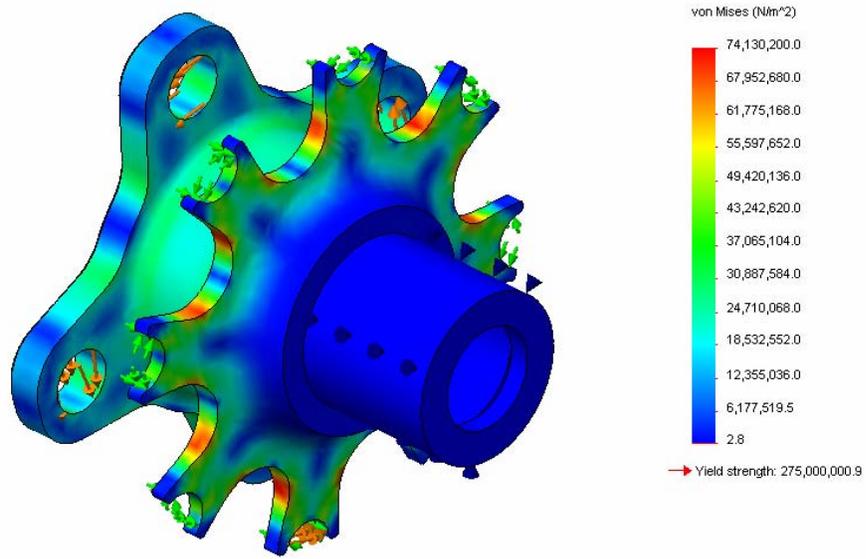r and in toe. This would not negatively affect the behavior of the vehicle in any significant way. The minimum factor of safety recorded during this scenario is 13.4.

The upright design also benefited greatly from the use of FEA to find and change locations where stresses were either too high or low enough that material could be taken away. After the initial design was complete a series of simulations were performed for final design changes. The lower support between the steering pickup and lower ball joint was added to reduce deflection on the steering tab during braking and was found to be a very light weight solution to high deflections. Additionally the large pockets were found to be acceptable and no webbing is required for those areas. This will allow the upright to be machined much more quickly and reduces the weight even further. The last change caused by FEA is the small pocket in the brake tab structure. The stresses in this area were minimal and the material removed was unnecessary.

**Figure 40: Upright Stress under 2g Braking**



**Figure 41: Upright Displacement under 2g Braking**

**Figure 42: Upright Stress under 2g Cornering**



**Figure 43: Upright Deflection under 2g Cornering**

## 5.5 Fabrication

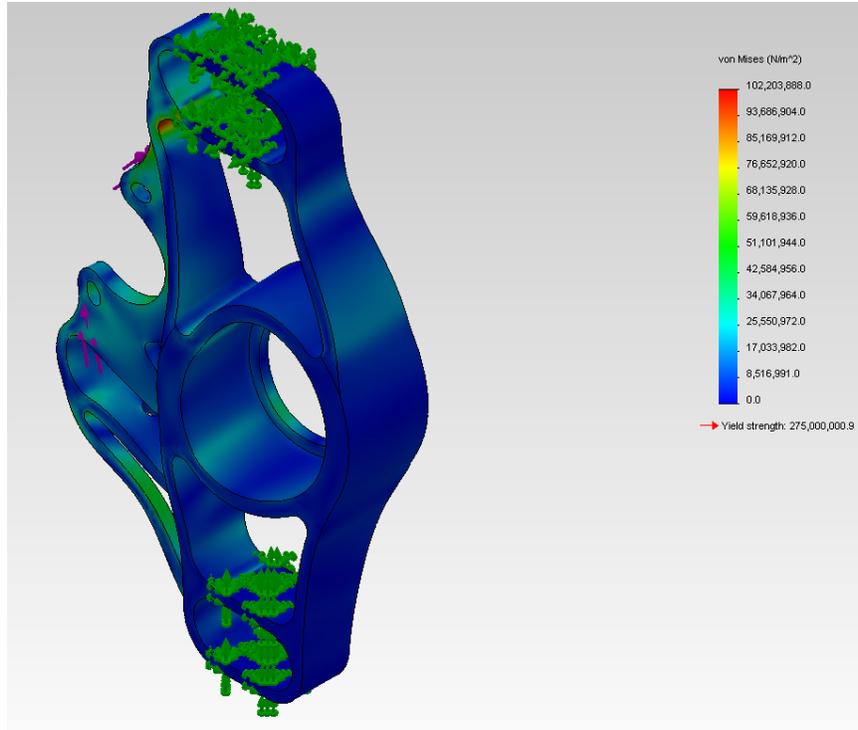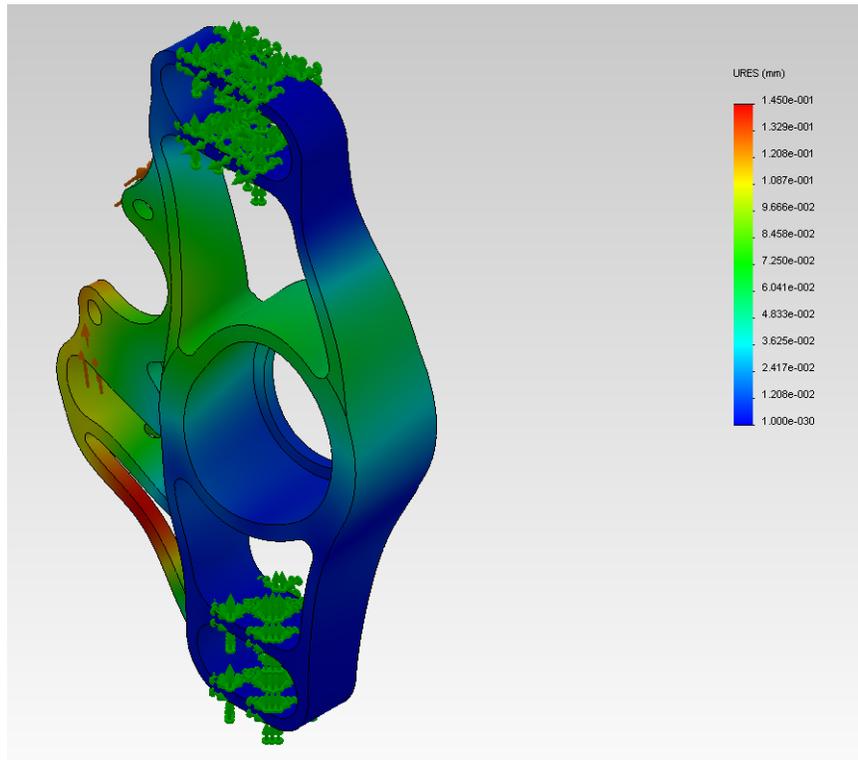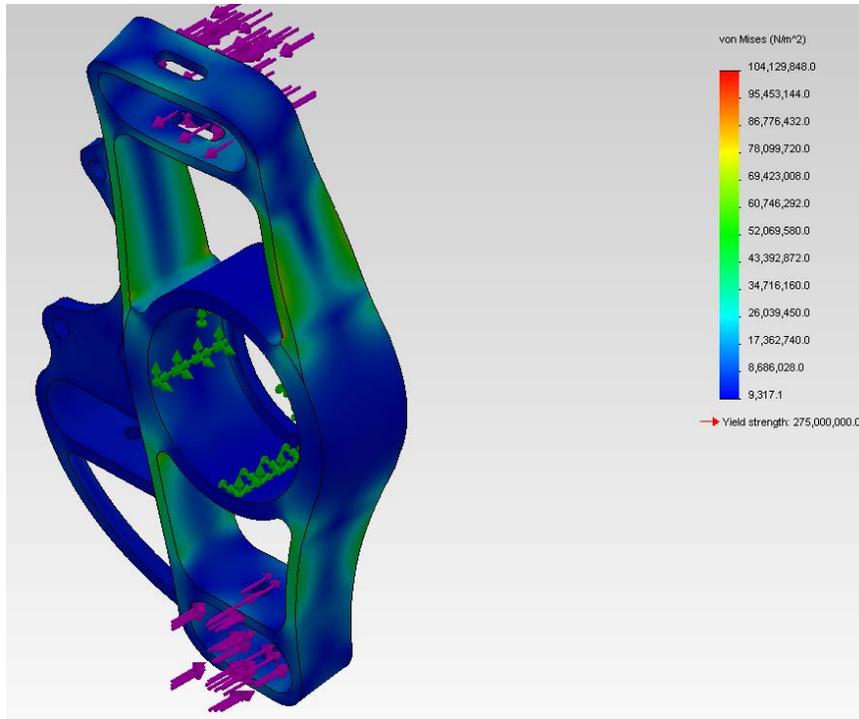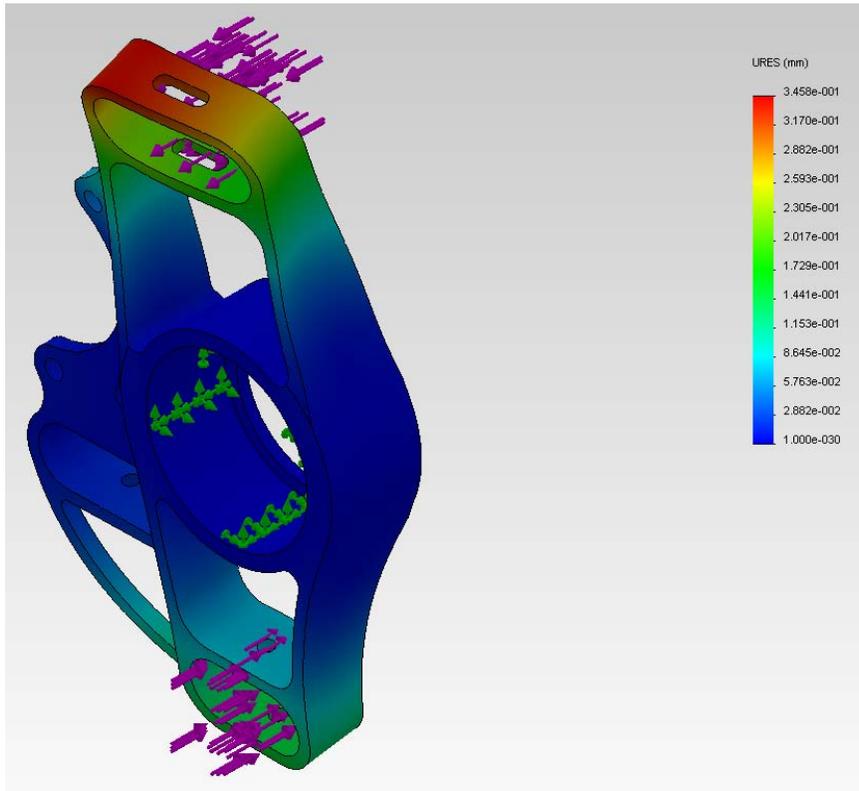As mentioned before, the design and manufacturing team worked very closely on the design of the upright. This allowed for the upright to be machined with only 5 re-fixturings in the machine and no exotic fixture methods. In the one off environment often found in this FSAE environment the ability to fixture a workpiece with solely a vice is very important. In a more production orientated environment it would make sense to create some other fixture method to cut multiple parts in one cycle from one piece of stock.

The improvement of the manufacturing processor of the upright is still in the rapid evolution stage, and can still be improved upon. The initial upright required 3 days of machine time and 8 hours of spindle on time, by the time the third upright was manufactured it required 17 hours of machine time and 4 hours of spindle on time. There are still more gains to be had in both respects.

In respect to total cycle time, the process is theoretically very optimized. It has been reduced to the minimal number of fixturings required for the part to be made with a 3 axis cnc machine. This theoretical cycle time is also known as the optimal cycle time and is calculated based on stead state conditions. Steady state is achieved by an average trained employee who has sufficiently learned the specific process for the part. In order to reduce this time further it would require very specific fixturings for each process, which would eliminate the need to probe the workpiece on each fixturing. For the actual cycle time found through the making of the previous uprights, more repetition would lower the cycle time.

Spindle on time is a component of cycle time which is often most looked at in industry. As the name describes it is the amount of time machine is actually running. The largest gains in spindle on time come from optimizing tool paths as well as increasing feed rates. However, if the tooling is pushed too hard this can increase the cycle time as it can lead to increased tool wear rate and tool replacement rate. In order to reduce spindle on time for the uprights multiple different approaches were taken. First, the tool path for much of the material removal was changed from a typical concentric path to a trochoidal path.

The trochoidal tool path keeps the tool engaged to the part for a much higher percentage of time compared to a concentric path, which requires many more rapid (non-cutting) moves. The trochoidal path also favors small amounts of percent engagement of the tool, which allows for the entire flute length of the tool to be engaged as well as the use of radial chip thinning theory. Radial chip thinning occurs when less than 50% of the tool is engaged with the part, with less engagement the there is a smaller chip load on the tool and less chip to be evacuated through the flute of the tool. Tooling is designed and tested to handle a certain chip load, rather than certain feeds and speeds. As most feeds and speeds from the manufacturer are quoted at 50% engagement, calculating the radial chip thinning allows for a great increase in feed rate to create the same chip load on the tool.

The third and fastest to produce upright utilized this technique extensively. However depth of cut and feed rates were still conservative as it was the last piece of stock. If there were to be a fourth upright machined the depth of cut and feed rate could have been pushed closer to the limit, though this was not a risk to be taken with the last remaining piece of stock. However another hour of spindle on time can be removed from the manufacturing time just from moving to the more aggressive machining parameters.

Tooling will also impact the production time. In the size tooling required for the upright WPI only stocks general purpose/finish tooling. These tools are fine for most usages and for achieving the surface finishes required of this part. However, roughing tooling can be run at might higher material removal rates than this tooling and would be more capable of faster roughing the workpiece without increased tool wear that would be experience with the current tooling. This would further serve to decrease the spindle on time of the process, with a slight addition of time spent changing tooling, as the finish tooling would still be required for finish machining.

The hub manufacturing, like the upright manufacturing was quite complicated. In order to manufacture the hubs the use of both a lathe and 3 axis milling machine is required. The lathe requires jaws bored to the stock diameter and the milling requires brass soft jaws bored to bearing surface diameter as well as a 4x100 fixture plate. There are also 2 additional pieces to the hub which require machining.

The main piece of the hub requires two different fixturings in the lathe. The first fixturings is used to face the end flat and clean the clamping surface for the next operation. Also the center bore drilled and bored with a boring bar. The boring bar portion of this operation is very difficult, such a long and slender boring bar experiences many issues with chatter and very specific feeds and speeds much be found though experimentation which result in both chatter free machining and proper chip breaking. Once the bore has been completed the work piece can be flipped and then outside diameter turning is required.

The OD turning operation roughs first with a trigon tool. The trigon tool is select because it is capable of taking very high chip loads with minimal deflection and also achieving very good surface finish. The bearing surface is finish machined first. This order of operation was chosen in order to minimize the amount of work piece flex during machining. If the bearing surface had been machined last, it is likely that the surface would be tapered and larger than intended. The surface still does have an immeasurable taper to it even with this operation; however it is impossible to avoid all taper even with the use of a steady rest. Also due to the tight tolerancing and the one off nature of these parts, the bearing surface with machined until the fit was perfect in one thousandth of an inch increments.

Once the bearing surface is complete the deep grooving tool is utilized in order to make the groove between the wheel flange and the brake rotor flange. A pecking operation is used to make this groove with an every other path. The every other path creates the same boundary conditions

on the tool, either material or air, on either side of the insert. This minimizes the amount of deflection of the deep groove tool, which is very important with such a long grooving tool. Finally the part is cut off from the stock in the chuck. Optimally this operation would fully cut off the part, however the Washburn Shops does not stock a sufficiency long cut off too and a hack saw was required to complete the cut off. There are two inches of waste material, in a production operation, depending on the throughput it may be beneficial to use a machine with a large enough bar feeder.

Once the turning operations have been completed on the hub, it is moved to the 3 axis milling center to have the wheel flange machined. In order to fixture the hub the 3 jaw chuck is used with bored jaws to clamp on the bearing surface. The soft jaws were made out of brass in order to reduce the likely hood of marring the bearing surface of the hub, and to allow a small deformation in the surface of the soft jaws to provide better clamping force. The wheel flange allows fox fixturings the hub in order to machine the brake flange to receive the buttons and rotor. A locating fixture plate is used for this. Special care needed to be taken to ensure that the machine would not collide with the large amount of hub above the cutting plane. Also conservative cutting forces were used in order to minimize the likelihood of deforming the brake flange.

The hub retaining plate, the other major component to the hub, was milled in two milling fixture using a three jaw chuck. However this part would be a great part to make on a lathe with live tooling as it is a round part with all of the features radially patterned. The amount of time to setup the machine for this operation did not justify if for a one off part. However with the use of a 2 inch bar feeder on the lathe the throughput of the operation could be very high. The final part is an internal plug in the hub which allowed for the center of the hub to be bored with tools available in the shop. A production version would have this piece of material integral to the main part of the hub.

The design for assembly of the hub and upright assembly became very apparent during assembly.  The hub into the upright was kept as an inline assembly, with the only difficulty being the extra part inside the hub bore. A specialized fixture tool was created to facilitate proper torque of the hub bolt which can be seen below in figure 45. Fixtures such as this would be utilized in all part of assembly of the car in accordance with lean manufacturing techniques. As well as well organized and specialized work areas.

**Figure 44: Hub Assembly Fixture**

## 5.6 Conclusion

The hub and upright design is unconventional with its lack of spindle. The major benefit to this design is the reduction of unsprung weight by using FEA to find areas of low stress and removing material without greatly impeding manufacturability, and by reducing the overall part count. Switching to the fixed caliper and floating rotor configuration also reduces overall compliance in the system, as the older brake setup cantilevered the caliper upon sliders that easily bind during operation.

## Chapter 6: Intake System

Since a CVT transmission is being used instead of a traditional gear-shift transmission, the intake runners can be optimized in conjunction with the peak power the engine will see. This is due to CVT lock-up, an event that holds the engine at a specific RPM and still allows for acceleration through infinitely variable gearing in the secondary clutch of the CVT. 7500RPM was chosen to be the desired peak engine RPM since it coincides with the peak power output of the Genesis 80fi engine without the engine choking flow through the 20mm restrictor. This will be made available through tuning the CVT, as the previous design allows the engine to operate over 9500RPM, missing the peak power output of the engine.

To reduce peak power output, Formula SAE rules mandate a 20mm restrictor to be placed on the intake manifold of any engine running gasoline. Because of this, the designs of the intake and exhaust systems are especially important to be tuned to allow for the maximum available power output. The following sections are dedicated to discussing the theoretical calculations used to provide a basis for designing these systems

### 6.1 2011 Intake System

The main issue found with the existing design of the intake system was the sizing of the intake runners. Previously, the diameter of the runners was determined to match the diameter of the stock runners of the Yamaha Phazer snowmobile. Formula SAE rules mandate a 20mm restrictor be placed on any engine running gasoline. This restrictor creates drastic changes to the flow rate into each cylinder, meaning the runner dimensions need to be adjusted from stock to accommodate the Formula SAE application.

The existing plenum was chosen to be adjustable to fine tune the volume of air it would store. However, due to poorly executed manufacturing, the adjustability was sacrificed to be able to properly seal the system, and was never adjusted from the minimum volume. The previous design relied on adjustment alone in determining the proper volume, as there are no specified calculations for an exact plenum displacement that could be investigated and used for the Genesis 80fi.

The existing intake restrictor, runners, and plenum were manufactured using a Rapid Prototyping machine. This machine allows for simple inputs prior to manufacturing, and eliminates the time consuming process caused by traditional CNC machining. However, this method of manufacturing does not have the tight tolerances as traditional CNC machining offers. This, combined with the porosity of the material, leads to poor sealing at joints and poor dimensioning for critical components. The intake restrictor from the existing design was measured to be less than 19mm after manufacturing. Simply boring out the intake to 20mm after manufacturing would not be possible because the ABS plastic was found to be too porous to safely manipulate.

The fuel injector manifold connects the intake runners to the intake ports on the cylinder head of the engine. The manifold that was used on the existing car was machined from aluminum and accommodates OEM Yamaha Phazer fuel rails and fuel injectors. Since there have been no known fuel delivery issues due to this manifold, it will be reused and taken into account for the new design.
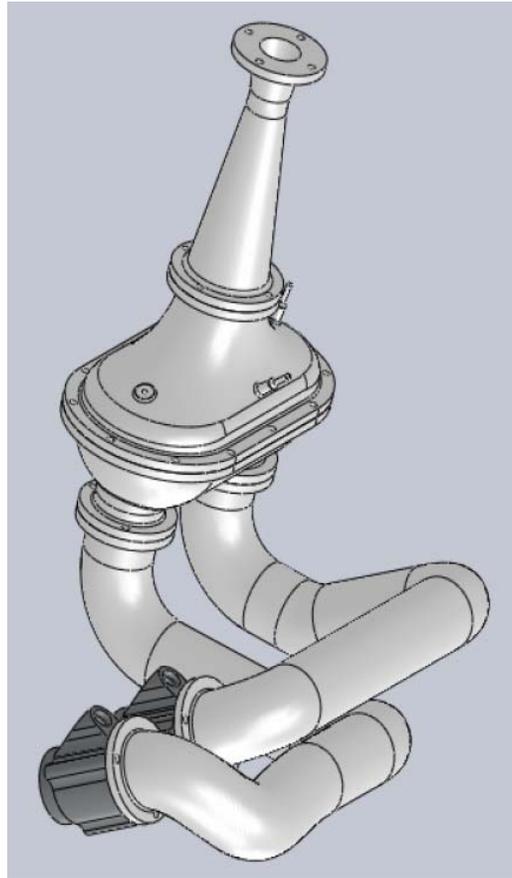


**Figure 45: Existing Intake Manifold Design**

## 6.2 Goal Statement and Task Specifications for the Intake

To prepare theoretical calculations to use as a basis for the design of the intake and exhaust systems for the 2011-2012 Formula SAE car.

- Calculations must be performed for the ideal peak operating range of 7500-8000RPM

- Calculations must be performed to prove the restrictor is not causing choked flow in the engine

- Calculations must be performed to ensure sufficient fueling given theoretical air flow into the cylinders of the engine

- Calculations must be performed to accommodate different packaging options to be considered for future design

## 6.3 Intake Calculations

The Genesis 80fi is found has a total displacement of 499cc. Consisting of two cylinders, each has a displacement of 15.225in$^3$. This, along with the specified peak speed of 7500RPM, dictates the total area each runner must occupy through a formula.

**Equation 6:**

$$A_{run} = \frac{\left[(RPM]_{pk} * Disp_{cyl} * \frac{min}{in^3}\right)}{86200}$$

This total area was then converted to resemble a circular cross section, and the diameter for each runner was found to be 1.284in.

After finding the runner diameter, it was important to determine the intake runner length. Adjusting the runner length allows for the potential to use the "natural supercharging" effects from pulsing air waves in the runner. When the intake valve opens, a vacuum is created that pulls air through the runners into the cylinder. When the valve closes, it sends an impulse backwards from all of the vacuumed air hitting the valve wall. This impulse wave then bounces back and forth through the runner at a specific velocity. Through previous MQP testing, the velocity of the wave was found to be 1275ft/s. If timed correctly, the runners can be tuned such that the intake valve begins to open just before the wave would meet the valve, forcing more available air into the cylinder. Depending on packaging concerns primarily, different waves can be chosen to have this effect and different runner lengths may be chosen.

In addition to knowing the speed of the waves, the lift duration of the intake valve must be found to understand the period of time available for air to enter the cylinder. Being a relatively unknown engine, these values were not readily available through research, and testing was necessary. This was executed by removing any timing covers on the Genesis 80fi, and carefully manipulating the engine through timing events by hand. Through multiple cycles, it was found that the overall intake valve duration was 288*, measured from the moment the first intake cam lobe began to open until the third intake cam lobe was fully closed. The duration can then be converted to effective cam duration (ECD), calculated by

**Equation 7:**

$$ECD = \frac{720° - Duration° - 30°}{degree}$$

Through this calculation, the ECD was found to equal 402*. After finding the ECD, the following calculation was used to determine runner length

$$L_{run} = \left[\frac{ECD * 0.25 * 2 * v_{sound}}{RPM * n} - \frac{d}{2}\right] * in$$

Where *n* represents the chosen reflective wave pulse. From this data, we were able to find runner lengths of 33.528in, 16.443in, 10.78in, 7.901in, or 6.192in to be acceptable, measured from the back face of the intake valve to the tip of the trumpet in the plenum.

## 6.4 Plenum Calculations

The goal of any plenum design is to allow for a certain immediate availability of air to each cylinder's intake stroke cycle. The longer the effective distance that the cylinder has to work to reach its air source, the more overall resistance there is to the airflow of that cylinder. The pressure difference created by that cylinder's stroke creates the flow of air back to the plenum. The important aspect to consider when sizing the plenum is to ensure there is enough air for the next cylinder's intake cycle. With an odd-fire engine, the time before the next cylinder's firing cycle is very short compared to an even –firing one. This results in the need for more air mass being required in less time, necessitating the use of a larger intake plenum. The downside of too large of an intake manifold is the loss of throttle response, due to the location of the location of the throttle body in relation to the cylinders. When the effective volume of the intake plenum is very large in respect to the required air mass needed by the cylinder, it means there is a large volume between the throttle body and the cylinder, and the instantaneous effect that throttle opening has on the airflow to the cylinders is hindered.  Also, when the throttle body bore or a restrictor limits the amount of mass airflow into the plenum, too large of a volume reduces the air density in the plenum, causing vacuum in the plenum. This vacuum negatively affects the pressure difference between the cylinder and the intake plenum, hurting efficiency.

For Formula SAE competition, there is specification for the diameter of the opening to the intake of the engine. This limits the amount of mass airflow that is available to the engine.  This leads to choke flow at high engine speeds. Calculations were done to figure out what this engine speed was to ensure that peak power was not attempted above that for intake runner and diameter sizing. As aforementioned, the plenum pressure decreases with increasing intake plenum volume for a set mass flow of air. Therefore, there is a volume for the plenum to be designed for that is between not supplying enough immediate mass airflow to the intake runners, while not being so large that it decreases the intake manifold pressure due to the mass airflow limit.

CFD was done on a basic intake manifold design that only had the parameters designed for and required, such as restrictor diameter, and intake runner dimensions. No bends for packaging were placed in the model, and very basic curves and surface designs were utilized as to not negatively affect airflow. A design table was used to quickly choose between appropriate intake plenum sizes. A base plenum volume of two times the engine displacement (499cc) was used for testing, as this is the existing size of the intake plenum, and currently provides exceptional throttle response. The boundary conditions were set with the ambient air pressure at 14.68 psi at a

temperature of 68°F, and an outlet flow from the intake runners set at the engines mass airflow usage of 0.041 lbm/s per cylinder.

A steady state flow test was done with both cylinders flowing at the same time to find the worst case flow, which also simplifies the calculations and inputs required for the test. Multiple tests were done on plenum volumes up to 3 times the engine displacement. The average intake plenum pressure at its centerline was plotted compared to plenum size to find the peak pressure that could be achieved. From this data, it was determined that a plenum at approximately 2.5 times the displacement of the engine would be best for this application.
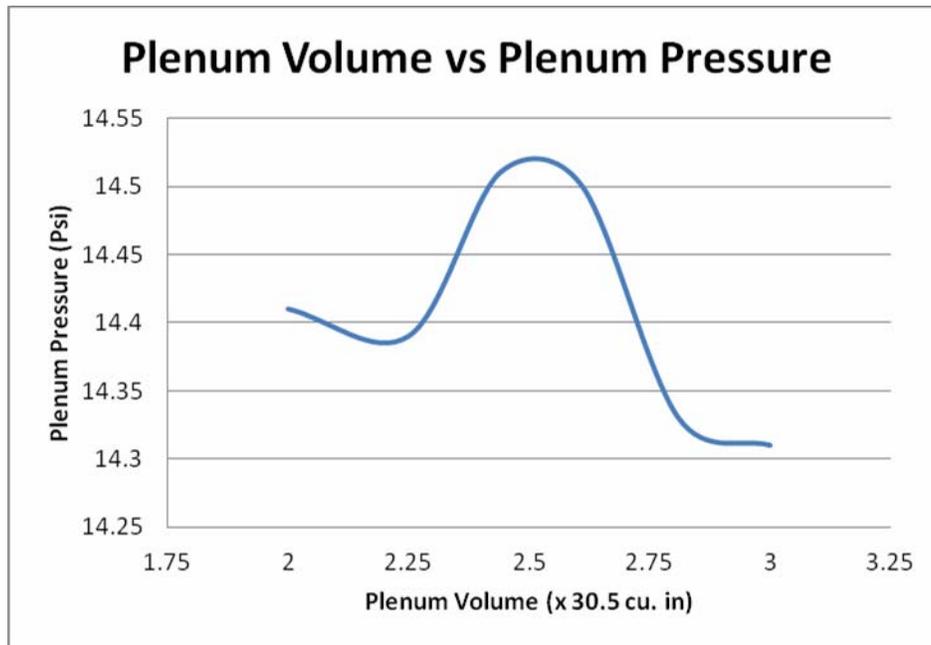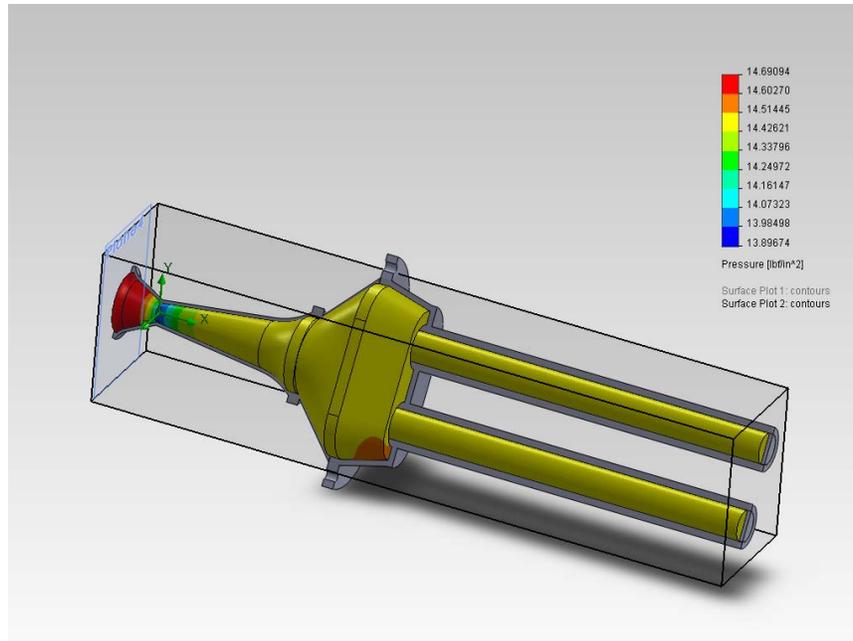


**Figure 46: Plenum Volume Study**

**Figure 47: Sample Pressure Surface Plot for a Restricted Intake Manifold**

## 6.5 Design Approach

Now that the intake runner diameter and lengths were calculated for, the team was able to make runner lengths based on which reflective wave wanted to be utilized as well as any specific diameter. The Yamaha Genesis 80fi has an intake port diameter of 1.62in, so the equations were reworked as to prevent a large trip boundary just before entering past the intake valves of the engine. This yielded a runner length of 16.275in to work in conjunction with the second reflective wave. The design needed to be packaged within the constraints of the seatback and engine head, as well as give an acceptable location of the throttle body. It was determined through multiple CAD iterations that the routing of the intake assembly would be to exit the left of the chassis, locating the throttle body just to the left of the seat. This set precedence for a series of bend for the runners to locate the plenum, then a plenum design that would be the correct volume, as well as locate the restrictor and throttle body. Design ideas were taken by shapes used for equal length headers to get the exit of each respective runner to be coplanar and have the same outlet angle. With the outlets parallel, the runners were found to be 0.5in displaced into the plenum, which was acceptable while maintaining equal length runners.

This allowed for the design of the intake plenum to begin. Since the study on the estimated desired plenum volume was completed, it was now a matter of flow and packaging analysis. The plenum primarily falls within the "shelf" dictated by the horizontal piece of the seat that spaces out the seat back from the engine. The plenum shape was determined by an estimated volume of two and half times the displacement of the engine as well as CFD analysis to minimize the swirling effects at the inlets of the intake runners. Several iterations later, the team was able to achieve a volume of 1272.97 cubic centimeters. This falls within an acceptable range of the goal

volume, so the next step was to perform flow studies. The first of which was a study to find out how air would flow to each respective runner outlet to the cylinder head.

**Table 4: Intake Study Results**

| Goal Name | Averaged Value | Minimum Value | Maximum Value |
|---|---|---|---|
| SG Mass Flow Rt 1 | -0.036497965 kg/s | -0.03656657 kg/s | -0.036306578 kg/s |
| SG Mass Flow Rt 2 | -0.03550183 kg/s | -0.035693867 kg/s | -0.035433552 kg/s |

The results of this test were created by putting the maximum allowable airflow through the restrictor of 0.072 kg/s (previously calculated) and placing the outlets of each runner to environmental pressure. The resulting data shows fewer than 3% differences in flow from each runner, and because the runner that is getting (at most) 3% more flow is the cylinder that fires second, this is absolutely acceptable. The flow trajectory study showed very promising results, in that there was no indication of swirling above the trumpets, as well as no pulling of air from one runner into the other. There were also negligible areas within the plenum that were displayed as zero velocity areas.
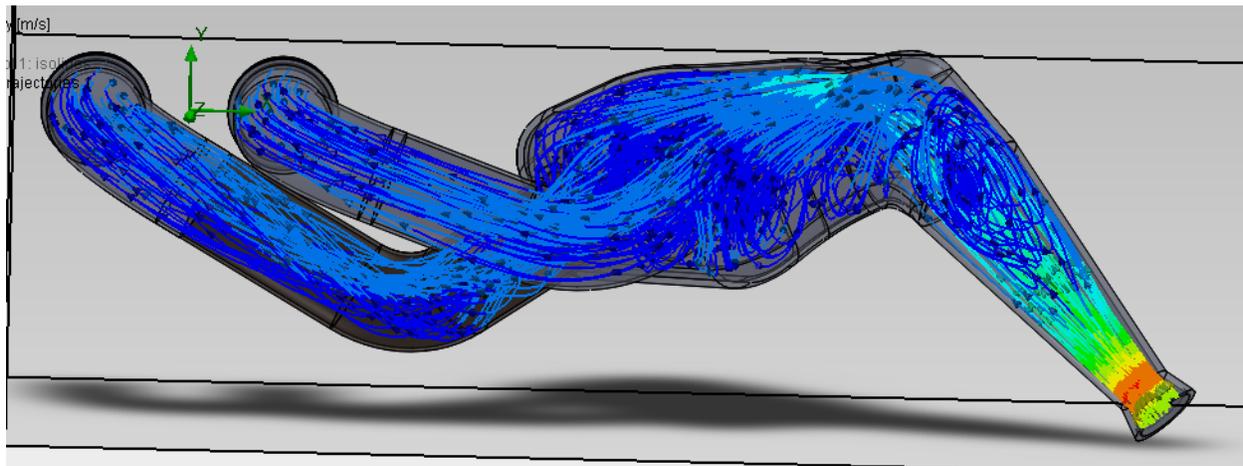


**Figure 48: Computational Fluid Dynamics on Intake**

The only initial concern from this flow model was the swirling that occurred shortly after the restrictor. The swirling was only found to be on the top side of the cone shaped inlet to the plenum. Because the goal volume was as close as it was, and because extending the cone length would place the throttle body below the upper side impact structure would mean structural reinforcement, the team looked into other modifications. Moving the angle of entry would either impact the seat, chassis, or make the throttle body fall outside of the roll envelope. Moving the cone further inwards only shifted the swirling into the plenum, which was also less than ideal. Transient flow analysis was unable to be properly completed using Solidworks Flow Simulation.

The results from the flow study did not seem to account for the reflective pulses in the runners, creating very misconstrued or inaccurate results.

## 6.6 Fabrication

Similarly to last year, the majority of the intake manifold was rapid prototyped. The simple advantage to this is in the rapid prototyping machine's ability to create very lightweight, complicated shapes at a reasonable cost. The physical size limitations of the machine meant that the intake would need to be made into four separate pieces: the restrictor, the plenum, and each respective intake runner. The machine prints parts in ABS plastic, which has had a few issues to be addressed. The first of which is the porosity of the material. Through this printing process, it was found that the material is not airtight. If the intake manifold is not airtight, then tuning the engine to respective vacuum and efficiencies becomes an unpredictable nightmare that will hurt overall performance. To allow the intake to be airtight, a sealant specifically intended for ABS plastic was purchased. The specific sealant chosen was picked because it was also intended to make the ABS fuel proof. This was important to the team because the beginning of the runners is directly connected to the fuel injector manifold.

## 6.7 Fuel Injector Manifold

The fuel injector manifold is intended to fasten the fuel rail and injectors to the intake manifold. Because the ABS plastic is susceptible to corrosion from gasoline, and the team did not trust the purchased sealant to resist constant fuel exposure, it was decided to be made from aluminum. The previous design for the fuel injector manifold was machined from a billet aluminum block that was sealed to the rapid prototyped intake runners.
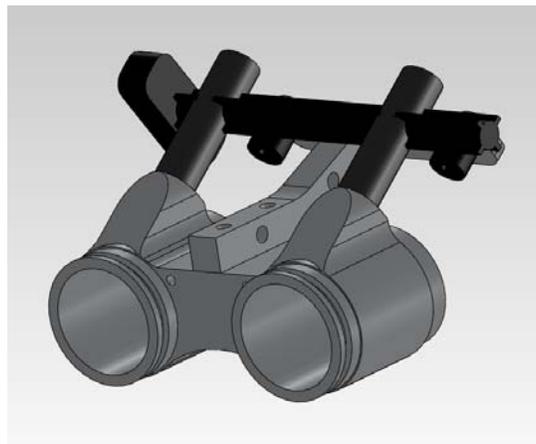


**Figure 49: Previous Fuel Injector Design**

While this design did work, several problems developed through this design. The biggest problem with this design is caused by the overall depth of the part. The packaging of the intake became unreasonably tight to the backside of the seat, causing the runners to angle very poorly into the fuel injector block. The second problem with this design is it is unreasonably heavy for its function, weighing 1.2lbs.

To connect the intake to the intake ports of the cylinder head, rings with matching grooves to the cylinder head were machined. These would allow for the intake to be mounted using the OEM intake mounts. These rings would be directly welded to sourced aluminum tight radius tubing with matching diameter to the rapid prototyped runners as well as the intake ports. This design allows for the aluminum tubing to double as part of the intake runners as well as serve as the mounting surface for the fuel injector block.

The fuel injector entry angle, distance from the intake ports, and injector placement into the runners was maintained from the OEM specifications. The injector manifold was also designed to connect both of the runners to allow for increased rigidity and appropriately hold the fuel rail during any vibrations or assembly, maintaining the runner entry angles to the engine. The final design weighed 0.2lbs, as opposed to the 1.2lbs from the previous design, while still providing adequate fuel rail support.
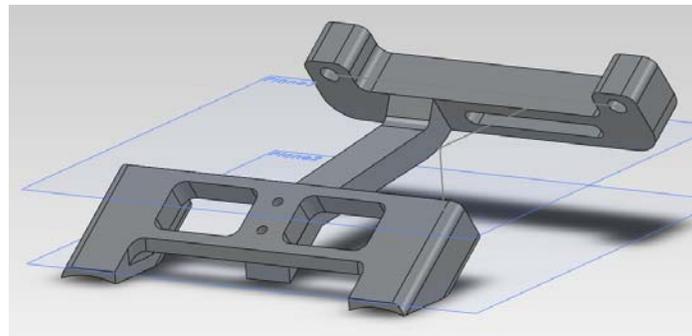


Figure 50: Fuel Injector Design

The final design provided a well thought out approach to solving the previous issues of the intake and fuel injector manifold systems. Sealing issues have been retested and have been solved utilizing the sealant over the rapid prototyped components, and fuel distribution has not seen any issues so far. A future design consideration would be to increase the overall wall thickness of the rapid prototyped components, as an intake backfire had caused one of the runners to fail. To remedy the brittle nature of the plastic, another recommendation would be to add a layer of carbon fiber or fiberglass to increase the overall rigidity without adding a considerable amount of weight. Sealing between the joints of the rapid prototyped components were originally designed to utilize O-rings. However, the only connection currently joined using an O-ring is the restrictor to the throttle body. Plastic to plastic connections were instead sealed using a high grade ABS epoxy.
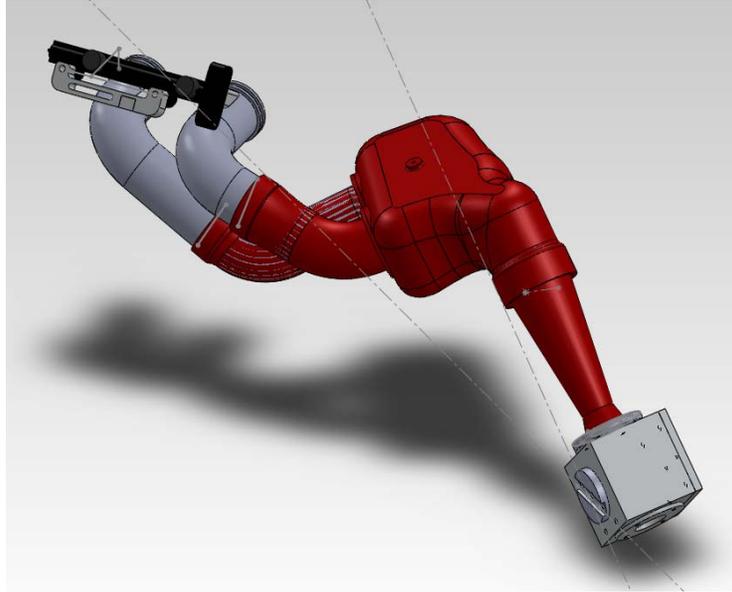
**Figure 51: Final Intake Manifold Design**

# Chapter 7: Exhaust System

## 7.1 2011 Exhaust System

After through analysis of the performance of the previous exhaust it became very apparent that something was not right. The Volumetric Efficiency chart and dynometer graphs showed valley where peaks were expected, as well as the exhaust being tune to much too high of an RPM range. The 2011 car exhaust was designed before it was discovered that the Genesis 80FI is an odd fire engine. In the case of an odd fire 2 cylinder using a merge collection in the exhaust is very detrimental to making power. Typically a merge collection allows for exhaust pulses to transfer between primary pipes and produce low pressure pulses at the valves at the certain tuned RPM. However, with the odd fire nature of this engine the merge collector creates high pressure at the valve at the RPM it is tuned at.

## 7.2 Goal Statement and Task Specifications for the Exhaust

To design and build a legal exhaust for a Formula SAE racecar.

- The exhaust must emit less than 120db at 16 inches from the exhaust exit at 8000 RPM on a sound meter with slow A weighting.

- The exhaust should be tuned to create the most power in conjunction with the intake and CVT.

- The exhaust should be manufacturable on a small and large scale.

- Weight should be kept to a minimum in the exhaust design.

- The exhaust should not break before the end of the of the endurance event in a FSAE competition.

## 7.3 Exhaust Calculations

Through similar methods for finding the intake cam duration, the exhaust cam duration was found to be 242*. Since the Genesis 80fi chokes flow above 7600RPM with the restrictor, calculations were based around 8000RPM peak in order to wring slightly more power out of the engine than setting the peak at 75000 RPM. This resulted in 50in, 24in, or 16in exhaust runner lengths depending on the first, second, or third pressure wave. For packaging concerns, the first pressure wave would not be feasible. With adjustments to the CVT, engine RPM should not exceed this peak. The resulting values for runner lengths will be much more viable than the existing exhaust system, as it was tuned to be effective well above peak power, hurting the effective power band.

Exhaust tuning is typically a fairly straight forward process. When the exhaust valve opens it creates a pressure wave which moves at the speed of sound down the primary runner of the exhaust system. Behind this wave is a pocket of low pressure. It gets reflected back as reduced amplitude when the area of the tubing changes. It will then go back towards the head and reflect off the closed exhaust valve. And it will keep bouncing back and forth until the next exhaust cycle of that cylinder. In this case the exhaust is said to be tuned when the pulse creates the low pressure zone right outside the valve during the time the exhaust valves are open. And obviously one would want this low pressure wave at they cylinder because it assists emptying the spent combustion gases out of the cylinder allowing for more fresh air/fuel to get into cylinder and thus make more power.

The engine is known to produce hot exhaust gases so a wave speed of 1700 ft/sec was used, from the higher end of the common spectrum.

## 7.4 Design Approach

The wave tuning can typically be multiplied on multi cylinder engines though the use of a merge collector. And the reflections will not only just bounce back but cross over to a different pipe at the merge collector. This works very well on engines which fire the cylinders evenly. Now, however, with an odd firing engine, such as the Genesis 80FI, that does not work out correctly. In that case the exhaust pulse from the previously firing cylinder would actually create high pressure at the exhaust valve making the engine have to push the spent gases out harder and likely not getting them all out. This would kill power.

Now typically, even if the merge collector is not being used for wave tuning it will be present in order for the exhaust header primaries to merge together into one pipe. Since the team cannot use a merge collector on an odd fire engine, we must utilize something else. It has been discovered that most teams which utilize this engine uses what is called an exhaust plenum. Essentially putting an intake manifold on the exhaust side of the engine. Both Sherbrooke and Melbourne University utilize this design. In this case one loses the additional merge collector savaging that one could have gotten from an even fire engine, however the pressure wave from the change of area will still be present. In that aspect it does have an advantage, because the area can be made much larger than with a merge collector. A larger area is better, as it makes for a smaller loss of amplitude on each reflection. After testing the exhaust plenum design on the previous car a 5% gain in Volumetric Efficiency (VE) was found. However that is still below the expected VE that should be seen on this engine with the restrictor.

Calculations involving the exhaust are the same as the intake. Taking the time expected for the exhaust valve to be closed (ECD) and desired peak power RPM, figuring out how long the wave has to travel down the pipe and reflect back to the valve can be found. Then it calculates how long the pipe needs to be based on the 1st, 2nd, and 3rd reflection utilizing wave speeds at a

common exhaust gas temperature. Another option for exhaust routing is to never merge the pipes at all, or if they are merged, it would happen in a chamber filled with sound deadening material. This would eliminate any sort of wave crossing between primary pipes. This is known as an individual runner exhaust with dual exhausts. It also allows for twice the amount of mufflers on the car which has reduced the sound level of the car significantly, however this does increase the weight of the car by approximately 8 pounds. It is believed that the teams which use the plenum design utilize it to even out the exhaust pulses before their turbochargers, which is something we lack. It is also a possibility that there are completely unknown wave effects occurring in the plenum, which could be reducing its improvement of VE. Also, the plenum sees a large amount of thermal stress which requires it to be quite robust essentially negating any weight advantages it could have had over the individual runner exhaust. Thus, after weighting the alternatives a dual muffler individual runner exhaust was designed and created.

The exhaust design included fabrication from the very beginning. Once the header flange was placed in the model and the constraints for muffler tip location placed a set of constant radius curves and straights can be created. The length of the line created by these shapes must equal to the tuned runner length minus the distance between the top of the exhaust valve and the header flange. Mandrel bends are available in a selection of radii and bend angle. It was decided that the radii would be kept constant if possible and that the minimal number of mid bend cuts would be made. Mid bend cuts are very difficult to make, they are even more difficult to weld and make smooth as the pipe needs to be cut perfectly perpendicular to the round area of the pipe, and this is nearly impossible to achieve. The final design utilized one 90deg bend, one 180deg bend, and one 70deg bend on each primary tube.

## 7.5 Fabrication

Since the exhaust design included fabrication from the very beginning fabrication was very smooth and simple. The minimal mid bend cuts made for very good dimensional accuracy as well as very clean weld joints. During welding the pipes were sealed and back purged with argon gas, this purging is required to maintain a strong and smooth inner weld when welding stainless steel. Minimal penetration was utilized on the weld joints in order to reduce flow disturbances in the piping. However the penetration is sufficient to provide almost maximum strength and complete sealing.

## 7.7 Conclusion

Based on initial testing this design appears to have increased VE further over the plenum design and though the use of the Ducati mufflers is much quieter than the 2011 exhaust. Therefore the exhaust has met all the goals which can be tested currently. The internal and external ceramic thermal coating on the header tubes also showed a 300*F reduction in header surface temperature after normal operation. Which indicates that the gases flowing through the exhaust should be at a higher temperature and velocity than on the 2011 exhaust which further increase flow. The power gain over the 2011 exhaust is pending dynamometer testing.

## Chapter 8: Belt Tensioning

The tensioner must move the jackshaft and its torque tube in order to properly place the secondary sheave of the CVT in relation to the primary sheave. The previous method of tensioning and aligning the belt was dubbed "the octopus" as it looks like a complicated tangle of tube members. It is, however, very robust and surprising light. The previous adjustment range does not allow for the smallest possible belt at proper tension. The tensioner needs to incorporate alignment adjustment in order to account for small dimensional inaccuracies in the manufacture of the chassis, engine mounts, engine block and torque tube. The tolerances on all of the above parts stack and create an angular misalignment on the belt. The misalignment along the axis of jackshaft is accounted for with spacers on the jackshaft and is less critical than the angular alignment of the sheaves.

### 8.1 2011 Belt Tensioner

The lower section of the octopus made of 4130 alloy steel and is welded directly to the chassis. 4130 alloy steel was chosen in order to allow it to be welded to the chassis, since a weld joint between two dissimilar steel alloys is significantly weaker than either of the alloys. It also provided the octopus with a larger factor of safety than many other materials work have. The top section of the octopus is the actual adjuster. This operates on the same principal as a turnbuckle, in this case there are rod ends on both the chassis and the torque tube and they are connected by connecting rods, often also referred to as radius rods. This is a hexagonal shaft with female left handed threads on one end and right handed threads on the other. There are also nuts on the rod ends used as jam nuts in order to prevent the adjustment from changing. This setup yields approximately 1.5 inches of travel of the adjuster.

This design was originally thought to be a slapped together fix on belt tension created after the chassis was complete. However, during analysis it became quite clear that the design was already very optimized. All of the structural members of the lower octopus account for all of the loading which the tensioner will see. It is also utilizing the lightest of the available sizes of tubing which do not fail during analysis. Any moves to a lighter tubing size, removal of members, or even noticeable movements of the pickups cause the design to fail analysis. Additionally this tensioner allows for relatively easy adjustment of the belt tension and alignment, and almost within the acceptable range.

### 8.2 Goal Statement and Task Specifications for the Belt Tensioner

To create and analyze a detailed design of belt tensioner for the 2011-2012 Formula SAE racecar that will be structurally sound and provides simple and effective belt tensioning and alignment.

- Two inches of travel.

- Simple adjustment.

- Needs to be able to adjust the angle of the secondary sheave relative to the primary to accommodate manufacturing flaws.

- Needs to keep the jackshaft close to the rear axle's rotation point to prevent changes in chain tension under suspension loading.

- Utilize the previous Jack Shaft and Torque Tube in order to reduce the cost of creating new ones (approx $600).

- Must not deform/comply more than 0.025 inch under assumed loading.

- Weight must be equal to or less than the previous solution.

## 8.3 Design Approach

It was felt that the best way to approach the design of a new belt tensioner would be to first analyze the previous design. It was first noted that the weight of the lower octopus was approximately 0.5 pounds. The design was then loaded independently with 40 pounds of side load toward the CVT and 1000 pounds to simulate the belt tension. It performed quite well and this provided a baseline for testing other designs.

The first design which was considered combined the lower mount for the tensioner and the rear axle mount while keeping the previous upper turnbuckle (see Figure 1). There were some major drawbacks to this design. Firstly, aluminum did not have satisfactory material properties for this part which will see strong cyclic loading and high forces. If it had not failed from static loading it would have fatigue failed. The part was then changed to steel, in this case the part marginally passed analysis. This is unacceptable as the suspension mount must be located much more precisely than this allows.
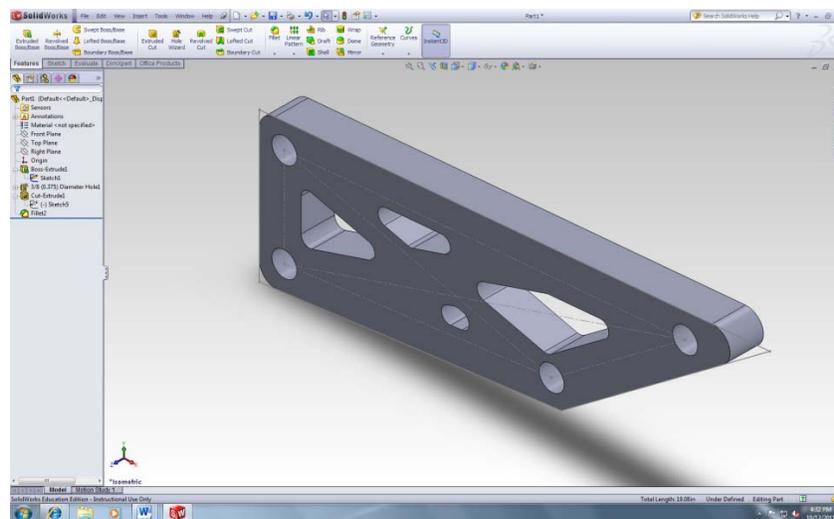


**Figure 52: Combined Tensioner and Rear Axle Mount**

Based on what was learned during the analysis of the original octopus a much less complicated version of a similar principal was designed. The design intent on this iteration was to replace the most important structural members of the octopus with stronger beams and adjust the triangulation to compensate, in order to produce a less complicated and lighter version which withstands the same loading. What was created can be seen below in figure 2, once in analysis it became clear that the members of the octopus were not as random as they seemed, while this part did not fail analysis, it is believe it passed on brute force. Also this design weighs three times as much as the octopus.
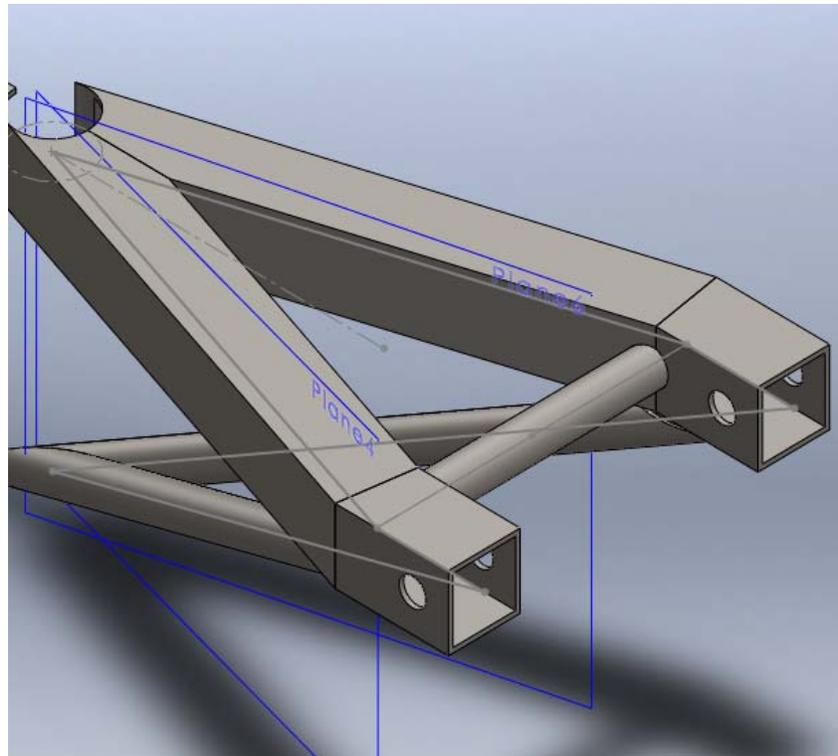


**Figure 53: Square Tubing Belt Tensioner**

Up until now the alternative designs have utilized the same turnbuckle previously used, although rod ends with longer threads have been planned to allow for more range of adjustment, and a slightly shorter connecting rod will be used to get the adjustment into the proper range. Designs for other methods of adjustment were brainstormed. All designs which required removing or adding spacers were instantly discarded as they do not allow for quick and simple adjustment. Optimally the alignment adjustment and the tension adjustment would be made independently; this would make adjustment very simple. However, with will almost certainly add weight, or create an adjuster which lacks enough strength to survive the loading, if it can survive the loading it would likely still create enough compliance that the adjustments are nullified. Even with that known such designs were considered.

The first of the independent adjustment adjusters involved a double turnbuckle. The previous turnbuckle would be shortened to allow for a 2nd single arm turnbuckle to go between the 1st turnbuckle and the chassis. This design was instantly thrown out, as it is impossible to package and allow anything resembling the required adjustment range. The 2nd adjuster considered involved placing the top mounts in sliders and using a shortened version of the previous turnbuckle to only cover alignment adjustment. While this design can actually be packaged it will be very difficult to achieve and maintain proper belt tension with a sliding design, which would only lock into position with the clamping force of its mounting bolts. Sketches of these designs can be seen in figures 3.
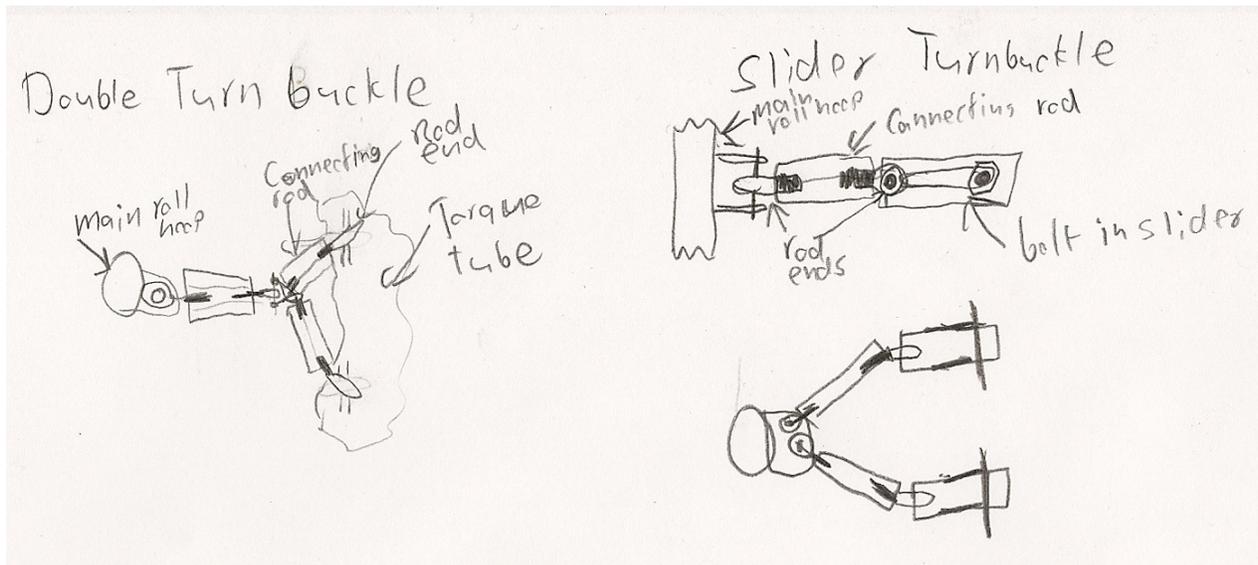
**Figure** 54**: Additional Turnbuckle Designs**

The last design of an alternative adjuster does not involve independent adjustments. Refereeing back to the square tubing replacement for the lower octopus, the end was extended and slotted to allow adjustment (as seen in figure 49). The part was then planned to be flipped upside down and used to replace the turnbuckle with either another version of itself or any other lower octopus design. However this design had many flaws. First, it is much heavier than the previous solution. Second, it once again runs into the same issues as slotted adjustment without a turn buckle, that achieving and maintains the proper adjustment is near impossible. As yet another drawback, the adjustment of the angular misalignment is very limited and almost impossible to achieve.

As an automatic chain tensioning system was designed this year, being able to adjust the belt independently of the chain is not a major issue. However the team still brainstormed designs. In this case the most promising design was one which there was two jackshafts, connected with another chain system and the belt side jackshaft would rotate around the chain side jackshaft to tension the belt. This is quite an un-reasonable design. It add an unreasonable amount of weight, more rotating mass, an extra layer of complexity, and it adds another chain which would require a solution for tensioning independently of the original chain and belt.

## 8.4 Design Analysis

It should have already become clear that the previous design already in use on the car (figure 5) is in fact the optimal design for this year as well. It meets all of the design specifications, except for the two inches of travel. It is fairly simple to adjust since it only requires loosening and tightening with a wrench with no removal of parts required. It accounts for angular misalignment as well as tensioning, and its range of misalignment adjustment is more than sufficient to accomplish aligning all but the most extreme manufacturing errors. It does not comply more than 0.025 inches under loading and is currently in use with the jackshaft and torque tube so it must work with them. One of the design considerations the 2009 MQP team used in their was also keeping the jackshaft as close the axle pivot point as possible to minimize chain tension change through suspension travel. It is a known quantity; it works in real life as well as in computer simulations.
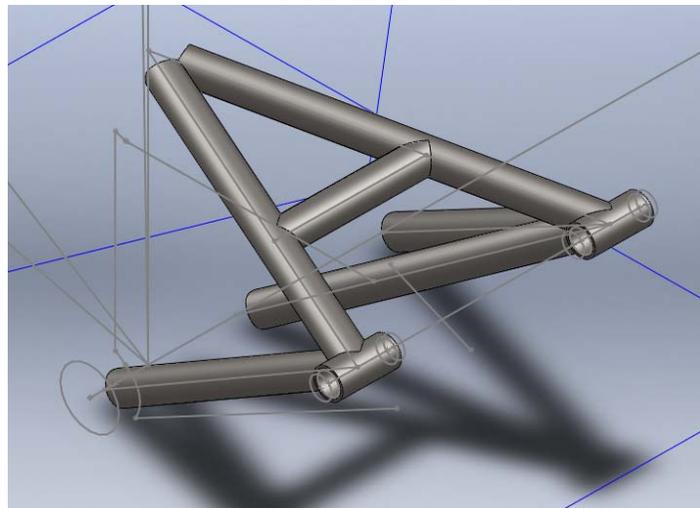


**Figure** 55**: Belt Tensioner Final Design**

## 8.5 Final Design

As this design is already known to stand up to real world loading, running failure analysis is a moot point. The only way in which the part could fail on the new car would be manufacturing error; either through defective material or poor welding. That said; analysis was already run on the lower octopus in order to gain a baseline for analysis of alternative designs (the results can be seen in figures 6-9 below). In the case of the turnbuckle, analysis is difficult as the main failure point would be threads in compressive loading modeling threads in SolidWorks is very time consuming and often not accurate. In this case its likelihood to fail is based on the rated values of the rod end components in use, all of which exceed the loading by multiple orders of magnitude.
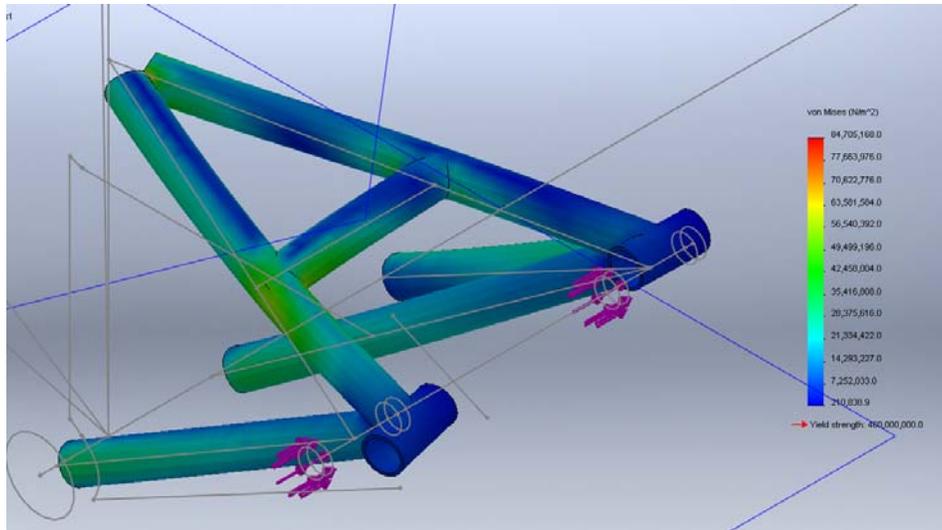
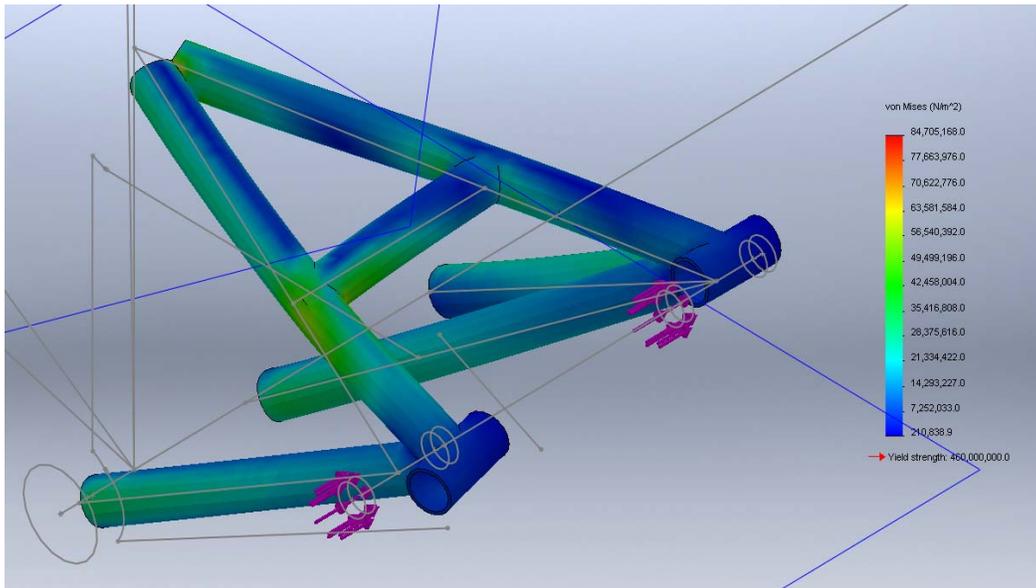**Figure 56: Belt Tensioner Lateral Stress**



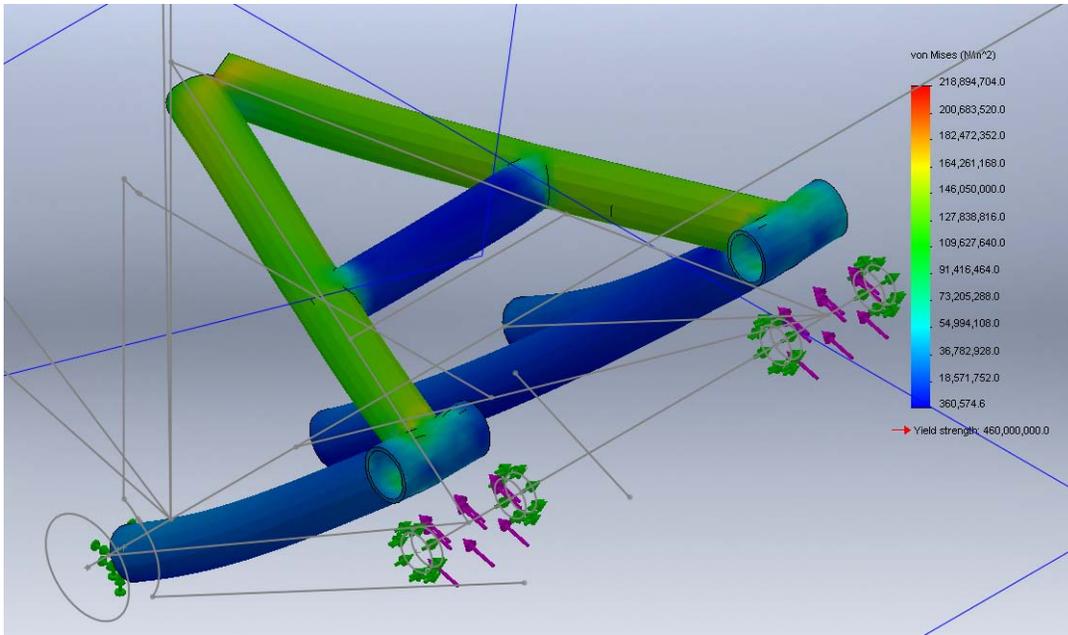**Figure 57: Belt Tensioner Lateral Displacement**

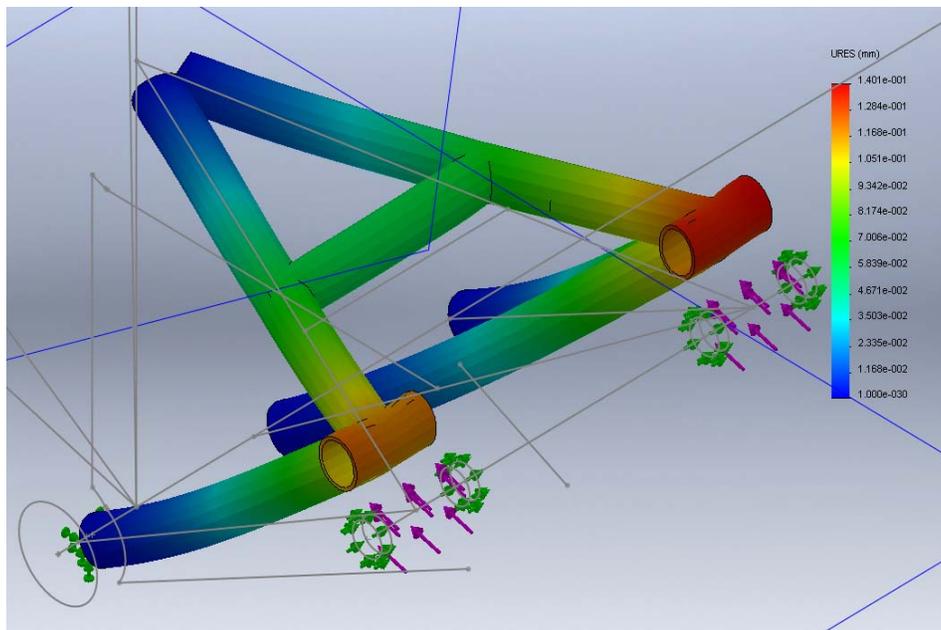**Figure 58: Stress on the Belt Tensioner due to Belt Tension**



**Figure 59: Displacement of Belt Tensioner due to Belt Tension**

As mentioned before, the previous design does not quite allow for the optimal adjustment range. In order to meet this design criteria rod ends with longer threaded shanks have already been source in the correct size which will allow for 2 inches of travel or very close to it. In order to allow for the new minimal size required a connecting rod of approximately ½ inch less length will be used. Previously, the belt tensioner was at its minimal setting and the belt was still

slightly too tight, this is causing some CVT efficiency issues along with being a small part of the hard starting issue.

One of the more important factors which was not discussed  at length as of yet is that the jacks shaft must be placed close to the rotation point of the axle to minimize the change in center to center distance on the chain drive. That is done in order to minimize transient changes in chain tension through suspension travel. It has already been shown that this placement is close enough to rotation point that it will not cause the chain to be thrown throughout the entire suspension travel. While this year we will have an independent automatic chain tensioner this constraint minimizes the work which that tensioner has to have and lowers its required response frequency.

## 8.6 Conclusion

While the intent of belt tensioner design for this project was to redesign the belt tensioner to meet our design specification and move away from the octopus, it was determine that the best engineering decision was to re-sue the octopus. It is the most elegant solution to a surprisingly very complex issue and meets all of the design criteria. Without a major redesign of the entire rear end of the car there does not seem to be another manner in which to adjust belt tension which is as effective and light weight. Even then one would struggle to keep the entire packaging change below the weight of the octopus.

# Chapter 9: Continuously Variable Transmission Tuning

The Continuously Variable Transmission (CVT) eliminates the limitations caused by fixed gear ratio, standard transmissions. Additionally, the CVT eliminates the use of a clutch pedal and shifter mechanism, allowing for a greater range of overall drivers. The CVT consists of two pulleys that are able to adjust depending on the force output of the engine, called the primary and secondary sheave. The primary sheave connects directly to the output shaft of the engine. Its primary function is to tune the engagement speed of the vehicle off of idle, and then control the engine RPM as a function of wheel speed. The secondary sheave focuses on the overall efficiency of the system, as well as back shifting. Back shifting is the ability of the CVT to "reset" when the throttle is released. Previously, the CVT was not adjusted past OEM specifications. This developed several issues with the previous car. The largest of which was the operating RPM of the engine.
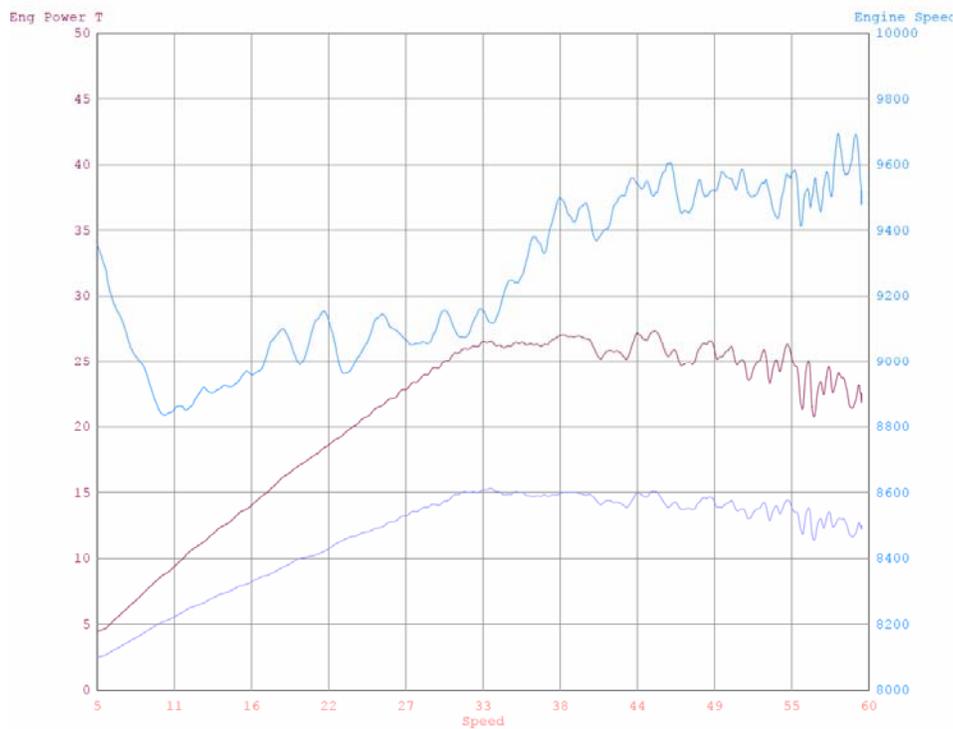


**Figure 60: 2011 FSAE CVT Graph**

According to the calculations completed for the intake design, the engine will choke flow anything above 7500RPM. As you can see by the figure above, the primary engages just above 8500RPM, then crawls to 9600RPM by the time the CVT is completely shifted out and in overdrive. This suggests that the previous car was severely underpowered because it was choking flow from engagement to overdrive. The second problem developed in the previous car was the

crawling from 9000 to 9500RPM. Ideally, the CVT operates in an extremely narrow powerband, differentiating no more than 200-300RPM from full engagement to overdrive. One of the primary benefits from the CVT is the ability to hold the engine in its peak torque output regardless of vehicle speed. This, unlike traditional transmissions which need to rev into their peak torque output as speed is increasing. This is especially beneficial coming out of corners.

## 9.1 Tuning

The most critical aspect of CVT function is maintaining the desired RPM throughout full engagement into overdrive, called the shift-out function. This is achieved by changing the weight of the flyweights in the CVT that drive the engagement and shifting out of the primary. The heavier the flyweights, the lower RPM is required to engage and physically shift out the primary. Because the CVT was engaging and shifting out so much higher than the desired 7500RPM, a 68g base weight was chosen. This was 18% heavier than the OEM weight. The flyweights that were chosen are also adjustable. This adjustment meant the flyweights could weigh anywhere between 68g to 82g. With an estimated flyweight weight of 76g, a 68g base weight put the primary in the middle of the adjustment range off of the theoretical value. Adjustment of this weight allows for weight distribution to be placed in the beginning, middle, and end of the cam. This adjustment coincides directly with the engagement and low speed, middle speed, and top end speed. This allows for further adjustment in the event that the climbing or falling of engine RPM during shift out in the event that the primary spring does not yield positive results.

After flyweights put the CVT in the desired operating range, the primary spring can be replaced. The function of the primary spring is to resist the centrifugal force of the flyweights as the primary is shifting out. If operating RPM climbs during primary shift out, then a spring with a lesser rate should be utilized to help flatten the RPM band throughout wheel speed. For this specific application, the RPM band crawled from 9000 to 9600RPM. This suggests using a lesser spring rate than OEM. However, because considerably heavier flyweights were chosen off of the OEM, the spring effectively will have less rate against the newer weights, so testing will need to be performed.

Engagement of the primary is also dictated by the pretension in the primary spring. To increase the engagement speed, increase the pretension of the spring while maintaining the same rate. Testing will need to be performed with the new flyweights to determine any necessary changes to the primary spring from the OEM.

Once engagement and shift out have been optimized for the specific application, the next step is to tune the secondary. As was stated before, the secondary deals primarily with back shifting as well as the efficiency of the system. Efficiency is dictated by the overall belt tension of the system as well as the ability for the secondary to backshift. Back shifting is dictated by the friction in the helical cam, rollers that manipulate it, and the secondary spring. It was found during testing that the back shifting characteristics of the secondary were very poor, and that the slow back shifting would cause the CVT to remain engaged after the throttle was disengaged.

This continued engagement would cause the vehicle to effectively "push" into corners, increasing required braking and causing unpredictable handling characteristics during turn in.

The helical cam in the secondary was Teflon coated to reduce the friction in the system. For future teams, finding a usable secondary that shares the Yamaha secondary spline that has complete roller conversion kits would be ideal. However, Teflon coating offers a 60% reduction in friction over the OEM system. Additionally, the pretension was increased as per the recommendations of CVT tuning professionals.

Overall, the system needs to be tested continuously to fully optimize the utility offered by the continuously variable transmission. Multiple tests with logging wheel speed vs. engine RPM should be conducted to fully understand the characteristics of the CVT, and how minute adjustments may affect the overall system. Currently, the vehicle is equipped with a vehicle speed sensor, but appropriate tuning to display the results of the changes made has not yet been performed.

# Chapter 10: Seat and Fuel Tank Design and Fabrication

The seat must be designed to meet with the Formula SAE rules relating to PERCY, previously described as the 95th percentile male. PERCY's "hips" must lay tangential to the floor pan as well as tangential to the diagonal face intended for the lower back of the driver. The "shoulders" must fall against this back plane, leaving the "head" in the acceptable range of the headrest supports of the chassis. The design is intended to maintain the fitment shown in figure 1 in chassis design, while also maintaining the spatial constraints dictated by the intake manifold. In the previous design, the angle of the lower back was dictated by the fuel engine mounting solution used. This caused drivers to sit in an unnaturally reclined position. Since the new engine mounts were not below the driver's seat, this angle was able to be increased to 32.3 degrees, as opposed to the original 29.5 degrees. While this is a minimal increase, the previous design did not meet Formula SAE regulations, and the seat had been further modified to recline the driver even further than originally designed. Additionally, clearance for the intake has been increased to allow for a smoother entry into the cylinder head.
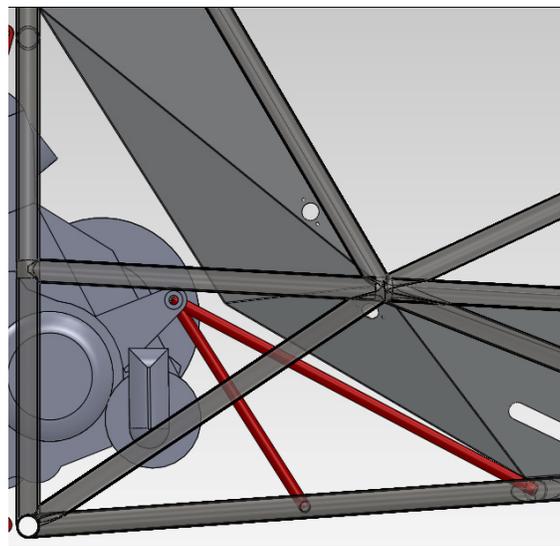


**Figure 61: Previous Seat Design, Engine Mount Constraint**

The chassis structure drove the majority of the seat geometry. The two primary design improvements from the previous design are the inclusion of an access panel and the addition of a "shelf" that offsets the seating position. As was previously mentioned, the previous design did not meet Formula SAE regulations. This was due, in part, to the addition of a similar shelf when it became apparent that there was only an inch or so clearance from the intake ports to the backside of the seat. This shifted seating position did not pass PERCY tests, and so the edge where the tangent of the floor pan to the diagonal lower back area had to be shifted forward.

Adding this shelf ahead of time would guarantee proper fitment for PERCY tests, while ensuring proper clearances for the intake.

Part of going through technical inspection requires visible, or simple access to any components that need to be inspected. This includes the mounting of the intake and fuel components to the engine. Previously, this required the complete removal of the seat, and was a tedious, time consuming action. The inclusion of the access panel allows for visual inspection of the intake and fuel component mounting with the actuation of two 90 degree fasteners.
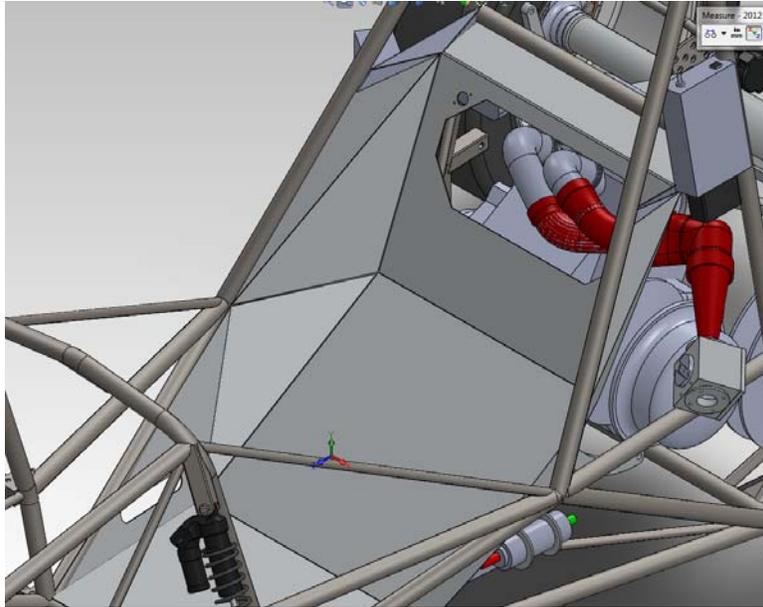


**Figure 62: Access Panel and Shelf Inclusion**

The fuel tank used in the previous car had a capacity of 2.5 gallons. With the intentions of being optimized for competition, the longest event that was required to be completed was the endurance event. It was found through competing last year that the car had used a total of 1.5 gallons during this event. Because of this, the overall capacity of the new fuel tank was changed to 1.7 gallons. Because the overall efficiency of the engine is being increased by operating in the desired powerband, this volume was decided to be a good balance between what was used and what is expected to be used during future endurance events.

The filler neck was changed from being a fixed position, side mounted neck. A number of issues arose with this design. The most prominent of which was the inability to remove the fuel tank from the car without cutting it out. Additionally, the seal to the side mounted neck never fully sealed, and consistently leaked. Instead, a top mounted fitting was welded directly to the fuel tank, and a flexible fuel hose was clamped to the fitting. This allowed for removal of the fuel tank, and minimized the potential for leaks in the system. Also, since this filler neck is clear, it will double as the sight tube for filling the fuel tank, decreasing the required components in the system.

Previously, fittings to the fuel tank were tapped directly into the sheet metal, and epoxy was used to seal them into place. For the new design, oversized holes were drilled into the tank, and aluminum bungs were welded into place. These bungs were then tapped, and sealant used on the threads. This allowed for 4x the thread engagement for each of the fittings.
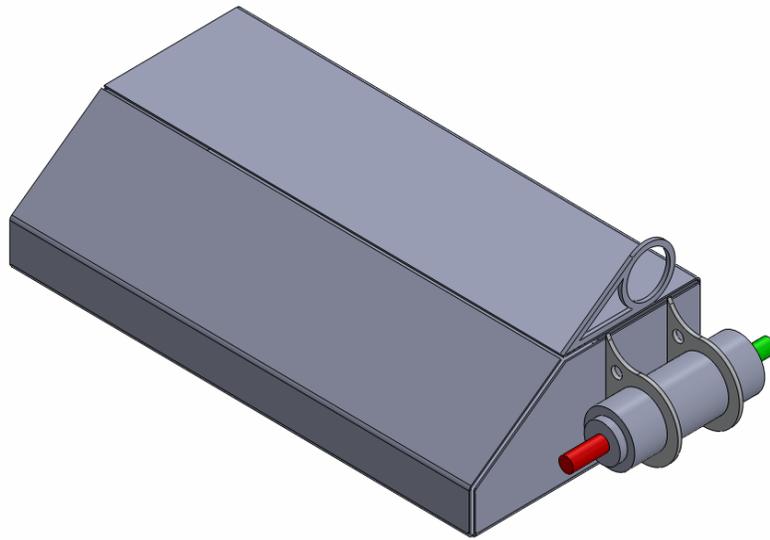
**Figure 63: Fuel Tank Assembly**

**Figure 64: Fuel Filler Neck**

## Conclusions and Recommendations

The team faced many challenges throughout the project. The biggest issue was with the chassis. The decision to outsource the notching the chassis tubes to CRD seemed like a good decision in the beginning, however after receiving the tubes it was determined that the difference in cost did not outweigh the quality and expected turnaround time that Cartesian could have offered. To future WPI Formula SAE teams, we strongly recommend outsourcing the chassis to Cartesian, or an equivalent company that is able to precision bend and notch the chassis members.

Time constraints were another issue the team faced. Designing and fabricating a compete formula style race car in an academic year is impossible. Most teams design a new iteration of their car every year that changes enough to qualify as a whole new car. This is the main reason for using several components from the 2012 car's predecessor such as the rear axle. Many teams also develop cars over a two year period.

# Works Cited

2011 FSAE MQP report…

Aho, Christopher, Scott Duncan, Dan Cullen, Dan Swan, Adam Panzica, and Ryan Lehrmitt.

    2009 Formula SAE Racecar.Tech. 2009. Print.

Ceviz, M.A. Intake plenum volume and its influence on the engine performance, cyclic

    variability and emissions, Energy Conversion and Management, Volume 48, Issue 3, March 2007,

    Pages 961-966, ISSN 0196-8904, 10.1016/j.enconman.2006.08.006.

    (http://www.sciencedirect.com/science/article/pii/S0196890406002391)

    Keywords: Intake manifold; Intake plenum; Engine performance; Cyclic variability; Emissions

Claywell, Mark, Donald Horkheimer, and Garrett Stockburger. University of Minnesota FSAE

    Coupled WAVE WAVE-VECTIS. Tech. Print.

Drake, Sam. Utah Formula SAE Final Design Report. Rep. Print.

Giaraffa, Matt. "Springs& Dampers."*OptimumG*.Optimum G, 2009.Web. 12 Oct. 2011.

    <http://www.optimumg.com/OptimumGWebSite/Others/TechTips.html>.

"Intake Manifold Design."Horsepower Calculators.Web. 20 Nov. 2011.

    <http://horsepowercalculators.net/intake-manifold-design/intake-manifold-design>.

Loiselle, James, John Paul McCann, and Alex Scott.Design and Analysis of a FSAE Racecar.

    Tech. 2010. Print.

McFarland, Jim. "Intake and Exhaust Size - How Inlet and Exhaust Path Sizing Impact Torque –

    Circle Track Magazine." Race Cars, Dirt & Stock Car Racing, Sprint Cars & Racing Tech - Circle Track Magazine. Jim McFarland, Jan. 2011. Web. 20 Nov. 2011. <http://www.circletrack.com/enginetech/ctrp_1101_intake_exhaust_size/viewall.html>

*Motorsports Spares International*.Web. 27 Sept. 2011.

      &lt;http://motorsportsspares.com/fsae.html&gt;.

*Pegasus Auto Racing Supplies* .Web. 26 April 2011.

      &lt; https://www.pegasusautoracing.com/&gt;.

*Woolf AircraftProducts* .Web. 26 April 2011.

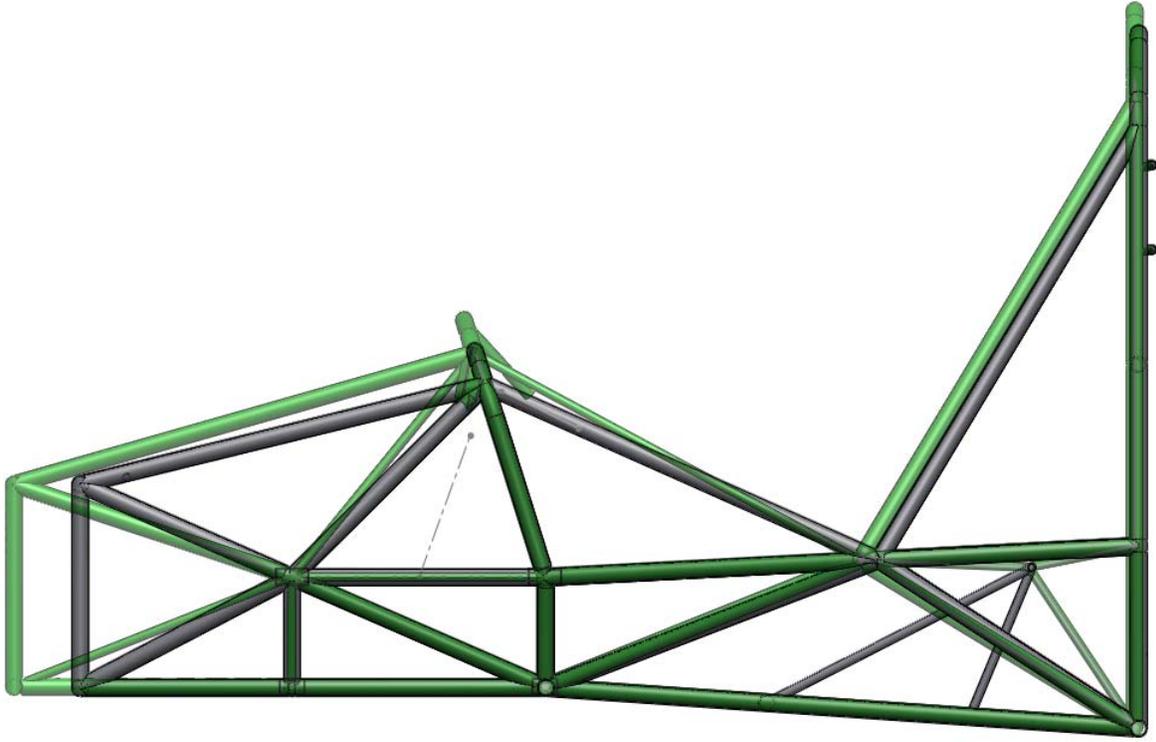      &lt; http://www.woolfaircraft.com/&gt;.

# Appendix A: Final Chassis Design Figures



**Figure 65: Final Design Projection: Side View**

Figures in this section show the projections of the newly designed chassis over the current one.
The new frame is projected in green, while the current one is grey.
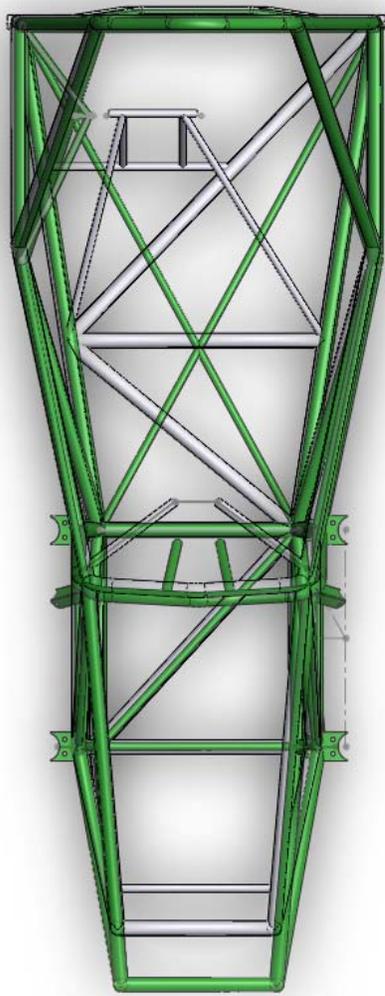
**Figure 66: Final Design Projection: Top View**
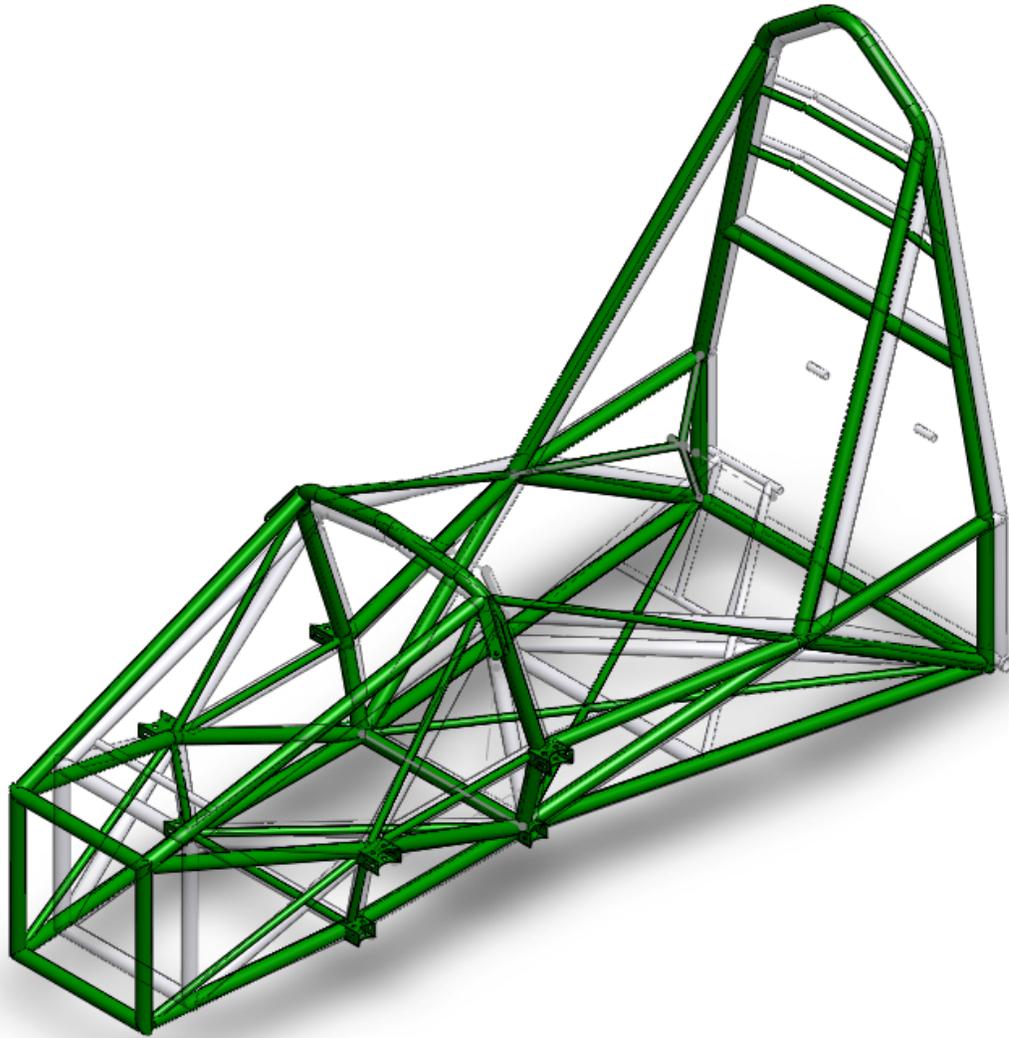
**Figure 67: Final Design Projection: Isometric View**

# Appendix B: Final Engine Mounting Figures
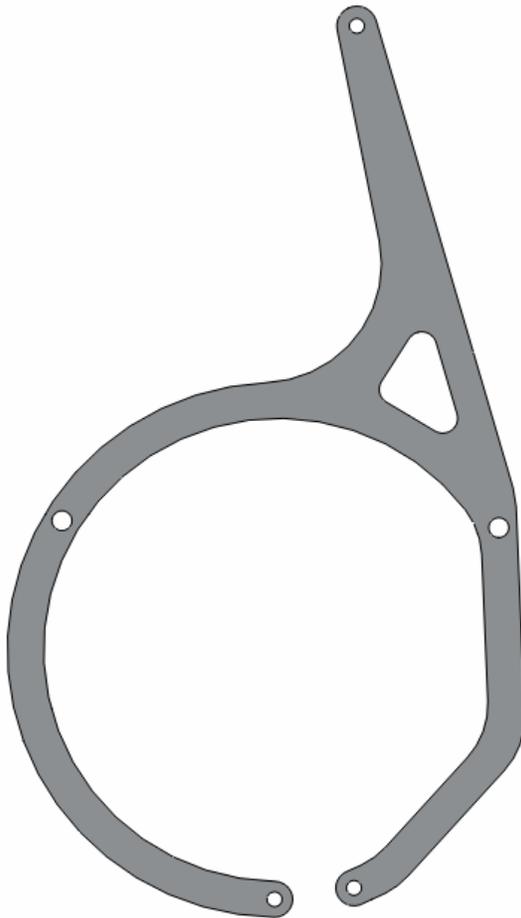
Mass properties of new claw ( Part Configuration - Default )

Output coordinate System: -- default --

Density = 0.10 pounds per cubic inch

Mass = 2.52 pounds

Volume = 25.86 cubic inches

Surface area = 157.61 square inches

Center of mass: ( inches )
 X = 0.25
 Y = 3.56
 Z = -0.98

Principal axes of inertia and principal moments of inertia: ( pounds * square inches )
Taken at the center of mass.
 Ix = (0.00, 0.95, -0.30)   Px = 34.04
 Iy = (0.00, 0.30, 0.95)   Py = 96.76
 Iz = (1.00, 0.00, 0.00)   Pz = 130.69

Moments of inertia: ( pounds * square inches )
Taken at the center of mass and aligned with the output coordinate system.

| Lxx = 130.69 | Lxy = 0.00 | Lxz = 0.00 |
|---|---|---|
| Lyx = 0.00 | Lyy = 39.57 | Lyz = -17.78 |
| Lzx = 0.00 | Lzy = -17.78 | Lzz = 91.23 |

Moments of inertia: ( pounds * square inches )
Taken at the output coordinate system.

| Ixx = 165.18 | Ixy = 2.25 | Ixz = -0.62 |
|---|---|---|
| Iyx = 2.25 | Iyy = 42.16 | Iyz = -26.62 |
| Izx = -0.62 | Izy = -26.62 | Izz = 123.44 |

**Figure 68: The Claw with Mass Properties**
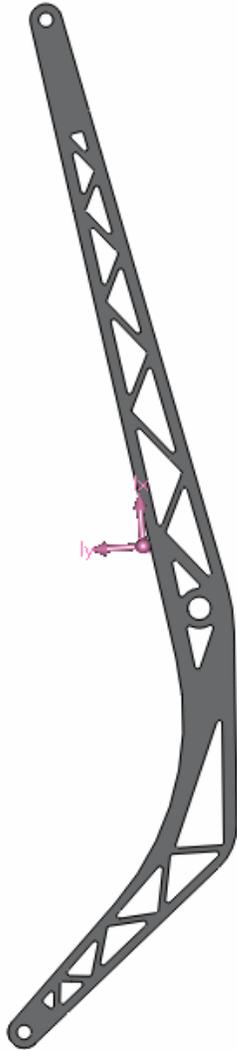
Mass properties of Banannav3 ( Part Configuration - Default )

Output coordinate System: -- default --

Density = 0.10 pounds per cubic inch

Mass = 0.85 pounds

Volume = 8.70 cubic inches

Surface area = 89.32 square inches

Center of mass: ( inches )
    X = 0.00
    Y = -0.12
    Z = 1.92

Principal axes of inertia and principal moments of inertia: ( pounds * square inches )
Taken at the center of mass.
    Ix = (0.00, 1.00, 0.08)    Px = 1.22
    Iy = (0.00, -0.08, 1.00)   Py = 34.00
    Iz = (1.00, 0.00, 0.00)    Pz = 35.18

Moments of inertia: ( pounds * square inches )
Taken at the center of mass and aligned with the output coordinate system.
    Lxx = 35.18         Lxy = 0.00          Lxz = 0.00
    Lyx = 0.00          Lyy = 1.43          Lyz = 2.61
    Lzx = 0.00          Lzy = 2.61          Lzz = 33.79

Moments of inertia: ( pounds * square inches )
Taken at the output coordinate system.
    Ixx = 38.33         Ixy = 0.00          Ixz = 0.00
    Iyx = 0.00          Iyy = 4.56          Iyz = 2.41
    Izx = 0.00          Izy = 2.41          Izz = 33.80

**Figure 69: The Banana with Mass Properties**
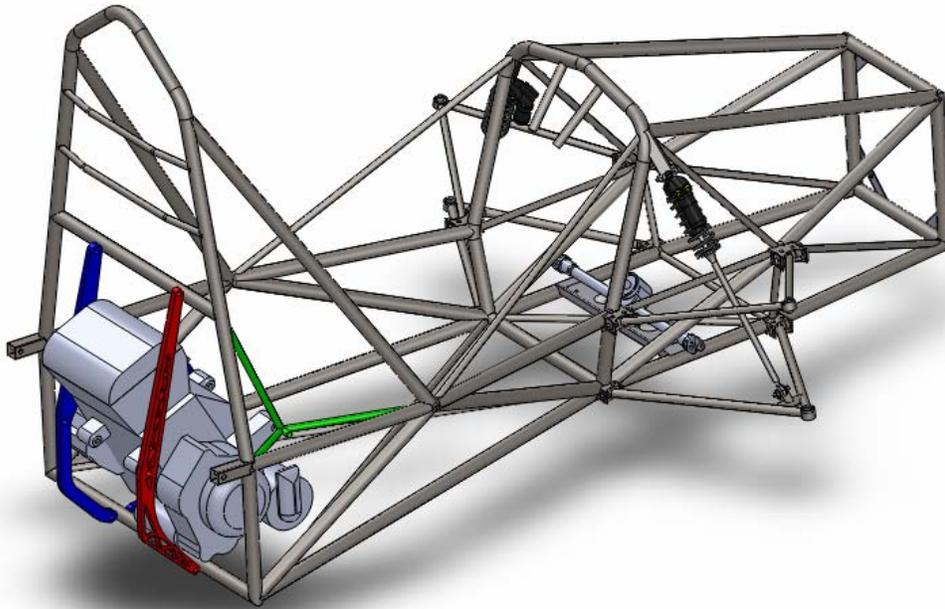
**Figure 70: Rear Isometric View of the Chassis with Engine Mounts (Chassis Engine Mounts: green, The Banana: red, The Claw: blue)**
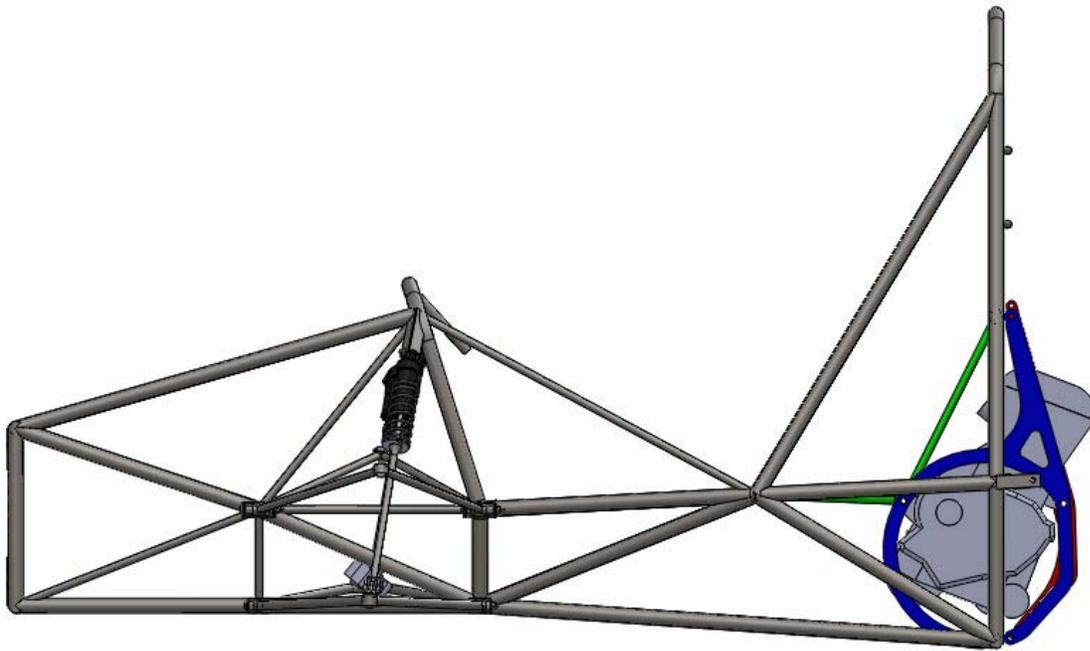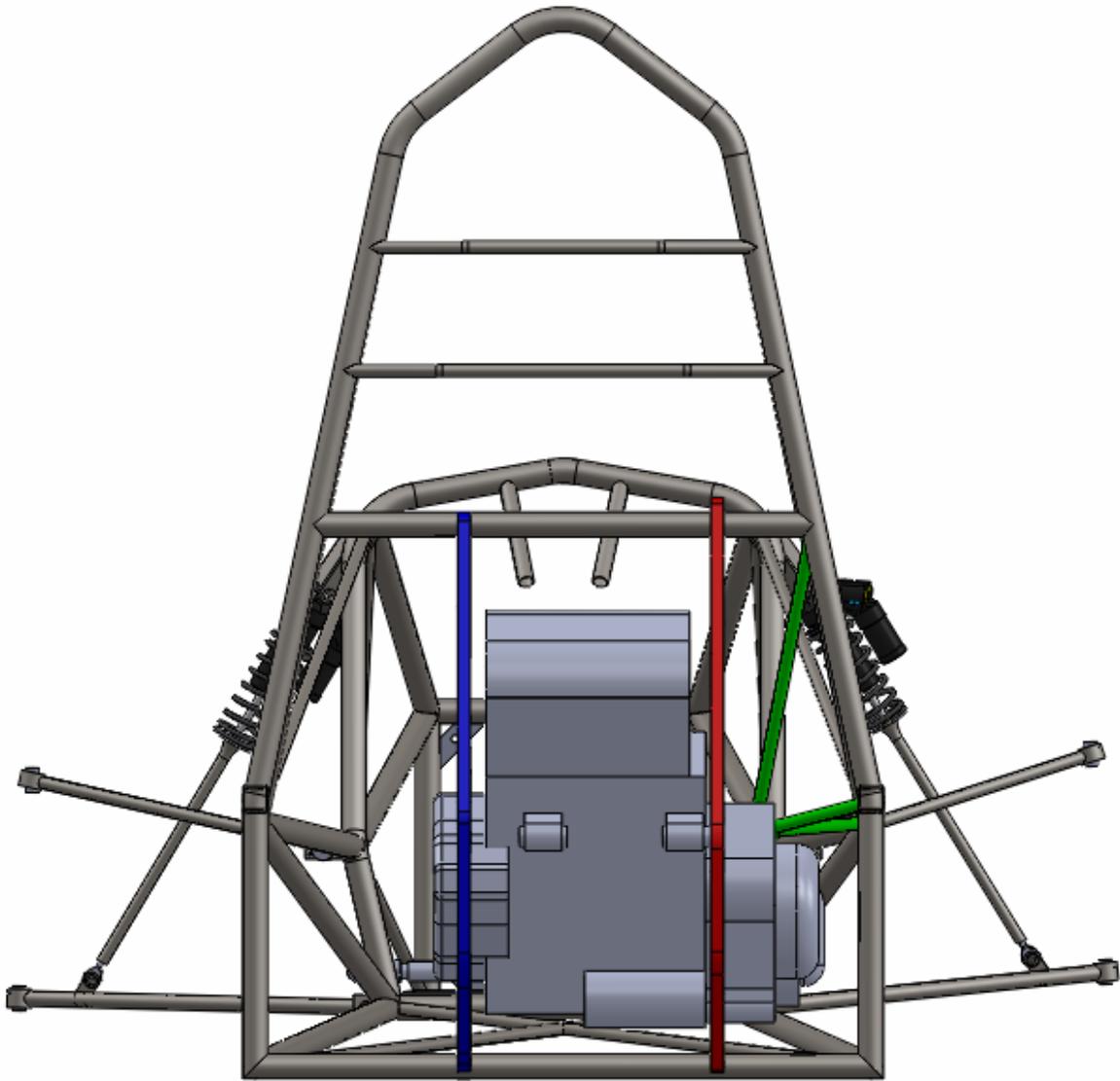
**Figure 71: Right View of Chassis with Engine Mounts**
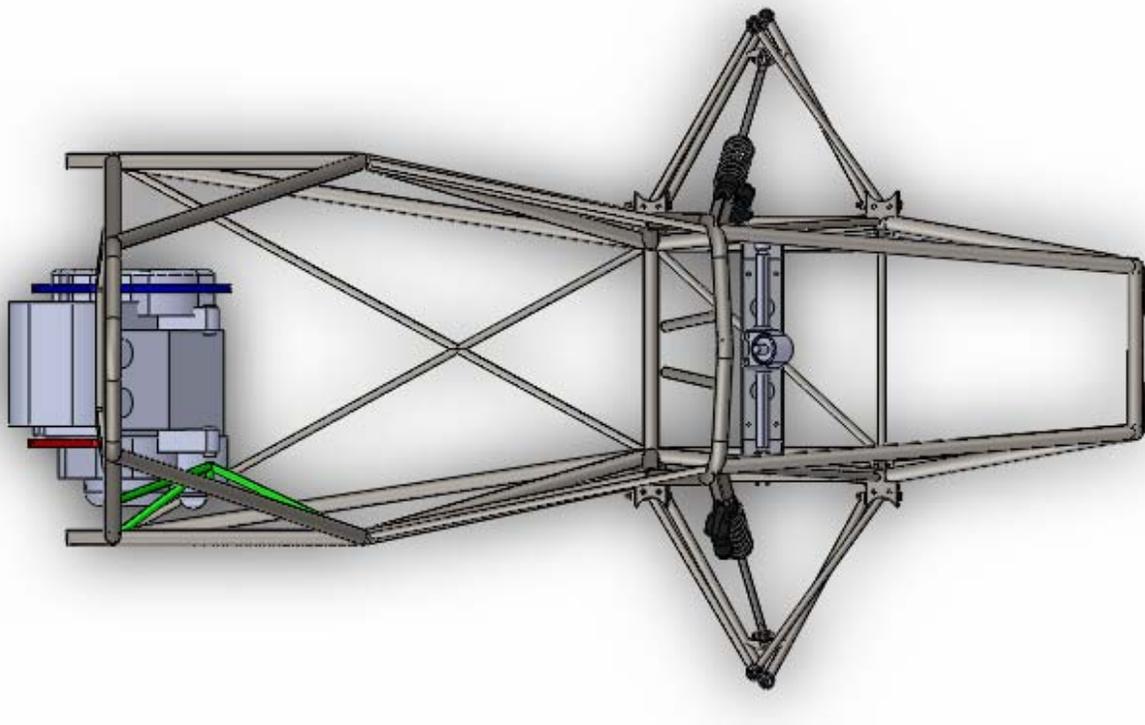
**Figure 72: Rear View of Chassis with Engine Mounts**

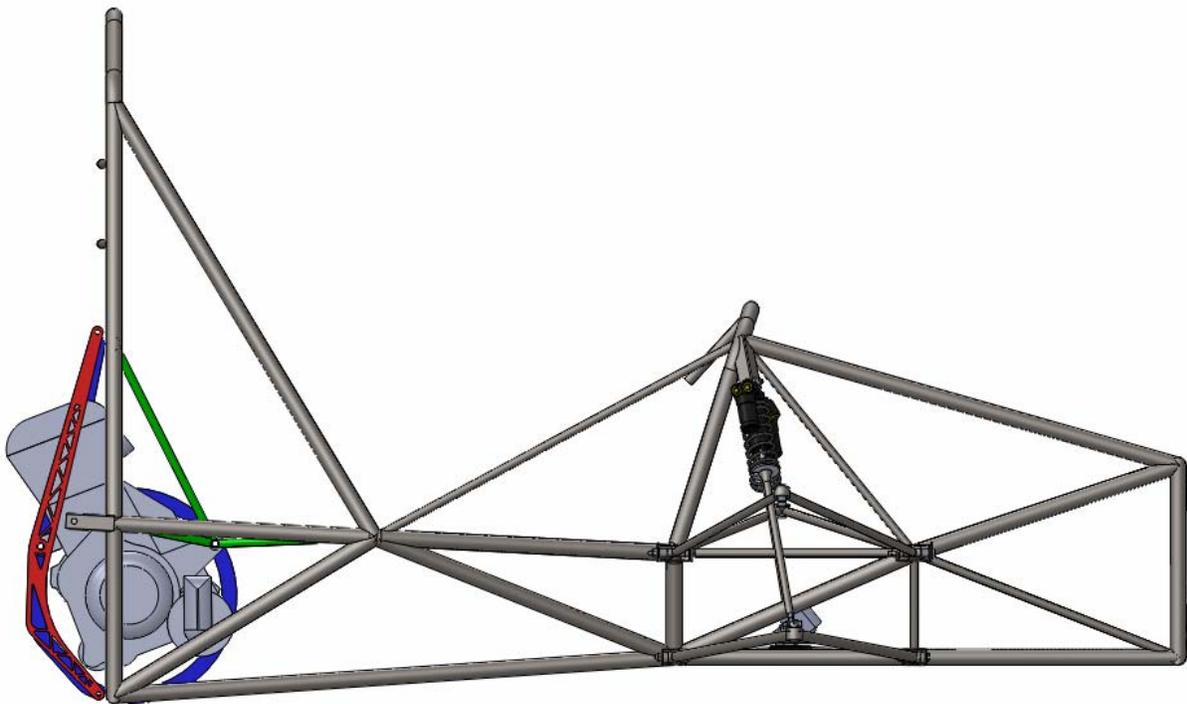**Figure 73: Top View of Chassis With Engine Mounts**



**Figure 74: Left View of Chassis with Engine Mounts**

# Appendix C: Suspension Calculations

**Front and rear motion ratios:**

$R_f := 1.46$

$R_r := 2$

**Weight Distribution:**

Car with Driver

$M := 550lb$

$M = 249.476\,kg$

**Front weight (assume 45/55 weight distribution)**

$W_f := M \cdot 0.45 = 112.264\,kg$        $W_{lf} := \dfrac{W_f}{2} = 56.132\,kg$        $W_{rf} := W_{lf}$

**Rear Weight**

$W_r := M \cdot 0.55 = 137.212\,kg$        $W_{lr} := \dfrac{W_r}{2} = 68.606\,kg$        $W_{rr} := W_{lr}$

**Front unsprung mass (one wheel)**

$m_{fus} := 25lb$        $m_{rus} := 55lb$

$m_{fus} = 11.34\,kg$        $m_{rus} = 24.948\,kg$

**Sprung Mass:**

Front

$m_{fsm} := W_{rf} - m_{fus} = 44.792\,kg$

$m_{fsm} = 98.75 \cdot lb$

Rear

$m_{rsm} := W_r - m_{rus} = 112.264\,kg$

Half of the rear sprung mass

$m_{rsm2} := \dfrac{m_{rsm}}{2} = 123.75 \cdot lb$

**Front Spring rate:**

Front ride frequency

$f_{rf} := 3.2Hz$

$K_{sf} := 4\,\pi^2 \cdot f_{rf}^2 \cdot m_{fsm} \cdot R_f^2 = 38.598 \cdot \dfrac{N}{mm}$        $K_{sf} = 220.402 \cdot \dfrac{lbf}{in}$

**Rear Spring rate:**

Rear ride frequency

$$f_{rr} := 2.8 Hz$$

$$K_{sr} := 4 \pi^2 \cdot f_{rr}^2 \cdot m_{rsm2} \cdot R_r^2 = 6.949 \times 10^4 \frac{kg}{s^2} \qquad K_{sr} = 396.82 \cdot \frac{lbf}{in}$$

**Wheel rate:**

Front: $\quad k_f := \dfrac{K_{sf}}{R_f^2} = 18.108 \cdot \dfrac{N}{mm}$ 

$\qquad\qquad\qquad\qquad\qquad$ Spring Rate of Tire: $\qquad\qquad k_f = 103.397 \cdot \dfrac{lbf}{in}$

Rear: $\quad k_r := \dfrac{K_{sr}}{R_r^2} = 1.737 \times 10^4 \dfrac{kg}{s^2}$ 

$\qquad\qquad k_{rt} := 500 \dfrac{lbf}{in} \quad k_{rt} = 8.756 \times 10^4 \dfrac{kg}{s^2}$

**Track width:**

Front: $\quad t_f := 44 \cdot in \qquad t_f = 1.118\, m$

Rear: $\quad t_r := 42 \cdot in \qquad t_r = 1.067\, m$

**Front Roll Rate:**

$$K_F := \frac{\left(\pi \cdot t_f^2 k_f^2\right)}{(180 \cdot 2 \cdot k_f) \cdot deg} = 197.371 \cdot \frac{N \cdot m}{deg} \qquad \text{per one degree of roll}$$

$$K_F = 1.747 \times 10^3 \cdot \frac{lbf \cdot in}{deg}$$

**Rear Roll Rate:**

$$K_R := \frac{\left(\pi \cdot t_r^2 k_{rt}^2\right)}{(180 \cdot 2 \cdot k_{rt}) \cdot deg} = 4.983 \times 10^4 \cdot (N \cdot m) \qquad \text{per one degree of roll}$$

$$K_R = 7.697 \times 10^3 \cdot \frac{lbf \cdot in}{deg}$$

Assume CG height $CG_h := 13 in \quad CG_h = 0.33\, m$

**Roll Gradient from the ride springs:**

$$r := \frac{(M) \cdot CG_h}{K_F + K_R} = 0.757 \cdot \frac{deg}{g}$$

**\*No anti-roll bars**

can we make the front suspension softer and get away with it? No

**Weight at the front wheel:**

$$W_{lf} = 56.132 \, \text{kg} \qquad W_{rr} = 68.606 \, \text{kg}$$

$$W_{rf} = 56.132 \, \text{kg} \qquad W_{lr} = 68.606 \, \text{kg}$$

**Force at front wheel at ride height:**

$$f_{fw} := W_{lf} \cdot g = 550.467 \, \text{N} \qquad f_{fw} = 123.75 \cdot \text{lbf} \qquad \text{at each wheel}$$

$$f_{rw} := W_{lr} \cdot g = 672.794 \, \text{N} \qquad f_{rw} = 151.25 \cdot \text{lbf}$$

**How much the wheel moves at ride height**

$$W_{mf} := \frac{f_{fw}}{k_f} = 30.4 \cdot \text{mm} \qquad W_{mf} = 1.197 \cdot \text{in}$$

$$W_{mr} := \frac{f_{rw}}{k_r} = 38.725 \cdot \text{mm} \qquad W_{mr} = 1.525 \cdot \text{in}$$

**How Much the Shock Moves (spring compression):**

$$S_{cf} := \frac{W_{mf}}{R_f} = 0.021 \, \text{m} \qquad S_{cf} = 0.82 \cdot \text{in}$$

$$S_{cr} := \frac{W_{mr}}{R_r} = 0.019 \, \text{m} \qquad S_{cr} = 0.762 \cdot \text{in}$$

**Force on Shock:**

$$f_{sf} := \frac{f_{fw}}{R_f^2} = 258.241 \, \text{N} \qquad f_{sf} = 58.055 \cdot \text{lbf}$$

$$f_{sr} := f_{rw} \cdot R_r = 1.346 \times 10^3 \, \text{N} \qquad f_{sr} = 302.5 \cdot \text{lbf}$$

**Damping Calculations:**

Critical Damping:

$$C_{crf} := 2\sqrt{k_f \cdot m_{fsm}} = 1.801 \times 10^3 \frac{kg}{s} \qquad\qquad C_{crf} = 3.971 \times 10^3 \cdot \frac{lb}{s}$$

$$C_{crr} := 2\sqrt{k_r \cdot m_{rsm}} = 2.793 \times 10^3 \frac{kg}{s} \qquad\qquad C_{crr} = 6.158 \times 10^3 \cdot \frac{lb}{s}$$

Damping Ratio: $:= .7$

A good base line for a damping ratio is .65 to .7 look at figure 6: Effect of damping ratio to a sprung mass system.

**Damping force:**

$$C_f := \cdot C_{crf} = 1.261 \cdot \frac{N}{\left(\frac{mm}{s}\right)} \qquad\qquad C_r := \cdot C_{crr} = 1.955 \times 10^3 \frac{kg}{s}$$

**Crossover point:** nknee in the dyno graph- defines where you go from low to high frequency

$$P_{crossf} := \sqrt{2} \cdot f_{rf} = 4.525 \cdot Hz \qquad\qquad v := 15\frac{in}{s} = 381 \cdot \frac{mm}{s}$$

$$P_{crossr} := \sqrt{2} \cdot f_{rr} = 3.96 \cdot Hz$$

Consider 1 inch to be the movement of the schock before the body moves,

$$d := 1in \qquad d_r := .625in$$

any velocity above Vcross the damping ratio is 0.2, anything below has a damping ratio of 0.7

**Velocities at the crossover point**

$$V_{crossf} := P_{crossf} \cdot d = 4.525 \cdot \frac{in}{s}$$

$$V_{crossf} = 114.947 \cdot \frac{mm}{s}$$

$$V_{crossr} := P_{crossr} \cdot d_r = 2.475 \cdot \frac{in}{s}$$

Initial slope

$$IS_f := 4 \quad \cdot f_{rf} \cdot m_{fsm} = 1.261 \times 10^3 \cdot \frac{N}{\left(\frac{m}{s}\right)}$$

$$IS_r := 4 \quad \cdot f_{rr} \cdot m_{rsm2} = 1.383 \times 10^3 \cdot \frac{N}{\left(\dfrac{m}{s}\right)}$$

## Compressions Slope

### Front

$$CS_{lsf} := \frac{2}{3} IS_f = 840.561 \cdot \frac{N}{\left(\dfrac{m}{s}\right)}$$

$$CS_{hsf} := \frac{1}{3} IS_f = 420.281 \cdot \frac{N}{\left(\dfrac{m}{s}\right)}$$

### Rear

$$CS_{lsr} := \frac{2}{3} IS_r = 921.692 \cdot \frac{N}{\left(\dfrac{m}{s}\right)}$$

$$CS_{hsr} := \frac{1}{3} IS_r = 460.846 \cdot \frac{N}{\left(\dfrac{m}{s}\right)}$$

## Rebound Slope:

$$RS_{lsf} := \frac{-3}{2} IS_f = -1.891 \times 10^3 \cdot \frac{N}{\left(\dfrac{m}{s}\right)}$$

$$RS_{hsf} := \frac{-3}{4} IS_f = -945.632 \cdot \frac{N}{\left(\dfrac{m}{s}\right)}$$

$$RS_{lsr} := \frac{-3}{2} IS_r = -2.074 \times 10^3 \cdot \frac{N}{\left(\dfrac{m}{s}\right)}$$

$$RS_{hsr} := \frac{-3}{4} IS_r = -1.037 \times 10^3 \cdot \frac{N}{\left(\dfrac{m}{s}\right)}$$

Front equations

## Compression

$$y_{clsf} := CS_{lsf} \cdot V_{crossf} = 96.62 \, N$$

$$x := 15 \frac{in}{s}$$

$$y_{chsf} := CS_{hsf} \cdot (x - V_{crossf}) + y_{clsf} = 208.437 \, N$$

intercept
$$b_c := CS_{hsf} \cdot (0 - V_{crossf}) + y_{clsf} = 48.31 \, N$$

$$V_c := 0 \frac{in}{s}, 0.1 \frac{in}{s} .. 20 \frac{in}{s}$$

$$f(V_c) := if\left(V_c < V_{crossf}, CS_{lsf} \cdot V_c, CS_{hsf} \cdot V_c + b_c\right)$$

**Rebound**

$$y_{rlsf} := RS_{lsf} \cdot V_{crossf} = -217.396 \, N$$

$$y_{rhsf} := RS_{hsf} \cdot \left(x - V_{crossf}\right) + y_{clsf} = -154.968 \, N$$

intercept
$$b_r := RS_{hsf} \cdot \left(0 - V_{crossf}\right) + y_{rlsf} = -108.698 \, N$$

$$b(V_c) := if\left(V_c < V_{crossf}, RS_{lsf} \cdot V_c, RS_{hsf} \cdot V_c + b_r\right)$$
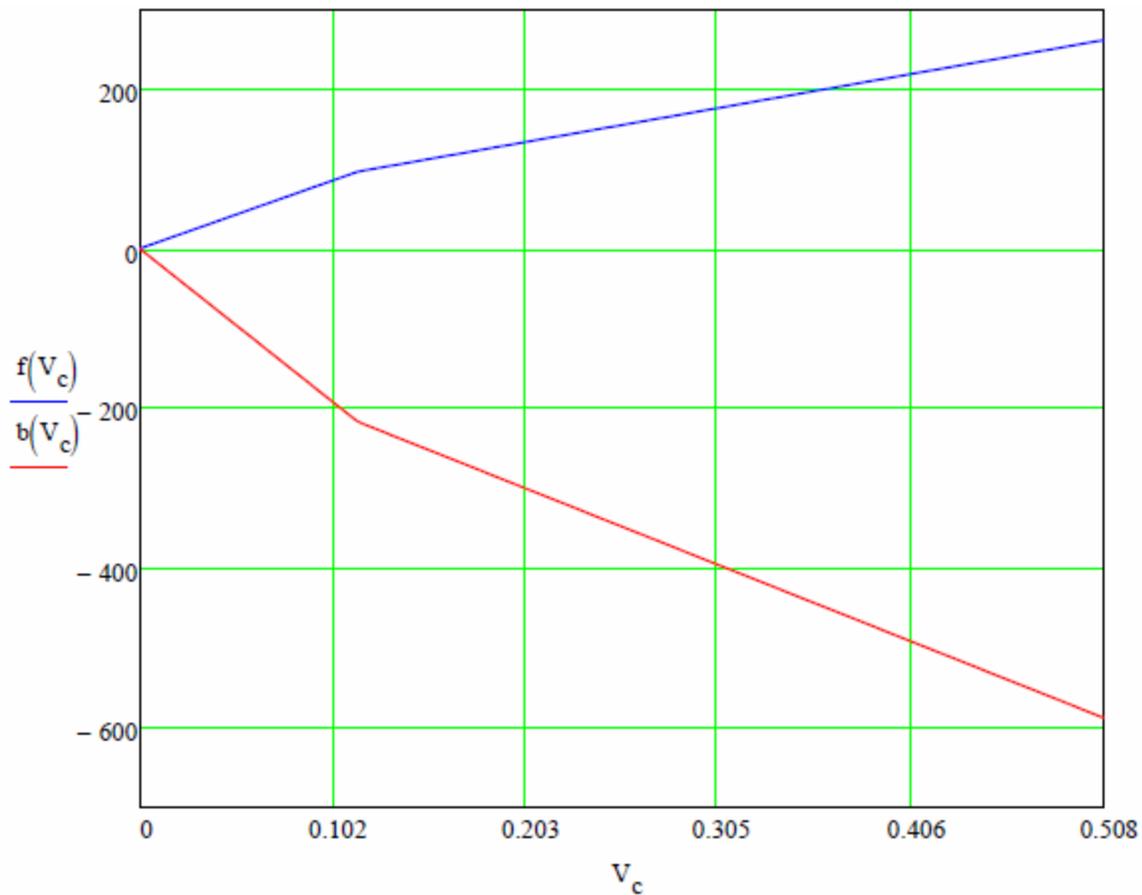
Note: the units of the above graph are in m/s and N

$$V_{crossf} = 0.115 \frac{m}{s}$$

$$20 \frac{in}{s} = 0.508 \frac{m}{s}$$

$$V_{crossf} = 4.525 \cdot \frac{in}{s}$$

$$f(V_{crossf}) = 21.721 \cdot lbf$$

$$b(V_{crossf}) = -48.872 \cdot lbf$$

Link to 2010 TTX25:
http://motorsportsspares.com/files/2010_ttx25_e.pdf

Link to 2011 TTX25 MKII:
http://motorsportsspares.com/files/2011_ttx25mkii_e.pdf

**For the shocks we have: (2010TTCX25)**
With our crossover point and slopes for compression we need C23 24-0 setting on the cane creek
for rebound we would need R23 18-1 settings

**For the 2011 TTX25 MKII:**
we want C11 R11 12-2 for compression and a quarter of the way between 4-4 and 0-5 (so 3-4.25)

24= clicks from low speed from fully closed (clockwise)
0=click from high speed from fully open (counter clockwise)
18=

Cost of new shocks:

$$C_s := 610$$

$$2 \cdot C_s = 1.22 \times 10^3 \quad \text{Dollars}$$

rear shock equations:

## Compression

$$y_{clsr} := CS_{lsr} \cdot V_{crossr} = 57.939 \, N$$

$$x := 15 \frac{in}{s}$$

$$y_{chsr} := CS_{hsr} \cdot (x - V_{crossr}) + y_{clsr} = 204.552 \, N$$

intercept

$$b_{cr} := CS_{hsr} \cdot (0 - V_{crossr}) + y_{clsr} = 28.97 \, N$$

$$V_{cr} := 0 \frac{in}{s}, 0.1 \frac{in}{s} .. 20 \frac{in}{s}$$

$$f_r(V_{cr}) := if(V_{cr} < V_{crossr}, CS_{lsr} \cdot V_{cr}, CS_{hsr} \cdot V_{cr} + b_{cr})$$

## Rebound

$$y_{rlsr} := RS_{lsr} \cdot V_{crossr} = -130.363 \, N$$

$$y_{rhsr} := RS_{hsr} \cdot (x - V_{crossr}) + y_{clsr} = -271.939 \, N$$

intercept

$$b_{rr} := RS_{hsr} \cdot (0 - V_{crossr}) + y_{rlsr} = -65.182 \, N$$

$$b_R(V_{cr}) := if(V_{cr} < V_{crossr}, RS_{lsr} \cdot V_{cr}, RS_{hsr} \cdot V_{cr} + b_{rr})$$

# Appendix D: Intake Calculations

Cross sectional area of runners

$$RPM_{pk} := 7500 \cdot \frac{1}{min}$$

$$D_{tot} := 499 cm^3 = 30.451 \cdot in^3$$

$$D_{cyl} := \frac{D_{tot}}{2} = 15.225 \cdot in^3$$

$$A_{run} := \frac{RPM_{pk} \cdot min \cdot \frac{D_{cyl}}{in^3}}{88200} = 1.295$$

$$r_{run} := \sqrt{\frac{A_{run}}{\pi}} = 0.642$$

$$d_{run} := r_{run} \cdot 2in = 1.284 \cdot in$$

Runner Length

$$Duration := 288 deg$$

$$ECD := \frac{720 deg - Duration - 30 deg}{deg} = 402$$

$$v_{sound} := 1275$$

$$n := 2$$

$$RPM := RPM_{pk} \cdot min$$

$$d := \frac{d_{run}}{in}$$

$$L_{run} := \left[ \frac{\left( ECD \cdot .25 \cdot 2 \cdot v_{sound} \right)}{RPM \cdot n} - \frac{d}{2} \right] \cdot in = 16.443 \cdot in$$

Plenum Sizing

$$D_{engine} := 499 cm^3 = 30.451 \cdot in^3$$

$$D_{cyl} := \frac{D_{engine}}{2} = 249.5 \cdot cm^3 \qquad\qquad RPM_{pk} := \frac{7500}{min}$$

$$VE := 80\%$$

$$Q_{cyl} := VE \cdot RPM_{pk} \cdot \frac{D_{cyl}}{2} = 26.433 \cdot \frac{ft^3}{min}$$

Max Air Flow through restrictor

$$d_r := 20mm$$

$$r_r := \frac{d_r}{2} = 10 \cdot mm$$

$$A_r := \pi \cdot r_r^2 = 314.159 \cdot mm^2$$

$$P_0 := 14.7 psi$$

$$k := 1.4$$

$$T_0 := 294 K$$

$$R := 287.04 \frac{J}{kg \cdot K}$$

$$m_{dotmax} := A_r \cdot P_0 \cdot \sqrt{\frac{k}{R \cdot T_0}} \cdot \left(\frac{2}{k+1}\right)^{\frac{(k+1)}{2(k-1)}} = 0.075 \cdot \frac{kg}{s}$$

$$R_s := 287.04 \frac{J}{kg \cdot K}$$

do we choke flow

$$T := 294 K$$

$$deg_{min} := 360 deg \cdot 7500 \cdot \frac{1}{min} = 2.7 \times 10^6 \cdot \frac{deg}{min}$$

$$p := 14.7 psi$$

$$t_{open} := \frac{144 deg}{deg_{min}} = 3.2 \times 10^{-3} s$$

$$\rho := \frac{p}{R_s \cdot T} = 1.201 \frac{kg}{m^3}$$

$$V_1 := Q_{cyl} \cdot t_{open} = 39.92 \cdot cm^3$$

$$Q_{max} := \frac{m_{dotmax}}{\rho} = 132.41 \cdot \frac{ft^3}{min}$$

Injector sizing

$$\rho_g := 720 \frac{kg}{m^3}$$

$$afr := 12$$

$$m_{dotg} := \frac{m_{dotmax}}{afr} = 6.254 \times 10^{-3} \frac{kg}{s}$$

$$Q_{inj} := \frac{m_{dotg}}{2 \cdot \rho_g} = 260.597 \cdot \frac{cm^3}{min}$$

$$250 cm^3 \cdot .8 = 200 \cdot cm^3$$

$$V_p := 500 cm^3$$

$$t_{180} := \frac{180 deg}{deg_{min}} = 4 \times 10^{-3} s$$

$$t_{12} := t_{180} - t_{open} = 8 \times 10^{-4} s$$

$$t_1 := 3 \cdot t_{180} = 0.012 s$$

$$V_2 := Q_{max} \cdot t_{12} = 49.993 \cdot cm^3$$

$$V_{cyl1} := Q_{max} \cdot t_1 = 749.888 \cdot cm^3$$

new peak torque velocity

$$Q_r := 240 \frac{ft}{s} \cdot A_{run} \cdot in^2 = 2.158 \cdot \frac{ft^3}{s}$$

$$m_{dotr} := \rho \cdot Q_r = 0.073 \frac{kg}{s}$$

$$Q_{new} := \frac{m_{dotr}}{\rho_2} = \blacksquare \cdot \frac{ft^3}{s}$$

$$v_{new} := \frac{Q_{new}}{A_{run} \cdot in^2} = \blacksquare \cdot \frac{ft}{s}$$